Journal of Physics A: Mathematical and Theoretical

TOPICAL REVIEW • **OPEN ACCESS**

Quantum Fisher information matrix and multiparameter estimation

To cite this article: Jing Liu *et al* 2020 *J. Phys. A: Math. Theor.* **53** 023001

OPEN ACCESS
IOP Publishing
Journal of Physics A: Mathematical and Theoretical
J. Phys. A: Math. Theor. **53** (2020) 023001 (68pp)
https://doi.org/10.1088/1751-8121/ab5d4d

Topical Review

Quantum Fisher information matrix and multiparameter estimation

Jing Liu[1,5], Haidong Yuan[2], Xiao-Ming Lu[3] and Xiaoguang Wang[4]

[1] MOE Key Laboratory of Fundamental Physical Quantities Measurement & Hubei Key Laboratory of Gravitation and Quantum Physics, PGMF and School of Physics, Huazhong University of Science and Technology, Wuhan 430074, People's Republic of China
[2] Department of Mechanical and Automation Engineering, The Chinese University of Hong Kong, Shatin, Hong Kong Special Administrative Region of China
[3] Department of Physics, Hangzhou Dianzi University, Hangzhou 310018, People's Republic of China
[4] Department of Physics, Zhejiang Institute of Modern Physics, Zhejiang University, Hangzhou 310027, People's Republic of China

E-mail: liujingphys@hust.edu.cn, hdyuan@mae.cuhk.edu.hk, lxm@hdu.edu.cn and xgwang1208@zju.edu.cn

Received 23 July 2019, revised 19 November 2019
Accepted for publication 29 November 2019
Published 18 December 2019

Abstract

Quantum Fisher information matrix (QFIM) is a core concept in theoretical quantum metrology due to the significant importance of quantum Cramér–Rao bound in quantum parameter estimation. However, studies in recent years have revealed wide connections between QFIM and other aspects of quantum mechanics, including quantum thermodynamics, quantum phase transition, entanglement witness, quantum speed limit and non-Markovianity. These connections indicate that QFIM is more than a concept in quantum metrology, but rather a fundamental quantity in quantum mechanics. In this paper, we summarize the properties and existing calculation techniques of QFIM for various cases, and review the development of QFIM in some aspects of quantum mechanics apart from quantum metrology. On the other hand, as the main application of QFIM, the second part of this paper reviews the quantum multiparameter Cramér–Rao bound, its attainability condition and the associated optimal measurements. Moreover, recent developments in a few typical scenarios of quantum multiparameter estimation and the quantum advantages are also thoroughly discussed in this part.

[5] Author to whom any correspondence should be addressed.

Keywords: quantum metrology, quantum multiparameter estimation, quantum Fisher information matrix

(Some figures may appear in colour only in the online journal)

Contents

1. Introduction

After decades of rapid development, quantum mechanics has now gone deep into almost every corner of modern science, not only as a fundamental theory, but also as a technology. The technology originated from quantum mechanics is usually referred to as quantum technology, which is aiming at developing brand new technologies or improving current existing technologies with the association of quantum resources, quantum phenomena or quantum effects. Some aspects of quantum technology, such as quantum communications, quantum computation, quantum cryptography and quantum metrology, have shown great power in both theory and laboratory to lead the next industrial revolution. Among these aspects, quantum metrology is the most promising one that can step into practice in the near future.

Quantum metrology focuses on making high precision measurements of given parameters using quantum systems and quantum resources. Generally, a complete quantum metrological process contains four steps: (1) preparation of the probe state; (2) parameterzation; (3) measurement and (4) classical estimation, as shown in figure 1. The last step has been well studies in classical statistics, hence, the major concern of quantum metrology is the first three steps.

Quantum parameter estimation is the theory for quantum metrology, and quantum Cramér–Rao bound is the most well-studied mathematical tool for quantum parameter estimation [1, 2]. In quantum Cramér–Rao bound, the quantum Fisher information (QFI) and quantum Fisher information matrix (QFIM) are the key quantities representing the precision limit for single parameter and multiparameter estimations. In recent years, several outstanding reviews on quantum metrology and quantum parameter estimation have been provided from different perspectives and at different time, including the ones given by Giovannetti *et al* on the quantum-enhanced measurement [3] and the advances in quantum metrology [4], the ones given by Paris [5] and Toth *et al* [6] on the QFI and its applications in quantum metrology, the one by Braun *et al* on the quantum enhanced metrology without entanglement [7], the ones by Pezzè *et al* [8] and Huang *et al* [9] on quantum metrology with cold atoms, the one by Degen *et al* on general quantum sensing [10], the one by Pirandola *et al* on the photonic quantum sensing [11], the ones by Dowling on quantum optical metrology with high-N00N state [12] and Dowling and Seshadreesan on theoretical and experimental optical technologies in quantum metrology, sensing and imaging [13], the one by Demkowicz-Dobrzański *et al* on the quantum limits in optical interferometry [14], the one by Sidhu and Kok on quantum parameter estimation from a geometric perspective [15], and the one by Szczykulska *et al* on simultaneous multiparameter estimation [16]. Petz *et al* also wrote a thorough technical introduction on QFI [17].

Apart from quantum metrology, the QFI also connects to other aspects of quantum physics, such as quantum phase transition [18–20] and entanglement witness [21, 22]. The widespread application of QFI may be due to its connection to the Fubini-study metric, a Kähler metric in the complex projective Hilbert space. This relation gives the QFI a strong geometric meaning and makes it a fundamental quantity in quantum physics. Similarly, the QFIM shares this connection since the diagonal entries of QFIM simply gives the QFI. Moreover, the QFIM also

Figure 1. Schematic of a complete quantum metrological process, which contains four steps: (1) preparation of the probe state; (2) parameterzation; (3) measurement; (4) classical estimation.

connects to other fundamental quantity like the quantum geometric tensor [23]. Thus, besides the role in multiparameter estimation, the QFIM should also be treated as a fundamental quantity in quantum mechanics.

In recent years, the calculation techniques of QFIM have seen a rapid development in various scenarios and models. However, there lack papers that thoroughly summarize these techniques in a structured manner for the community. Therefore, this paper not only reviews the recent developments of quantum multiparameter estimation, but also provides comprehensive techniques on the calculation of QFIM in a variety of scenarios. For this purpose, this paper is presented in a way similar to a textbook with many technical details given in the appendices, which could help the readers to follow and better understand the corresponding results.

2. Quantum Fisher information matrix

2.1. Definition

Consider a vector of parameters $\vec{x} = (x_0, x_1, ..., x_a, ...)^{\mathrm{T}}$ with x_a the ath parameter. $\vec{x}$ is encoded in the density matrix $\rho = \rho(\vec{x})$. In the entire paper we denote the QFIM as $\mathcal{F}$, and an entry of $\mathcal{F}$ is defined as [1, 2]

$$\mathcal{F}_{ab} := \frac{1}{2}\mathrm{Tr}\left(\rho\{L_a, L_b\}\right), \tag{1}$$

where $\{\cdot,\cdot\}$ represents the anti-commutation and L_a (L_b) is the symmetric logarithmic derivative (SLD) for the parameter x_a (x_b), which is determined by the equation[6]

$$\partial_a \rho = \frac{1}{2}\left(\rho L_a + L_a \rho\right). \tag{2}$$

The SLD operator is a Hermitian operator and the expected value $\mathrm{Tr}(\rho L_a) = 0$. Utilizing the equation above, $\mathcal{F}_{ab}$ can also be expressed by [24]

$$\mathcal{F}_{ab} = \mathrm{Tr}\left(L_b \partial_a \rho\right) = -\mathrm{Tr}(\rho \partial_a L_b). \tag{3}$$

Based on equation (1), the diagonal entry of QFIM is

$$\mathcal{F}_{aa} = \mathrm{Tr}\left(\rho L_a^2\right), \tag{4}$$

which is exactly the QFI for parameter x_a.

[6] In the entire paper the notation ∂_a (∂_t) is used as an abbreviation of $\frac{\partial}{\partial x_a}$ ($\frac{\partial}{\partial t}$).

The definition of Fisher information matrix originated from classical statistics. For a probability distribution $\{p(y|\vec{x})\}$ where $p(y|\vec{x})$ is the conditional probability for the outcome result y, an entry of Fisher information matrix is defined as

$$\mathcal{I}_{ab} := \int \frac{[\partial_a p(y|\vec{x})]\,[\partial_b p(y|\vec{x})]}{p(y|\vec{x})}\,\mathrm{d}y. \tag{5}$$

For discrete outcome results, it becomes $\mathcal{I}_{ab} := \sum_y \frac{[\partial_a p(y|\vec{x})][\partial_b p(y|\vec{x})]}{p(y|\vec{x})}$. With the development of quantum metrology, the Fisher information matrix concerning classical probability distribution is usually referred to as *classical Fisher information matrix* (CFIM), with the diagonal entry referred to as *classical Fisher information* (CFI). In quantum mechanics, it is well known that the choice of measurement will affect the obtained probability distribution, and thus result in different CFIM. This fact indicates the CFIM is actually a function of measurement. However, while the QFI is always attained by optimizing over the measurements [30], i.e. $\mathcal{F}_{aa} = \max_{\{\Pi_y\}} \mathcal{I}_{aa}(\rho, \{\Pi_y\})$, where $\{\Pi_y\}$ represents a positive-operator valued measure (POVM), in general there may not be any measurement that can attain the QFIM.

The QFIM based on SLD is not the only quantum version of CFIM. Another well-used ones are based on the right and left logarithmic derivatives [2, 25], defined by $\partial_a\rho = \rho R_a$ and $\partial_a\rho = R_a^\dagger\rho$, with the corresponding QFIM $\mathcal{F}_{ab} = \mathrm{Tr}(\rho R_a R_b^\dagger)$. Different with the one based on SLD, which are real symmetric, the QFIM based on right and left logarithmic derivatives are complex and Hermitian. All versions of QFIMs belong to a family of Riemannian monotone metrics established by Petz [26, 27] in 1996, which will be further discussed in section 2.4. All the QFIMs can provide quantum versions of Cramér–Rao bound, yet with different achievability. For instance, for the D-invariant models only the one based on right logarithmic derivative provides an achievable bound [28]. The quantum Cramér–Rao bound will be further discussed in section 3. For pure states, Fujiwara and Nagaoka [29] also extended the SLD to a family via $\partial_a\rho = \frac{1}{2}(\rho L_a + L_a^\dagger\rho)$, in which L_a is not necessarily to be Hermitian, and when it is, it reduces to the SLD. An useful example here is the anti-symmetric logarithmic derivative $L_a^\dagger = -L_a$. This paper focuses on the QFIM based on the SLD, thus, the QFIM in the following only refers to the QFIM based on SLD without causing any confusion.

The properties of QFI have been well organized by Tóth *et al* in [6]. Similarly, the QFIM also has some powerful properties that have been widely applied in practice. Here we organize these properties as below.

Proposition 2.1. *Properties and useful formulas of the QFIM.*

- $\mathcal{F}$ *is real symmetric, i.e.* $\mathcal{F}_{ab} = \mathcal{F}_{ba} \in \mathbb{R}$[7].
- $\mathcal{F}$ *is positive semi-definite, i.e.* $\mathcal{F} \geqslant 0$. *If* $\mathcal{F} > 0$, *then* $[\mathcal{F}^{-1}]_{aa} \geqslant 1/\mathcal{F}_{aa}$ *for any a.*
- $\mathcal{F}(\rho) = \mathcal{F}(U\rho U^\dagger)$ *for a* $\vec{x}$*-independent unitary operation U.*
- *If* $\rho = \bigotimes_i \rho_i(\vec{x})$, *then* $\mathcal{F}(\rho) = \sum_i \mathcal{F}(\rho_i)$.
- *If* $\rho = \bigoplus_i \mu_i\rho_i(\vec{x})$ *with* μ_i *a* $\vec{x}$*-independent weight, then* $\mathcal{F}(\rho) = \sum_i \mu_i\mathcal{F}(\rho_i)$.
- *Convexity:* $\mathcal{F}(p\rho_1 + (1-p)\rho_2) \leqslant p\mathcal{F}(\rho_1) + (1-p)\mathcal{F}(\rho_2)$ *for* $p \in [0, 1]$.
- $\mathcal{F}$ *is monotonic under completely positive and trace preserving map* Φ, *i.e.* $\mathcal{F}(\Phi(\rho)) \leqslant \mathcal{F}(\rho)$ *[27].*
- *If* $\vec{y}$ *is function of* $\vec{x}$, *then the QFIMs with respect to* $\vec{y}$ *and* $\vec{x}$ *satisfy* $\mathcal{F}(\rho(\vec{x})) = J^{\mathrm{T}}\mathcal{F}(\rho(\vec{y}))J$, *with J the Jacobian matrix, i.e.* $J_{ij} = \partial y_i/\partial x_j$.

[7] $\mathbb{R}$ represents the set of real numbers.

2.2. Parameterization processes

Generally, the parameters are encoded into the probe state via a parameter-dependent dynamics. According to the types of dynamics, there exist three types of parameterization processes: Hamiltonian parameterization, channel parameterization and hybrid parameterization, as shown in figure 2. In the Hamiltonian parameterization, $\vec{x}$ is encoded in the probe state ρ_0 through the Hamiltonian $H_{\vec{x}}$. The dynamics is then governed by the Schrödinger equation

$$\partial_t \rho = -\mathrm{i}[H_{\vec{x}}, \rho], \tag{6}$$

and the parameterized state can be written as

$$\rho = \mathrm{e}^{-\mathrm{i}H_{\vec{x}}t}\rho_0 \mathrm{e}^{\mathrm{i}H_{\vec{x}}t}. \tag{7}$$

Thus, the Hamiltonian parameterization is a unitary process. In some other scenarios the parameters are encoded via the interaction with another system, which means the probe system here has to be treated as an open system and the dynamics is governed by the master equation. This is the channel parameterization. The dynamics for the channel parameterization is

$$\partial_t \rho = -\mathrm{i}[H, \rho] + \mathcal{L}_{\vec{x}}(\rho), \tag{8}$$

where $\mathcal{L}_{\vec{x}}(\rho)$ represents the decay term dependent on $\vec{x}$. A well-used form of $\mathcal{L}_{\vec{x}}$ is the Lindblad form

$$\mathcal{L}(\rho) = \sum_j \gamma_j \left(\Gamma_j \rho \Gamma_j^\dagger - \frac{1}{2} \left\{ \Gamma_j^\dagger \Gamma_j, \rho \right\} \right), \tag{9}$$

where Γ_j is the jth Lindblad operator and γ_j is the jth decay rate. All the decay rates are unknown parameters to be estimated. The third type is the hybrid parameterization, in which both the Hamiltonian parameters and decay rates in equation (8) are unknown and need to be estimated.

2.3. Calculating QFIM

In this section we review the techniques in the calculation of QFIM and some analytic results for specific cases.

2.3.1. General methods. The traditional derivation of QFIM usually assumes the rank of the density matrix is full, i.e. all the eigenvalues of the density matrix are positive. Specifically if we write $\rho = \sum_{i=0}^{\dim(\rho)-1} \lambda_i |\lambda_i\rangle\langle\lambda_i|$, with λ_i and $|\lambda_i\rangle$ the eigenvalue and the corresponding eigenstate, it is usually assumed that $\lambda_i > 0$ for all $0 \leqslant i \leqslant \dim(\rho) - 1$. Under this assumption the QFIM can be obtained as follows.

Theorem 2.1. *The entry of QFIM for a full-rank density matrix with the spectral decomposition* $\rho = \sum_{i=0}^{d-1} \lambda_i |\lambda_i\rangle\langle\lambda_i|$ *can be written as*

$$\mathcal{F}_{ab} = \sum_{i,j=0}^{d-1} \frac{2\mathrm{Re}(\langle\lambda_i|\partial_a\rho|\lambda_j\rangle\langle\lambda_j|\partial_b\rho|\lambda_i\rangle)}{\lambda_i + \lambda_j}, \tag{10}$$

where $d := \dim(\rho)$ *is the dimension of the density matrix.*

One can easily see that if the density matrix is not of full rank, there can be divergent terms in the above equation. To extend it to the general density matrices which may not have full rank, we can manually remove the divergent terms as

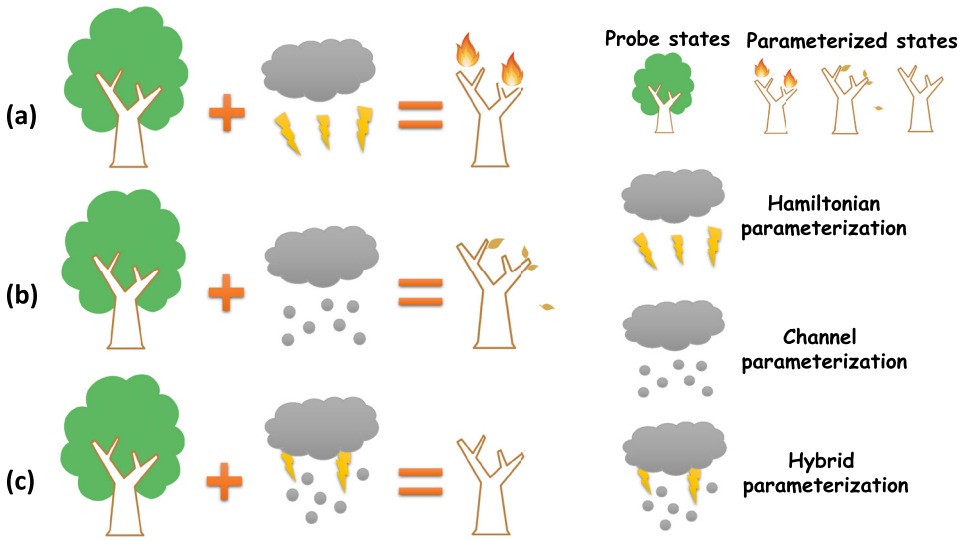

Figure 2. The schematic of multiparameter parameterization processes. (a) Hamiltonian parameterization (b) Channel parameterization (c) Hybrid parameterization.

$$\mathcal{F}_{ab} = \sum_{i,j=0,\lambda_i+\lambda_j\neq 0}^{d-1} \frac{2\mathrm{Re}(\langle\lambda_i|\partial_a\rho|\lambda_j\rangle\langle\lambda_j|\partial_b\rho|\lambda_i\rangle)}{\lambda_i+\lambda_j}. \tag{11}$$

By substituting the spectral decomposition of ρ into the equation above, it can be rewritten as [5]

$$\mathcal{F}_{ab} = \sum_{i=0}^{d-1} \frac{(\partial_a\lambda_i)(\partial_b\lambda_i)}{\lambda_i} + \sum_{i\neq j,\lambda_i+\lambda_j\neq 0} \frac{2(\lambda_i-\lambda_j)^2}{\lambda_i+\lambda_j}\mathrm{Re}\left(\langle\lambda_i|\partial_a\lambda_j\rangle\langle\partial_b\lambda_j|\lambda_i\rangle\right). \tag{12}$$

Recently, it has been rigorously proved that the QFIM for a finite dimensional density matrix can be expressed with the support of the density matrix [31]. The support of a density matrix, denoted by $\mathcal{S}$, is defined as $\mathcal{S} := \{\lambda_i \in \{\lambda_i\}|\lambda_i \neq 0\}$ ($\{\lambda_i\}$ is the full set of ρ's eigenvalues), and the spectral decomposition can then be modified as $\rho = \sum_{\lambda_i\in\mathcal{S}} \lambda_i|\lambda_i\rangle\langle\lambda_i|$. The QFIM can then be calculated via the following theorem.

Theorem 2.2. *Given the spectral decomposition of a density matrix, $\rho = \sum_{\lambda_i\in\mathcal{S}} |\lambda_i\rangle\langle\lambda_i|$ where $\mathcal{S} = \{\lambda_i \in \{\lambda_i\}|\lambda_i \neq 0\}$ is the support, an entry of QFIM can be calculated as [31]*

$$\begin{aligned}\mathcal{F}_{ab} = &\sum_{\lambda_i\in\mathcal{S}} \frac{(\partial_a\lambda_i)(\partial_b\lambda_i)}{\lambda_i} + \sum_{\lambda_i\in\mathcal{S}} 4\lambda_i\mathrm{Re}\left(\langle\partial_a\lambda_i|\partial_b\lambda_i\rangle\right)\\ &- \sum_{\lambda_i,\lambda_j\in\mathcal{S}} \frac{8\lambda_i\lambda_j}{\lambda_i+\lambda_j}\mathrm{Re}(\langle\partial_a\lambda_i|\lambda_j\rangle\langle\lambda_j|\partial_b\lambda_i\rangle).\end{aligned} \tag{13}$$

The detailed derivation of this equation can be found in appendix B. It is a general expression of QFIM for a finite-dimensional density matrix of arbitrary rank. Due to the relation between the QFIM and QFI, one can easily obtain the following corollary.

Corollary 2.2.1. *Given the spectral decomposition of a density matrix, $\rho = \sum_{\lambda_i \in \mathcal{S}} |\lambda_i\rangle\langle\lambda_i|$, the QFI for the parameter x_a can be calculated as [32–36]*

$$\mathcal{F}_{aa} = \sum_{\lambda_i \in \mathcal{S}} \frac{(\partial_a \lambda_i)^2}{\lambda_i} + \sum_{\lambda_i \in \mathcal{S}} 4\lambda_i \langle \partial_a \lambda_i | \partial_a \lambda_i \rangle - \sum_{\lambda_i, \lambda_j \in \mathcal{S}} \frac{8\lambda_i \lambda_j}{\lambda_i + \lambda_j} |\langle \partial_a \lambda_i | \lambda_j \rangle|^2. \quad (14)$$

The first term in equations (12) and (13) can be viewed as the counterpart of the classical Fisher information as it only contains the derivatives of the eigenvalues which can be regarded as the counterpart of the probability distribution. The other terms are purely quantum [5, 36]. The derivatives of the eigenstates reflect the local structure of the eigenspace on $\vec{x}$. The effect of this local structure on QFIM can be easily observed via equations (12) and (13).

The SLD operator is important since it is not only related to the calculation of QFIM, but also contains the information of the optimal measurements and the attainability of the quantum Cramér–Rao bound, which will be further discussed in sections 3.1.2 and 3.1.3. In terms of the eigen-space of ρ, the entries of the SLD operator for $\lambda_i, \lambda_j \in \mathcal{S}$ can be obtained as follows[8]

$$\langle \lambda_i | L_a | \lambda_j \rangle = \delta_{ij} \frac{\partial_a \lambda_i}{\lambda_i} + \frac{2(\lambda_j - \lambda_i)}{\lambda_i + \lambda_j} \langle \lambda_i | \partial_a \lambda_j \rangle; \quad (15)$$

for $\lambda_i \in \mathcal{S}$ and $\lambda_j \notin \mathcal{S}$, $\langle \lambda_i | L_a | \lambda_j \rangle = -2\langle \lambda_i | \partial_a \lambda_j \rangle$; and for $\lambda_i, \lambda_j \notin \mathcal{S}$, $\langle \lambda_i | L_a | \lambda_j \rangle$ can take arbitrary values. Fujiwara and Nagaoka [29, 37] first proved that this randomness does not affect the value of QFI and all forms of SLD provide the same QFI. As a matter of fact, this conclusion can be extended to the QFIM for any quantum state [31, 38], i.e. the entries that can take arbitrary values do not affect the value of QFIM. Hence, if we focus on the calculation of QFIM we can just set them zeros. However, this randomness plays a role in the search of optimal measurement, which will be further discussed in section 3.1.3.

In control theory, equation (2) is also referred to as the Lyapunov equation and the solution can be obtained as [5]

$$L_a = 2 \int_0^\infty \mathrm{e}^{-\rho s} \left(\partial_a \rho\right) \mathrm{e}^{\rho s} \mathrm{d}s, \quad (16)$$

which is independent of the representation of ρ. This can also be written in an expanded form [38]

$$L_a = -2 \lim_{s \to \infty} \sum_{n=0}^{\infty} \frac{(-s)^{n+1}}{(n+1)!} \mathcal{R}_\rho^n(\partial_a \rho), \quad (17)$$

here $\mathcal{R}_\rho(\cdot) := \{\rho, \cdot\}$ denotes the anti-commutator. Using the fact that $\mathcal{R}_\rho^n(\partial_a \rho) = \sum_{m=0}^n \binom{n}{m} \rho^m \left(\partial_a \rho\right) \rho^{n-m}$, where $\binom{n}{m} = \frac{n!}{m!(n-m)!}$, equation (17) can be rewritten as

$$L_a = -2 \lim_{s \to \infty} \sum_{n=0}^{\infty} \sum_{m=0}^{n} \frac{(-s)^{n+1}}{(n+1)!} \binom{n}{m} \rho^m \left(\partial_a \rho\right) \rho^{n-m}. \quad (18)$$

This form of SLD can be easy to calculate if $\rho^m(\partial_a \rho)\rho^{n-m}$ is only non-zero for limited number of terms or has some recursive patterns.

Recently, Safránek [39] provided another method to compute the QFIM utilizing the density matrix in Liouville space. In Liouville space, the density matrix is a vector containing all the entries of the density matrix in Hilbert space. Denote $\mathrm{vec}(A)$ as the *column* vector of A

[8] The derivation is in appendix B.

in Liouville space and $\mathrm{vec}(A)^\dagger$ as the conjugate transpose of $\mathrm{vec}(A)$. The entry of $\mathrm{vec}(A)$ is $[\mathrm{vec}(A)]_{id+j} = A_{ij}$ $(i,j \in [0, d-1])$. The QFIM can be calculated as follows.

Theorem 2.3. *For a full-rank density matrix, the QFIM can be expressed by [39]*

$$\mathcal{F}_{ab} = 2\mathrm{vec}(\partial_a \rho)^\dagger \left(\rho \otimes \mathbb{1} + \mathbb{1} \otimes \rho^*\right)^{-1} \mathrm{vec}(\partial_b \rho), \tag{19}$$

where ρ^* is the conjugate of ρ, and the SLD operator in Liouville space, denoted by $\mathrm{vec}(L_a)$, reads

$$\mathrm{vec}(L_a) = 2\left(\rho \otimes \mathbb{1} + \mathbb{1} \otimes \rho^*\right)^{-1} \mathrm{vec}(\partial_a \rho). \tag{20}$$

This theorem can be proved by using the facts that $\mathrm{vec}(AB\mathbb{1}) = (A \otimes \mathbb{1})\mathrm{vec}(B) = (\mathbb{1} \otimes B^{\mathrm{T}})\mathrm{vec}(A)$ (B^{T} is the transpose of B) [40–42] and $\mathrm{Tr}(A^\dagger B) = \mathrm{vec}(A)^\dagger \mathrm{vec}(B)$.

Bloch representation is another well-used tool in quantum information theory. For a d-dimensional density matrix, it can be expressed by

$$\rho = \frac{1}{d}\left(\mathbb{1} + \sqrt{\frac{d(d-1)}{2}}\vec{r} \cdot \vec{\kappa}\right), \tag{21}$$

where $\vec{r} = (r_1, r_2 ..., r_m, ...)^{\mathrm{T}}$ is the Bloch vector ($|\vec{r}|^2 \leqslant 1$) and $\vec{\kappa}$ is a (d^2-1)-dimensional vector of $\mathfrak{su}(d)$ generator satisfying $\mathrm{Tr}(\kappa_i) = 0$. The anti-commutation relation for them is $\{\kappa_i, \kappa_j\} = \frac{4}{d}\delta_{ij}\mathbb{1} + \sum_{m=1}^{d^2-1} \mu_{ijm}\kappa_m$, and the commutation relation is $[\kappa_i, \kappa_j] = \mathrm{i}\sum_{m=1}^{d^2-1} \epsilon_{ijm}\kappa_m$, where μ_{ijm} and ϵ_{ijm} are the symmetric and antisymmetric structure constants. Watanabe *et al* recently [43–45] provided the formula of QFIM for a general Bloch vector by considering the Bloch vector itself as the parameters to be estimated. Here we extend their result to a general case as the theorem below.

Theorem 2.4. *In the Bloch representation of a d-dimensional density matrix, the QFIM can be expressed by*

$$\mathcal{F}_{ab} = (\partial_b \vec{r})^{\mathrm{T}} \left(\frac{d}{2(d-1)}G - \vec{r}\,\vec{r}^{\mathrm{T}}\right)^{-1} \partial_a \vec{r}, \tag{22}$$

where G is a real symmetric matrix with the entry

$$G_{ij} = \frac{1}{2}\mathrm{Tr}(\rho\{\kappa_i, \kappa_j\}) = \frac{2}{d}\delta_{ij} + \sqrt{\frac{d-1}{2d}}\sum_m \mu_{ijm} r_m. \tag{23}$$

The most well-used scenario of this theorem is single-qubit systems, in which $\rho = (\mathbb{1} + \vec{r} \cdot \vec{\sigma})/2$ with $\vec{\sigma} = (\sigma_x, \sigma_y, \sigma_z)$ the vector of Pauli matrices. For a single-qubit system, we have the following corollary.

Corollary 2.4.1. *For a single-qubit mixed state, the QFIM in Bloch representation can be expressed by*

$$\mathcal{F}_{ab} = (\partial_a \vec{r}) \cdot (\partial_b \vec{r}) + \frac{(\vec{r} \cdot \partial_a \vec{r})(\vec{r} \cdot \partial_b \vec{r})}{1 - |\vec{r}|^2}, \tag{24}$$

where $|\vec{r}|$ is the norm of $\vec{r}$. For a single-qubit pure state, $\mathcal{F}_{ab} = (\partial_a \vec{r}) \cdot (\partial_b \vec{r})$.

The diagonal entry of equation (24) is exactly the one given by [47]. The proofs of the theorem and corollary are provided in appendix C.

2.3.2. Pure states. A pure state satisfies $\rho = \rho^2$, i.e. the purity $\mathrm{Tr}(\rho^2)$ equals 1. For a pure state $|\psi\rangle$, the dimension of the support is 1, which means only one eigenvalue is non-zero (it has to be 1 since $\mathrm{Tr}\rho = 1$), with which the corresponding eigenstate is $|\psi\rangle$. For pure states, the QFIM can be obtained as follows.

Theorem 2.5. *The entries of the QFIM for a pure parameterized state $|\psi\rangle := |\psi(\vec{x})\rangle$ can be obtained as [1, 2]*

$$\mathcal{F}_{ab} = 4\mathrm{Re}(\langle\partial_a\psi|\partial_b\psi\rangle - \langle\partial_a\psi|\psi\rangle\langle\psi|\partial_b\psi\rangle). \tag{25}$$

The QFI for the parameter x_a is just the diagonal element of the QFIM, which is given by

$$\mathcal{F}_{aa} = 4(\langle\partial_a\psi|\partial_a\psi\rangle - |\langle\partial_a\psi|\psi\rangle|^2), \tag{26}$$

and the SLD operator corresponding to x_a is $L_a = 2\left(|\psi\rangle\langle\partial_a\psi| + |\partial_a\psi\rangle\langle\psi|\right)$.

The SLD formula is obtained from the fact $\rho^2 = \rho$ for a pure state, then $\partial_a\rho = \rho\partial_a\rho + (\partial_a\rho)\rho$. Compared this equation to the definition equation, it can be seen that $L = 2\partial_a\rho$. A simple example is $|\psi\rangle = \mathrm{e}^{-\mathrm{i}\sum_j H_j x_j t}|\psi_0\rangle$ with $[H_a, H_b] = 0$ for any a and b, here $|\psi_0\rangle$ denotes the initial probe state. In this case, the QFIM reads

$$\mathcal{F}_{ab} = 4t^2\mathrm{cov}_{|\psi_0\rangle}(H_a, H_b), \tag{27}$$

where $\mathrm{cov}_{|\varphi\rangle}(A, B)$ denotes the covariance between A and B on $|\varphi\rangle$, i.e.

$$\mathrm{cov}_{|\varphi\rangle}(A, B) := \frac{1}{2}\langle\varphi|\{A, B\}|\varphi\rangle - \langle\varphi|A|\varphi\rangle\langle\varphi|B|\varphi\rangle. \tag{28}$$

A more general case where H_a and H_b do not commute will be discussed in section 2.3.4.

2.3.3. Few-qubit states. The simplest few-qubit system is the single-qubit system. A single-qubit pure state can always be written as $\cos\theta|0\rangle + \sin\theta\mathrm{e}^{\mathrm{i}\phi}|1\rangle$ ($\{|0\rangle, |1\rangle\}$ is the basis), i.e. it only has two degrees of freedom, which means only two independent parameters ($\vec{x} = (x_0, x_1)^{\mathrm{T}}$) can be encoded in a single-qubit pure state. Assume θ, ϕ are the parameters to be estimated, the QFIM can then be obtained via equation (25) as

$$\mathcal{F}_{\theta\theta} = 4,\ \mathcal{F}_{\phi\phi} = \sin^2(2\theta),\ \mathcal{F}_{\theta\phi} = 0. \tag{29}$$

If the unknown parameters are not θ, ϕ, but functions of θ, ϕ, the QFIM can be obtained from formula above with the assistance of Jacobian matrix.

For a single-qubit mixed state, when the number of encoded parameters is larger than three, the determinant of QFIM would be zero, indicating that these parameters cannot be simultaneously estimated. This is due to the fact that there only exist three degrees of freedom in a single-qubit mixed state, thus, only three or fewer independent parameters can be encoded into the density matrix ρ. However, more parameters may be encoded if they are not independent. Since ρ here only has two eigenvalues λ_0 and λ_1, equation (13) then reduces to

$$\mathcal{F}_{ab} = \frac{(\partial_a\lambda_0)(\partial_b\lambda_0)}{\lambda_0(1-\lambda_0)} + 4(1-2\lambda_0)^2\mathrm{Re}\left(\langle\partial_a\lambda_0|\lambda_1\rangle\langle\lambda_1|\partial_b\lambda_0\rangle\right). \tag{30}$$

In the case of single qubit, equation (30) can also be written in a basis-independent formula [46] below.

Theorem 2.6. *The basis-independent expression of QFIM for a single-qubit mixed state ρ is of the following form*

$$\mathcal{F}_{ab} = \mathrm{Tr}\left[(\partial_a\rho)(\partial_b\rho)\right] + \frac{1}{\det(\rho)}\mathrm{Tr}\left[\rho(\partial_a\rho)\rho(\partial_b\rho)\right], \tag{31}$$

where $\det(\rho)$ *is the determinant of* ρ. *For a single-qubit pure state,* $\mathcal{F}_{ab} = 2\mathrm{Tr}[(\partial_a\rho)(\partial_b\rho)]$.

Equation (31) is the reduced form of the one given in [46]. The advantage of the basis-independent formula is that the diagonalization of the density matrix is avoided. Now we show an example for single-qubit. Consider a spin in a magnetic field which is in the z-axis and suffers from dephasing noise also in the z-axis. The dynamics of this spin can then be expressed by

$$\partial_t\rho = -\mathrm{i}[B\sigma_z, \rho] + \frac{\gamma}{2}(\sigma_z\rho\sigma_z - \rho), \tag{32}$$

where σ_z is a Pauli matrix. B is the amplitude of the field. Take B and γ as the parameters to be estimated. The analytical solution for $\rho(t)$ is

$$\rho(t) = \begin{pmatrix} \rho_{00}(0) & \rho_{01}(0)\mathrm{e}^{-\mathrm{i}2Bt-\gamma t} \\ \rho_{10}(0)\mathrm{e}^{\mathrm{i}2Bt-\gamma t} & \rho_{11}(0) \end{pmatrix}. \tag{33}$$

The derivatives of $\rho(t)$ on both B and γ are simple in this basis. Therefore, the QFIM can be directly calculated from equation (31), which is a diagonal matrix ($\mathcal{F}_{B\gamma} = 0$) with the diagonal entries

$$\mathcal{F}_{BB} = 16|\rho_{01}(0)|^2\mathrm{e}^{-2\gamma t}t^2, \tag{34}$$

$$\mathcal{F}_{\gamma\gamma} = \frac{4\rho_{00}(0)\rho_{11}(0)|\rho_{01}(0)|^2t^2}{\rho_{00}(0)\rho_{11}(0)\mathrm{e}^{2\gamma t} - |\rho_{01}(0)|^2}. \tag{35}$$

For a general two-qubit state, the calculation of QFIM requires the diagonalization of a 4 by 4 density matrix, which is difficult to solve analytically. However, some special two-qubit states, such as the X state, can be diagonalized analytically. An X state has the form (in the computational basis $\{|00\rangle, |01\rangle, |10\rangle, |11\rangle\}$) of

$$\rho = \begin{pmatrix} \rho_{00} & 0 & 0 & \rho_{03} \\ 0 & \rho_{11} & \rho_{12} & 0 \\ 0 & \rho_{21} & \rho_{22} & 0 \\ \rho_{30} & 0 & 0 & \rho_{33} \end{pmatrix}. \tag{36}$$

By changing the basis into $\{|00\rangle, |11\rangle, |01\rangle, |10\rangle\}$, this state can be rewritten in the block diagonal form as $\rho = \rho^{(0)} \oplus \rho^{(1)}$, where $\oplus$ represents the direct sum and

$$\rho^{(0)} = \begin{pmatrix} \rho_{00} & \rho_{03} \\ \rho_{30} & \rho_{33} \end{pmatrix}, \quad \rho^{(1)} = \begin{pmatrix} \rho_{11} & \rho_{12} \\ \rho_{21} & \rho_{22} \end{pmatrix}. \tag{37}$$

Note that $\rho^{(0)}$ and $\rho^{(1)}$ are not density matrices as their trace is not normalized. The QFIM for this block diagonal state can be written as $\mathcal{F}_{ab} = \mathcal{F}^{(0)}_{ab} + \mathcal{F}^{(1)}_{ab}$ [36], where $\mathcal{F}^{(0)}_{ab}$ ($\mathcal{F}^{(1)}_{ab}$) is the QFIM for $\rho^{(0)}$ ($\rho^{(1)}$). The eigenvalues of $\rho^{(i)}$ are $\lambda^{(i)}_{\pm} = \frac{1}{2}\left(\mathrm{Tr}\rho^{(i)} \pm \sqrt{\mathrm{Tr}^2\rho^{(i)} - 4\det\rho^{(i)}}\right)$ and corresponding eigenstates are

$$|\lambda_{\pm}^{(i)}\rangle = \mathcal{N}_{\pm}^{(i)}\left(\frac{1}{2\mathrm{Tr}(\rho^{(i)}\sigma_{+})}\left[\mathrm{Tr}\left(\rho^{(i)}\sigma_{z}\right) \pm \sqrt{\mathrm{Tr}^{2}\rho^{(i)} - 4\det\rho^{(i)}}\right], 1\right)^{\mathrm{T}}, \tag{38}$$

for non-diagonal $\rho^{(i)}$ with $\mathcal{N}_{\pm}^{(i)}$ $(i = 0, 1)$ the normalization coefficient. Here the specific form of σ_z and σ_+ are

$$\sigma_z = \begin{pmatrix} 1 & 0 \\ 0 & -1 \end{pmatrix}, \quad \sigma_+ = \begin{pmatrix} 0 & 1 \\ 0 & 0 \end{pmatrix}. \tag{39}$$

Based on above information, $\mathcal{F}_{ab}^{(i)}$ can be specifically written as

$$\begin{aligned}\mathcal{F}_{ab}^{(i)} = &\sum_{k=\pm}\frac{(\partial_a\lambda_k^{(i)})(\partial_b\lambda_k^{(i)})}{\lambda_k^{(i)}} + \lambda_k^{(i)}\mathcal{F}_{ab}\left(|\lambda_k^{(i)}\rangle\right) \\ &- \frac{16\det\rho^{(i)}}{\mathrm{Tr}\rho^{(i)}}\mathrm{Re}(\langle\partial_a\lambda_+^{(i)}|\lambda_-^{(i)}\rangle\langle\lambda_-^{(i)}|\partial_b\lambda_+^{(i)}\rangle),\end{aligned} \tag{40}$$

where $\mathcal{F}_{ab}(|\lambda_k^{(i)}\rangle)$ is the QFIM entry for the state $|\lambda_k^{(i)}\rangle$. For diagonal $\rho^{(i)}$, $|\lambda_{\pm}^{(i)}\rangle$ is just $(0, 1)^{\mathrm{T}}$ and only the classical contribution term remains in above equation.

2.3.4. Unitary processes. Unitary processes are the most fundamental dynamics in quantum mechanics since it can be naturally obtained via the Schrödinger equation. For a $\vec{x}$-dependent unitary process $U = U(\vec{x})$, the parameterized state ρ can be written as $\rho = U\rho_0 U^{\dagger}$, where ρ_0 is the initial probe state which is $\vec{x}$-independent. For such a process, the QFIM can be calculated via the following theorem.

Theorem 2.7. *For a unitary parametrization process U, the entry of QFIM can be obtained as [48]*

$$\begin{aligned}\mathcal{F}_{ab} = &\sum_{\eta_i\in\mathcal{S}} 4\eta_i\mathrm{cov}_{|\eta_i\rangle}(\mathcal{H}_a, \mathcal{H}_b) \\ &- \sum_{\eta_i,\eta_j\in\mathcal{S},i\neq j}\frac{8\eta_i\eta_j}{\eta_i+\eta_j}\mathrm{Re}\left(\langle\eta_i|\mathcal{H}_a|\eta_j\rangle\langle\eta_j|\mathcal{H}_b|\eta_i\rangle\right),\end{aligned} \tag{41}$$

where η_i and $|\eta_i\rangle$ are ith eigenvalue and eigenstate of the initial probe state ρ_0. $\mathrm{cov}_{|\eta_i\rangle}(\mathcal{H}_a, \mathcal{H}_b)$ is defined in equation (28). The operator $\mathcal{H}_a$ is defined as [49, 50]

$$\mathcal{H}_a := \mathrm{i}\left(\partial_a U^{\dagger}\right)U = -\mathrm{i}U^{\dagger}\left(\partial_a U\right). \tag{42}$$

$\mathcal{H}_a$ is a Hermitian operator for any parameter x_a due to above definition.

For the unitary processes, the parameterized state will remain pure for a pure probe state. The QFIM for this case is given as follows.

Corollary 2.7.1. *For a unitary process U with a pure probe state $|\psi_0\rangle$, the entry of QFIM is in the form*

$$\mathcal{F}_{ab} = 4\mathrm{cov}_{|\psi_0\rangle}(\mathcal{H}_a, \mathcal{H}_b), \tag{43}$$

where $\mathrm{cov}_{|\psi_0\rangle}(\mathcal{H}_a, \mathcal{H}_b)$ is defined by equation (28) and the QFI for x_a can then be obtained as $\mathcal{F}_{aa} = 4\mathrm{var}_{|\psi_0\rangle}(\mathcal{H}_a)$. Here $\mathrm{var}_{|\psi_0\rangle}(\mathcal{H}_a) := \mathrm{cov}_{|\psi_0\rangle}(\mathcal{H}_a, \mathcal{H}_a)$ is the variance of $\mathcal{H}_a$ on $|\psi_0\rangle$.

For a single-qubit mixed state ρ_0 under a unitary process, the QFIM can be written as

$$\mathcal{F}_{ab} = 4\left[2\mathrm{Tr}(\rho_0^2) - 1\right]\mathrm{cov}_{|\eta_0\rangle}(\mathcal{H}_a, \mathcal{H}_b) \tag{44}$$

with $|\eta_0\rangle$ an eigenstate of ρ_0. This equation is equivalent to

$$\mathcal{F}_{ab} = 4\left[2\mathrm{Tr}(\rho_0^2) - 1\right]\mathrm{Re}\left(\langle\eta_0|\mathcal{H}_a|\eta_1\rangle\langle\eta_1|\mathcal{H}_b|\eta_0\rangle\right). \tag{45}$$

The diagonal entry reads $\mathcal{F}_{aa} = 4\left[2\mathrm{Tr}(\rho_0^2) - 1\right]|\langle\eta_0|\mathcal{H}_a|\eta_1\rangle|^2$. Recall that theorem 2.6 provides the basis-independent formula for single-qubit mixed state, which leads to the next corollary.

Corollary 2.7.2. *For a single-qubit mixed state ρ_0 under a unitary process, the basis-independent formula of QFIM is*

$$\begin{aligned}\mathcal{F}_{ab} = {} & \mathrm{Tr}(\rho_0^2\{\mathcal{H}_a, \mathcal{H}_b\}) - 2\mathrm{Tr}(\rho_0\mathcal{H}_a\rho_0\mathcal{H}_b) \\ & + \frac{1}{\det\rho_0}\left[\mathrm{Tr}\left(\rho_0\mathcal{H}_a\rho_0\left\{\rho_0^2, \mathcal{H}_b\right\}\right) - 2\mathrm{Tr}(\rho_0^2\mathcal{H}_a\rho_0^2\mathcal{H}_b)\right].\end{aligned} \tag{46}$$

The diagonal entry reads

$$\begin{aligned}\mathcal{F}_{aa} = {} & 2\mathrm{Tr}(\rho_0^2\mathcal{H}_a^2) - 2\mathrm{Tr}[(\rho_0\mathcal{H}_a)^2] \\ & + \frac{2}{\det\rho_0}\left[\mathrm{Tr}\left(\rho_0\mathcal{H}_a\rho_0^3\mathcal{H}_a\right) - \mathrm{Tr}[(\rho_0^2\mathcal{H}_a)^2]\right].\end{aligned} \tag{47}$$

Under the unitary process, the QFIM for pure probe states, as given in equation (1), can be rewritten as

$$\mathcal{F}_{ab} = \frac{1}{2}\langle\psi_0|\left\{L_{a,\mathrm{eff}}, L_{b,\mathrm{eff}}\right\}|\psi_0\rangle, \tag{48}$$

where $L_{a,\mathrm{eff}} := U^\dagger L_a U$ can be treated as an effective SLD operator, which leads to the following theorem.

Theorem 2.8. *Given a unitary process, U, with a pure probe state, $|\psi_0\rangle$, the effective SLD operator $L_{a,\mathrm{eff}}$ can be obtained as*

$$L_{a,\mathrm{eff}} = \mathrm{i}2\left[\mathcal{H}_a, |\psi_0\rangle\langle\psi_0|\right]. \tag{49}$$

In equation (41), all the information of the parameters is involved in the operator set $\{\mathcal{H}_a\}$, which might benefit the analytical optimization of the probe state in some scenarios. Generally, the unitary operator can be written as $\exp(-\mathrm{i}tH)$ where $H = H(\vec{x})$ is a time-independent Hamiltonian for the parametrization. $\mathcal{H}_a$ can then be calculated as

$$\mathcal{H}_a = -\int_0^t \mathrm{e}^{\mathrm{i}sH}\left(\partial_a H\right)\mathrm{e}^{-\mathrm{i}sH}\mathrm{d}s, \tag{50}$$

where the technique $\partial_x \mathrm{e}^A = \int_0^1 \mathrm{e}^{sA}\partial_x A\mathrm{e}^{(1-s)A}\mathrm{d}s$ (A is an operator) is applied. Denote $H^\times(\cdot) := [H, \cdot]$, the expression above can be rewritten in an expanded form [48]

$$\mathcal{H}_a = -\sum_{n=0}^{\infty}\frac{t^{n+1}}{(n+1)!}\left(\mathrm{i}H^\times\right)^n\partial_a H. \tag{51}$$

In some scenarios, the recursive commutations in expression above display certain patterns, which can lead to analytic expressions for the $\mathcal{H}$ operator. The simplest example is $H = \sum_a x_a H_a$, with all H_a commute with each other. In this case $\mathcal{H}_a = -tH_a$ since only the zeroth order term in equation (51) is nonzero. Another example is the interaction of a collective spin system with a magnetic field with the Hamiltonian $H = -BJ_{\vec{n}_0}$, where B is the amplitude of the external magnetic field, $J_{\vec{n}_0} = \vec{n}_0 \cdot \vec{J}$ with $\vec{n}_0 = (\cos\theta, 0, \sin\theta)$ and $\vec{J} = (J_x, J_y, J_z)$. θ is the angle between the field and the collective spin. $J_i = \sum_k \sigma_i^{(k)}/2$ for $i = x, y, z$ is the collective spin operator. $\sigma_i^{(k)}$ is the Pauli matrix for kth spin. In this case, the $\mathcal{H}$ operator for θ can be analytically calculated via equation (51), which is [48]

$$\mathcal{H}_\theta = -2\sin\left(\frac{1}{2}Bt\right) J_{\vec{n}_1}, \tag{52}$$

where $J_{n_1} = \vec{n}_1 \cdot \vec{J}$ with $\vec{n}_1 = (\cos(Bt/2)\sin\theta, \sin(Bt/2), -\cos(Bt/2)\cos\theta)$.

Recently, Sidhu and Kok [51, 52] use this $\mathcal{H}$-representation to study the spatial deformations, epecially the grid deformations of classical and quantum light emitters. By calculating and analyzing the QFIM, they showed that the higher average mode occupancies of the classical states performs better in estimating the deformation when compared with single photon emitters.

An alternative operator that can be used to characterize the precision limit of unitary process is [50, 53, 54]

$$\mathcal{K}_a := \mathrm{i}\left(\partial_a U\right) U^\dagger = -\mathrm{i}U\left(\partial_a U^\dagger\right). \tag{53}$$

As a matter of fact, this operator is the infinitesimal generator of U of parameter x_a. Assume $\vec{x}$ is shifted by $\mathrm{d}x_a$ along the direction of x_a and other parameters are kept unchanged. Then $U(\vec{x} + \mathrm{d}x_a)$ can be expanded as $U(\vec{x} + \mathrm{d}x_a)\partial_a U(\vec{x})$. The density matrix $\rho_{\vec{x}+\mathrm{d}x_a}$ can then be approximately calculated as $\rho_{\vec{x}+\mathrm{d}x_a} = \mathrm{e}^{-\mathrm{i}\mathcal{K}_a \mathrm{d}x_a}\rho\mathrm{e}^{\mathrm{i}\mathcal{K}_a \mathrm{d}x_a}$ [53], which indicates that $\mathcal{K}_a$ is the generator of U along parameter x_a. The relation between $\mathcal{H}_a$ and $\mathcal{K}_a$ can be easily obtained as

$$\mathcal{K}_a = -U\mathcal{H}_a U^\dagger. \tag{54}$$

With this relation, the QFIM can be easily rewritten with $\mathcal{K}_a$ as

$$\begin{aligned}\mathcal{F}_{ab} = &\sum_{\lambda_i \in \mathcal{S}} 4\lambda_i \mathrm{cov}_{|\lambda_i\rangle}(\mathcal{K}_a, \mathcal{K}_b) \\ &- \sum_{\lambda_i, \lambda_j \in \mathcal{S}, i \neq j} \frac{8\lambda_i\lambda_j}{\lambda_i + \lambda_j} \mathrm{Re}\left(\langle\lambda_i|\mathcal{K}_a|\lambda_j\rangle\langle\lambda_j|\mathcal{K}_b|\lambda_i\rangle\right),\end{aligned} \tag{55}$$

where $|\lambda_i\rangle = U|\eta_i\rangle$ is the ith eigenstate of the parameterized state ρ. And $\mathrm{cov}_{|\lambda_i\rangle}(\mathcal{K}_a, \mathcal{K}_b)$ is defined by equation (28). The difference between the calculation of QFIM with $\{\mathcal{K}_a\}$ and $\{\mathcal{H}_a\}$ is that the expectation is taken with the eigenstate of the probe state ρ_0 for the use of $\{\mathcal{H}_a\}$ but with the parameterized state ρ for $\{\mathcal{K}_a\}$. For a pure probe state $|\psi_0\rangle$, the expression above reduces to $\mathcal{F}_{ab} = 4\mathrm{cov}_{|\psi\rangle}(\mathcal{K}_a, \mathcal{K}_b)$ with $|\psi\rangle = U|\psi_0\rangle$. Similarly, for a mixed state of single qubit, the QFIM reads $\mathcal{F}_{ab} = 4\left(2\mathrm{Tr}\rho_0^2 - 1\right)\mathrm{cov}_{|\lambda_0\rangle}(\mathcal{K}_a, \mathcal{K}_b)$.

2.3.5. Gaussian states. Gaussian state is a widely-used quantum state in quantum physics, particularly in quantum optics, quantum metrology and continuous variable quantum information processes. Consider a m-mode bosonic system with a_i ($a_i^\dagger$) as the annihilation (creation) operator for the ith mode. The quadrature operators are [55, 56] $\hat{q}_i := \frac{1}{\sqrt{2}}(a_i + a_i^\dagger)$ and

$\hat{p}_i := \frac{1}{i\sqrt{2}}(a_i - a_i^\dagger)$, which satisfy the commutation relation $[\hat{q}_i, \hat{p}_j] = \mathrm{i}\delta_{ij}$ ($\hbar = 1$). A vector of quadrature operators, $\vec{R} = (\hat{q}_1, \hat{p}_1, ..., \hat{q}_m, \hat{p}_m)^{\mathrm{T}}$ satisfies

$$[R_i, R_j] = \mathrm{i}\Omega_{ij} \tag{56}$$

for any i and j where Ω is the symplectic matrix defined as $\Omega := \mathrm{i}\sigma_y^{\oplus m}$ where $\oplus$ denote the direct sum. Now we introduce the covariance matrix $C(\vec{R})$ with the entries defined as $C_{ij} := \mathrm{cov}_\rho(R_i, R_j) = \frac{1}{2}\mathrm{Tr}(\rho\{R_i, R_j\}) - \mathrm{Tr}(\rho R_i)\mathrm{Tr}(\rho R_j)$. C satisfies the uncertainty relation $C + \frac{\mathrm{i}}{2}\Omega \geqslant 0$ [57, 58]. According to the Williamson's theorem, the covariance matrix can be diagonalized utilizing a symplectic matrix S [58, 59], i.e.

$$C = SC_{\mathrm{d}}S^{\mathrm{T}}, \tag{57}$$

where $C_{\mathrm{d}} = \bigoplus_{k=1}^{m} c_k \mathbb{1}_2$ with c_k the kth symplectic eigenvalue and $\mathbb{1}_2$ is a 2-dimensional identity matrix. S is a $2m$-dimensional real matrix which satisfies $S\Omega S^{\mathrm{T}} = \Omega$.

A very useful quantity for Gaussian states is the characteristic function

$$\chi(\vec{s}) = \mathrm{Tr}\left(\rho\, \mathrm{e}^{\mathrm{i}\vec{R}^{\mathrm{T}}\Omega\vec{s}}\right), \tag{58}$$

where $\vec{s}$ is a $2m$-dimensional real vector. Another powerful function is the Wigner function, which can be obtained by taking the Fourier transform of the characteristic function

$$W(\vec{R}) = \frac{1}{(2\pi)^{2m}} \int_{\mathbb{R}^{2m}} \mathrm{e}^{-\mathrm{i}\vec{R}^{\mathrm{T}}\Omega\vec{s}}\, \chi(\vec{s})\, \mathrm{d}^{2m}\vec{s}. \tag{59}$$

Considering the scenario with first and second moments, a state is a Gaussian state if $\chi(\vec{s})$ and $W(\vec{R})$ are Gaussian, i.e. [55, 56, 58, 60, 61]

$$\chi(\vec{s}) = \mathrm{e}^{-\frac{1}{2}\vec{s}^{\mathrm{T}}\Omega C\Omega^{\mathrm{T}}\vec{s} - \mathrm{i}(\Omega\langle\vec{R}\rangle)^{\mathrm{T}}\vec{s}}, \tag{60}$$

$$W(\vec{R}) = \frac{1}{(2\pi)^m\sqrt{\det C}} \mathrm{e}^{-\frac{1}{2}\left(\vec{R}-\langle\vec{R}\rangle\right)^{\mathrm{T}}C^{-1}\left(\vec{R}-\langle\vec{R}\rangle\right)}, \tag{61}$$

where $\langle\vec{R}\rangle_j = \mathrm{Tr}(R_j\rho)$ is the first moment. A pure state is Gaussian if and only if its Wigner function is non-negative [58].

The study of QFIM for Gaussian states started from the research of QFI. The expression of QFI was first given in 2013 by Monras for the multi-mode case [62] and Pinel *et al* for the single-mode case [63]. In 2018, Nichols *et al* [65] and Šafránek [66] provided the expression of QFIM for multi-mode Gaussian states independently, which was obtained based on the calculation of SLD [7]. The SLD operator for Gaussian states has been given in [62, 65, 67], and we organize the corresponding results in the following theorem.

Theorem 2.9. *For a continuous variable bosonic m-mode Gaussian state with the displacement vector (first moment) $\langle\vec{R}\rangle$ and the covariance matrix (second moment) C, the SLD operator is [62, 64–67, 69]*

$$L_a = L_a^{(0)}\mathbb{1}_{2m} + \vec{L}_a^{(1),\mathrm{T}}\vec{R} + \vec{R}^{\mathrm{T}}G_a\vec{R}, \tag{62}$$

where $\mathbb{1}_{2m}$ is the 2m-dimensional identity matrix and the coefficients read

$$G_a = \sum_{j,k=1}^{m}\sum_{l=0}^{3} \frac{g_l^{(jk)}}{4c_jc_k + (-1)^{l+1}} \left(S^{\mathrm{T}}\right)^{-1} A_l^{(jk)} S^{-1}, \tag{63}$$

$$\vec{L}_a^{(1)} = C^{-1}(\partial_a\langle\vec{R}\rangle) - 2G_a\langle\vec{R}\rangle, \tag{64}$$

$$L_a^{(0)} = \langle\vec{R}\rangle^{\mathrm{T}} G_a\langle\vec{R}\rangle - (\partial_a\langle\vec{R}\rangle)^{\mathrm{T}} C^{-1}\langle\vec{R}\rangle - \mathrm{Tr}(G_a C). \tag{65}$$

Here

$$A_l^{(jk)} = \frac{1}{\sqrt{2}}\mathrm{i}\sigma_y^{(jk)},\ \frac{1}{\sqrt{2}}\sigma_z^{(jk)},\ \frac{1}{\sqrt{2}}\mathbb{1}_2^{(jk)},\ \frac{1}{\sqrt{2}}\sigma_x^{(jk)} \tag{66}$$

for $l = 0, 1, 2, 3$ *and* $g_l^{(jk)} = \mathrm{Tr}[S^{-1}(\partial_a C)(S^{\mathrm{T}})^{-1}A_l^{(jk)}]$. $\sigma_i^{(jk)}$ *is a* $2m$*-dimensional matrix with all the entries zero expect a* 2×2 *block, shown as below*

$$\sigma_i^{(jk)} = \begin{pmatrix} & 1\mathrm{st} & \cdots & k\mathrm{th} & \cdots \\ 1\mathrm{st} & 0_{2\times 2} & 0_{2\times 2} & 0_{2\times 2} & 0_{2\times 2} \\ \vdots & 0_{2\times 2} & \vdots & \vdots & \vdots \\ j\mathrm{th} & 0_{2\times 2} & \cdots & \sigma_i & \cdots \\ \vdots & \vdots & \vdots & \vdots & \vdots \end{pmatrix}, \tag{67}$$

where $0_{2\times 2}$ *represents a 2 by 2 block with zero entries.* $\mathbb{1}_2^{(jk)}$ *is similar to* $\sigma_i^{(jk)}$ *but replace the block* σ_i *with* $\mathbb{1}_2$[9].

Being aware of the expression of SLD operator given in theorem 2.9, the QFIM can be calculated via equation (1). Here we show the result explicitly in following theorem.

Theorem 2.10. *For a continuous variable bosonic m-mode Gaussian state with the displacement vector (first moment)* $\langle\vec{R}\rangle$ *and the covariance matrix (second moment) C, the entry of QFIM can be expressed by [64–66]*

$$\mathcal{F}_{ab} = \mathrm{Tr}\left(G_a\partial_b C\right) + (\partial_a\langle\vec{R}\rangle^{\mathrm{T}})C^{-1}\partial_b\langle\vec{R}\rangle, \tag{68}$$

and the QFI for an m-mode Gaussian state with respect to x_a *can be immediately obtained as [62]*

$$\mathcal{F}_{aa} = \mathrm{Tr}\left(G_a\partial_a C\right) + (\partial_a\langle\vec{R}\rangle^{\mathrm{T}})C^{-1}\partial_a\langle\vec{R}\rangle. \tag{69}$$

The expression of right logarithmic derivative for a general Gaussian state and the corresponding QFIM was provided by Gao and Lee [64] in 2014, which is an appropriate tool for the estimation of complex numbers [25], such as the number α of a coherent state $|\alpha\rangle$. The simplest case is a single-mode Gaussian state. For such a state, G_a can be calculated as following.

Corollary 5. *For a single-mode Gaussian state* G_a *can be expressed as*[10]

$$G_a = \frac{4c^2-1}{4c^2+1}\Omega(\partial_a J)\Omega, \tag{70}$$

where $c = \sqrt{\det C}$ *is the symplectic eigenvalue of C and*

[9] The derivation of this theorem is in appendix E.1.
[10] The derivation of this corollary is in appendix E.2.

$$J = \frac{1}{4c^2 - 1} C. \tag{71}$$

For pure states, $\det \boldsymbol{C}$ *is a constant,* G_a *then reduces to*

$$G_a = \frac{1}{4c^2 + 1} \Omega(\partial_a C)\Omega. \tag{72}$$

From this G_a, $\vec{L}_a^{(1)}$ and $L_a^{(0)}$ can be further obtained, which can be used to obtain the SLD operator via equation (62) and the QFIM via equation (68).

Another widely used method to obtain the QFI for Gaussian states is through the fidelity (see section 2.4.2 for the relation between fidelity and QFIM). The QFI for pure Gaussian states is studied in [68]. The QFI for single-mode Gaussian states has been obtained through the fidelity by Pinel *et al* in [63], and for two-mode Gaussian states by Šafránek *et al* in [69] and Marian *et al* [70] in 2016, based on the expressions of the fidelity given by Scutaru [71] and Marian *et al* in [72]. The expressions of the QFI and the fidelity for multi-mode Gaussian states are given by Monras [62], Safranek *et al* [69] and Banchi *et al* [73], and reproduced by Oh *et al* [74] with a Hermitian operator related to the optimal measurement of the fidelity.

There are other approaches, such as the exponential state [76], Husimi Q function [77], that can obtain the QFI and the QFIM for some specific types of Gaussian states. Besides, a general method to find the optimal probe states to optimize the QFIM of Gaussian unitary channels is also provided by Šafránek and Fuentes in [78], and Matsubara *et al* [75] in 2019. Matsubara *et al* performed the optimization of the QFI for Gaussian states in a passive linear optical circuit. For a fixed total photon number, the optimal Gaussian state is proved to be a single-mode squeezed vacuum state and the optimal measurement is a homodyne measurement.

2.4. QFIM and geometry of quantum mechanics

2.4.1. Fubini-study metric. In quantum mechanics, the pure states is a normalized vector because of the basic axiom that the norm square of its amplitude represents the probability. The pure states thus can be represented as rays in the projective Hilbert space, on which Fubini–Study metric is a Kähler metric. The squared infinitesimal distance here is usually expressed as [79]

$$\mathrm{d}s^2 = \frac{\langle \mathrm{d}\psi | \mathrm{d}\psi \rangle}{\langle \psi | \psi \rangle} - \frac{\langle \mathrm{d}\psi | \psi \rangle \langle \psi | \mathrm{d}\psi \rangle}{\langle \psi | \psi \rangle^2}. \tag{73}$$

As $\langle \psi | \psi \rangle = 1$ and $|\mathrm{d}\psi\rangle = \sum_\mu |\partial_{x_\mu} \psi\rangle \mathrm{d}x_\mu$, $\mathrm{d}s^2$ can be expressed as

$$\mathrm{d}s^2 = \sum_{\mu\nu} \frac{1}{4} \mathcal{F}_{\mu\nu} \mathrm{d}x_\mu \mathrm{d}x_\nu, \tag{74}$$

here $\mathcal{F}_{\mu\nu}$ is the $\mu\nu$ element of the QFIM. This means the Fubini–Study metric is a quarter of the QFIM for pure states. This is the intrinsic reason why the QFIM can depict the precision limit. Intuitively, the precision limit is just a matter of distinguishability. The best precision means the maximum distinguishability, which is naturally related to the distance between the states. The counterpart of Fubini-study metric for mixed states is the Bures metric, a well-known metric in quantum information and closely related to the quantum fidelity, which will be discussed below.

2.4.2. Fidelity and Bures metric. In quantum information, the fidelity $f(\rho_1, \rho_2)$ quantifies the similarity between two quantum states ρ_1 and ρ_2, which is defined as [80]

$$f(\rho_1, \rho_2) := \mathrm{Tr}\sqrt{\sqrt{\rho_1}\rho_2\sqrt{\rho_1}}. \tag{75}$$

Here $f \in [0, 1]$ and $f = 1$ only when $\rho_1 = \rho_2$. Although the fidelity itself is not a distance measure, it can be used to construct the Bures distance, denoted as D_B, as [80]

$$D_\mathrm{B}^2(\rho_1, \rho_2) = 2 - 2f(\rho_1, \rho_2). \tag{76}$$

The relationship between the fidelity and the QFIM has been well studied in the literature [30, 31, 81–84]. In the case that the rank of $\rho(\vec{x})$ is unchanged with the varying of $\vec{x}$, the QFIM is related to the infinitestmal Bures distance in the same way as the QFIM related to the Fubini-study metric[11]

$$D_\mathrm{B}^2(\rho(\vec{x}), \rho(\vec{x} + \mathrm{d}\vec{x})) = \frac{1}{4}\sum_{\mu\nu}\mathcal{F}_{\mu\nu}\mathrm{d}x_\mu\mathrm{d}x_\nu. \tag{77}$$

In recent years it has been found that the fidelity susceptibility, the leading order (the second order) of the fidelity, can be used as an indicator of the quantum phase transitions [18]. Because of this deep connection between the Bures metric and the QFIM, it is not surprising that the QFIM can be used in a similar way. On the other hand, the enhancement of QFIM at the critical point indicates that the precision limit of the parameter can be improved near the phase transition, as shown in [85, 86].

In the case that the rank of $\rho(\vec{x})$ does not equal to that of $\rho(\vec{x} + \mathrm{d}\vec{x})$, Šafránek recently showed [87] that the QFIM does not exactly equal to the fidelity susceptibility. Later, Seveso *et al* further suggested [88] that the quantum Cramér–Rao bound may also fail at those points.

Besides the Fubini–Study metric and the Bures metric, the QFIM is also closely connected to the Riemannian metric due to the fact that the state space of a quantum system is actually a Riemannian manifold. In more concrete terms, the QFIM belongs to a family of contractive Riemannian metric [24, 26, 89, 90], associated with which the infinitesimal distance in state space is $\mathrm{d}s^2 = \sum_\mu g_{\mu\nu}\mathrm{d}x_\mu\mathrm{d}x_\nu$ with $g_{\mu\nu}$ as the contractive Riemannian metric. In the eigenbasis of the density matrix ρ, $g_{\mu\nu}$ takes the form as [91–93]

$$g_{\mu\nu} = \frac{1}{4}\sum_i \frac{\langle\lambda_i|\mathrm{d}\rho|\lambda_i\rangle^2}{\lambda_i} + \frac{1}{2}\sum_{i<j}\frac{|\langle\lambda_i|\mathrm{d}\rho|\lambda_j\rangle|^2}{\lambda_j h(\lambda_i/\lambda_j)}, \tag{78}$$

where $h(\cdot)$ is the Morozova–Čencov function, which is an operator monotone (for any positive semi-definite operators), self inverse ($xh(1/x) = 1/h(x)$) and normalized ($h(1) = 1$) real function. When $h(x) = (1 + x)/2$, the metric above reduces to the QFIM (based on the SLD). The QFIMs based on right and left logarithmic derivatives can also be obtained by taking $h(x) = x$ and $h(x) = 1$. The Wigner–Yanase information metric can be obtained from it by taking $h(x) = \frac{1}{4}(\sqrt{x} + 1)^2$.

2.4.3. Quantum geometric tensor. The quantum geometric tensor originates from a complex metric in the projective Hilbert space, and is a powerful tool in quantum information science that unifies the QFIM and the Berry connection. For a pure state $|\psi\rangle = |\psi(\vec{x})\rangle$, the quantum geometric tensor Q is defined as [23, 95]

[11] The derivation is given in appendix F.

$$Q_{\mu\nu} = \langle\partial_\mu\psi|\partial_\nu\psi\rangle - \langle\partial_\mu\psi|\psi\rangle\langle\psi|\partial_\nu\psi\rangle. \tag{79}$$

Recall the expression of QFIM for pure states, given in equation (25), the real part of $Q_{\mu\nu}$ is actually the QFIM up to a constant factor, i.e.

$$\mathrm{Re}(Q_{\mu\nu}) = \frac{1}{4}\mathcal{F}_{\mu\nu}. \tag{80}$$

In the mean time, due to the fact that

$$(\langle\partial_\mu\psi|\psi\rangle\langle\psi|\partial_\nu\psi\rangle)^* = \langle\psi|\partial_\mu\psi\rangle\langle\partial_\nu\psi|\psi\rangle = \langle\partial_\mu\psi|\psi\rangle\langle\psi|\partial_\nu\psi\rangle, \tag{81}$$

i.e. $\langle\partial_\mu\psi|\psi\rangle\langle\psi|\partial_\nu\psi\rangle$ is real, the imaginary part of $Q_{\mu\nu}$ then reads

$$\mathrm{Im}(Q_{\mu\nu}) = \mathrm{Im}(\langle\partial_\mu\psi|\partial_\nu\psi\rangle) = -\frac{1}{2}\left(\partial_\mu\mathcal{A}_\nu - \partial_\nu\mathcal{A}_\mu\right), \tag{82}$$

where $\mathcal{A}_\mu := \mathrm{i}\langle\psi|\partial_\mu\psi\rangle$ is the Berry connection [96] and $\Upsilon_{\mu\nu} := \partial_\mu\mathcal{A}_\nu - \partial_\nu\mathcal{A}_\mu$ is the Berry curvature. The geometric phase can then be obtained as [97]

$$\phi = \oint \mathcal{A}_\mu \mathrm{d}x_\mu, \tag{83}$$

where the integral is taken over a closed trajectory in the parameter space.

Recently, Guo *et al* [98] connected the QFIM and the Berry curvature via the Robertson uncertainty relation. Specifically, for a unitary process with two parameters, $\Upsilon_{\mu\nu} = \mathrm{i}\langle\psi_0|[\mathcal{H}_\mu, \mathcal{H}_\nu]|\psi_0\rangle$ with $\mathcal{H}_\mu$ defined in equation (42) and $|\psi_0\rangle$ the probe state, the determinants of the QFIM and the Berry curvature should satisfy

$$\det\mathcal{F} + 4\det\Upsilon \geqslant 0. \tag{84}$$

2.5. QFIM and thermodynamics

The density matrix of a quantum thermal state is

$$\rho = \frac{1}{Z}\mathrm{e}^{-\beta H}, \tag{85}$$

where $Z = \mathrm{Tr}(\mathrm{e}^{-\beta H})$ is the partition function and $\beta = 1/(k_\mathrm{B}T)$. k_B is the Boltzmann constant and T is the temperature. For such state we have $\partial_T\rho = \frac{1}{T^2}\left(\langle H\rangle - H\right)\rho$, where we have set $k_\mathrm{B} = 1$. If we take the temperature as the unknown parameter, the SLD, which is the solution to $\partial_T\rho = \frac{1}{2}(\rho L_T + L_T\rho)$, can then be obtained as

$$L_T = \frac{1}{T^2}\left(\langle H\rangle - H\right), \tag{86}$$

which commutes with ρ. The QFI for the temperature hence reads

$$\mathcal{F}_{TT} = \frac{1}{T^4}(\langle H^2\rangle - \langle H\rangle^2), \tag{87}$$

i.e. $\mathcal{F}_{TT}$ is proportional to the fluctuation of the Hamiltonian. Compared to the specific heat $C_v = \frac{\partial_T\langle H\rangle}{\partial T} = \frac{1}{T^2}(\langle H^2\rangle - \langle H\rangle^2)$, we have [18, 82, 99–101]

$$\mathcal{F}_{TT} = \frac{1}{T^2}C_v, \tag{88}$$

i.e. for a quantum thermal state, the QFI for the temperature is proportional to the specific heat of this system. For a system of which the Hamiltonian has no interaction terms, the relation above still holds for its subsystems [102].

The correlation function is an important concept in quantum physics and condensed matter physics due to the wide applications of the linear response theory. It is well known that the static susceptibility between two observables A and B, which represents the influence of $\langle A\rangle$'s perturbation on $\langle B\rangle$ under the thermal equilibrium, is proportional to the canonical correlation $\frac{1}{\beta}\int_0^\beta \frac{1}{Z}\mathrm{Tr}(\mathrm{e}^{-\beta H}\mathrm{e}^{sH}A\mathrm{e}^{-sH}B)\mathrm{d}s$ [103], which can be further written into $\int_0^1 \mathrm{Tr}(\rho^s A\rho^{1-s}B)\mathrm{d}s$. Denote $\int_0^1 \rho^s\tilde{L}_a\rho^{1-s}\mathrm{d}s = \partial_a\rho$ and replace A, B with $\tilde{L}_a$ and $\tilde{L}_b$, the canonical correlation reduces to the so-called Bogoliubov–Kubo–Mori Fisher information matrix $\int_0^1 \rho^s\tilde{L}_a\rho^{1-s}\tilde{L}_b\mathrm{d}s$ [27, 104–107]. However, this relation does not suggest how to connect the linear response function with the QFIM based on SLD. In 2007, You *et al* [18, 108] first studied the connection between the fidelity susceptibility and the correlation function, and then in 2016, Hauke *et al* [109] extended this connection between the QFI and the symmetric and asymmetric correlation functions to the thermal states. Here we use their methods to establish the relation between the QFIM and the cross-correlation functions.

Consider a thermal state corresponding to the Hamiltonian $H = \sum_a x_a O_a$, where O_a is a Hermitian generator for x_a and $[O_a, O_b] = 0$ for any a and b, the QFIM can be expressed as[12]

$$\mathcal{F}_{ab} = \frac{4}{\pi}\int_{-\infty}^{\infty}\tanh^2\left(\frac{\omega}{2T}\right)\mathrm{Re}(S_{ab}(\omega))\mathrm{d}\omega, \tag{89}$$

or equivalently,

$$\mathcal{F}_{ab} = \frac{4}{\pi}\int_{-\infty}^{\infty}\tanh\left(\frac{\omega}{2T}\right)\mathrm{Im}(\chi_{ab}(\omega))\mathrm{d}\omega. \tag{90}$$

Here $S_{ab}(\omega)$ is the symmetric cross-correlation spectrum defined as

$$S_{ab}(\omega) = \int_{-\infty}^{\infty}\frac{1}{2}\langle\{Q_a(t), O_b\}\rangle\mathrm{e}^{\mathrm{i}\omega t}\mathrm{d}t, \tag{91}$$

where $\langle\cdot\rangle = \mathrm{Tr}(\rho\cdot)$ and $O_{a(b)}(t) = \mathrm{e}^{\mathrm{i}Ht}O_{a(b)}\mathrm{e}^{-\mathrm{i}Ht}$. Its real part can also be written as

$$\mathrm{Re}(S_{ab}(\omega)) = \int_{-\infty}^{\infty}\frac{1}{2}\langle Q_a(t)O_b + O_b(t)O_a\rangle\mathrm{e}^{\mathrm{i}\omega t}\mathrm{d}t. \tag{92}$$

χ_{ab} is the asymmetric cross-correlation spectrum defined as

$$\chi_{ab}(\omega) = \int_{-\infty}^{\infty}\frac{\mathrm{i}}{2}\langle[O_a(t), O_b]\rangle\mathrm{e}^{\mathrm{i}\omega t}\mathrm{d}t. \tag{93}$$

Because of equations (89) and (90), and the fact that $S_{ab}(\omega)$ and $\chi_{ab}(\omega)$ can be directly measured in the experiments [110–114], $\mathcal{F}_{ab}$ becomes measurable in this case, which breaks the previous understanding that QFI is not observable since the fidelity is not observable. Furthermore, due to the fact that the QFI is a witness for multipartite entanglement [22], and a large QFI can imply Bell correlations [115], equations (89) and (90) provide an experimentally-friendly way to witness the quantum correlations in the thermal systems. As a matter of fact, Shitara and Ueda [94] showed that the relations in equations (89) and (90) can be

[12] The details of the derivation can be found in appendix G.

further extended to the family of metric described in equation (78) by utilizing the generalized fluctuation-dissipation theorem.

2.6. QFIM in quantum dynamics

Quantum dynamics is not only a fundamental topic in quantum mechanics, but also widely connected to various topics in quantum information and quantum technology. Due to some excellent mathematical properties, the QFIM becomes a good candidate for the characterization of certain behaviors and phenomena in quantum dynamics. In the following we show the roles of QFIM in quantum speed limit and the characterization of non-Markovianity.

2.6.1. Quantum speed limit. Quantum speed limit aims at obtaining the smallest evolution time for quantum processes [6, 49, 93, 116–121]. It is closely related to the geometry of quantum states since the dynamical trajectory with the minimum evolution time is actually the geodesic in the state space, which indicates that the QFIM should be capable to quantify the speed limit. As a matter of fact, the QFI and the QFIM have been used to bound the quantum speed limit in recent studies [6, 49, 116, 117]. For a unitary evolution, $U = \exp(-\mathrm{i}Ht)$, to steer a state away from the initial position with a Bures angle $D_{\mathrm{B}} = \arccos(f)$ (f is the fidelity defined in equation (75)), the evolution time t needs to satisfy [6, 49, 122]

$$t \geqslant \frac{2D_{\mathrm{B}}}{\sqrt{\mathcal{F}_{tt}}}, \tag{94}$$

where $\mathcal{F}_{tt}$ is the QFI for the time t. For a more general case, that the Hamiltonian is time-dependent, Taddei *et al* [49] provided an implicit bound based on the QFI,

$$\sqrt{\frac{1}{2}\frac{\mathrm{d}^2\mathcal{D}(f)}{\mathrm{d}f^2}\left(\frac{\mathrm{d}\mathcal{D}}{\mathrm{d}f}\right)^{-3}}\Bigg|_{f\to 1} \mathcal{D}(f(\rho(0),\rho(t))) \leqslant \int_0^t \sqrt{\frac{\mathcal{F}_{\tau\tau}}{4}}\mathrm{d}\tau, \tag{95}$$

where $\mathcal{D}$ is any metric on the space of quantum states via the fidelity f. In 2017, Beau and del Campo [123] discussed the nonlinear metrology of many-body open systems and established the relation between the QFI for coupling constants and the quantum speed limit, which indicates that the quantum speed limit directly determines the amplitude of the estimation error in such cases.

Recently, Pires *et al* [93] established an infinite family of quantum speed limits based on a contractive Riemannian metric discussed in section 2.4.2. In the case that $\vec{x}$ is time-dependent, i.e. $\vec{x} = \vec{x}(t)$, the geodesic distance $D(\rho_0, \rho_t)$ gives a lower bound of general trajectory,

$$D(\rho_0,\rho_t) \leqslant \int_0^t \left(\frac{\mathrm{d}s}{\mathrm{d}t}\right)\mathrm{d}t = \int_0^t \mathrm{d}t\sqrt{\sum_{\mu\nu} g_{\mu\nu}\frac{\mathrm{d}x_\mu}{\mathrm{d}t}\frac{\mathrm{d}x_\nu}{\mathrm{d}t}}, \tag{96}$$

where $g_{\mu\nu}$ is defined in equation (78). Taking the maximum Morozova–Čencov function, the above inequality leads to the quantum speed limit with time-dependent parameters given in [49].

2.6.2. Non-Markovianity. Non-Markovianity is an emerging concept in open quantum systems. Many different quantification of the non-Markovianity based on monotonic quantities under the completely positive and trace-preserving maps have been proposed [124–126]. The QFI can also be used to characterize the non-Markovianity since it also satisfies the monotonicity [6]. For the master equation

$$\partial_t \rho = -\mathrm{i}[H_{\vec{x}}, \rho] + \sum_j \gamma_j(t) \left(\Gamma_j \rho \Gamma_j^\dagger - \frac{1}{2} \left\{ \Gamma_j^\dagger \Gamma_j, \rho \right\} \right), \tag{97}$$

the quantum Fisher information flow

$$\partial_t \mathcal{F}_{aa} = -\sum_j \gamma_j(t) \mathrm{Tr} \left(\rho [L_a, \Gamma_j]^\dagger [L_a, \Gamma_j] \right) \tag{98}$$

given by Lu *et al* [127] in 2010 is a valid witness for non-Markovianity. Later in 2015, Song *et al* [128] utilized the maximum eigenvalue of average QFIM flow to construct a quantitative measure of non-Markovianity. The average QFIM flow is the time derivative of average QFIM $\bar{\mathcal{F}} = \int \mathcal{F} \mathrm{d}\vec{x}$. Denote $\lambda_{\max}(t)$ as the maximum eigenvalue of $\partial_t \bar{\mathcal{F}}$ at time t, then the non-Markovianity can be alternatively defined as

$$\mathcal{N} := \int_{\lambda_{\max}>0} \lambda_{\max} \mathrm{d}t. \tag{99}$$

One may notice that this is not the only way to define non-Makovianity with the QFIM, similar constructions would also be qualified measures for non-Markovianity.

3. Quantum multiparameter estimation

3.1. Quantum multiparameter Cramér–Rao bound

3.1.1. Introduction. The main application of the QFIM is in the quantum multiparameter estimation, which has shown very different properties and behaviors compared to its single-parameter counterpart [16]. The quantum multiparameter Cramér–Rao bound, also known as Helstrom bound, is one of the most widely used asymptotic bound in quantum metrology [1, 2].

Theorem 3.1. *For a density matrix ρ in which a vector of unknown parameters $\vec{x} = (x_0, x_1, ..., x_m, ...)^{\mathrm{T}}$ is encoded, the covariance matrix $\mathrm{cov}(\hat{\vec{x}}, \{\Pi_y\})$ of an unbiased estimator $\hat{\vec{x}}$ under a set of POVM, $\{\Pi_y\}$, satisfies the following inequality*[13]

$$\mathrm{cov}(\hat{\vec{x}}, \{\Pi_y\}) \geqslant \frac{1}{n} \mathcal{I}^{-1}(\{\Pi_y\}) \geqslant \frac{1}{n} \mathcal{F}^{-1}, \tag{100}$$

where $\mathcal{I}(\{\Pi_y\})$ is the CFIM, $\mathcal{F}$ is the QFIM and n is the repetition of the experiment.

The second inequality is called the quantum multiparameter Cramér–Rao bound. In the derivation, we assume the QFIM can be inverted, which is reasonable since a singular QFIM usually means not all the unknown parameters are independent and the parameters cannot be estimated simultaneously. In such cases one should first identify the set of parameters that are independent, then calculate the corresponding QFIM for those parameters.

For cases where the number of unknown parameters is large, it may be difficult or even meaningless to know the error of every parameter, and the total variance or the average variance is a more appropriate macroscopic quantity to study. Recall that the ath diagonal entry of the covariance matrix is actually the variance of the parameter x_a. Thus, the bound for the total variance can be immediately obtained as following.

[13] The derivation of this theorem is given in appendix H.

Corollary 3.1.1. *Denote* $\mathrm{var}(\hat{x}_a, \{\Pi_y\})$ *as the variance of* x_a*, then the total variance* $\sum_a \mathrm{var}(x_a, \{\Pi_y\})$ *is bounded by the trace of* $\mathcal{F}^{-1}$*, i.e.*

$$\sum_a \mathrm{var}(\hat{x}_a, \{\Pi_y\}) \geqslant \frac{1}{n}\mathrm{Tr}\left(\mathcal{I}^{-1}(\{\Pi_y\})\right) \geqslant \frac{1}{n}\mathrm{Tr}\left(\mathcal{F}^{-1}\right). \tag{101}$$

The inverse of QFIM sometimes is difficult to obtain analytically and one may need a lower bound of $\mathrm{Tr}(\mathcal{F}^{-1})$ to roughly evaluate the precision limit. Being aware of the property of QFIM (given in section 2.1) that $[\mathcal{F}^{-1}]_{aa} \geqslant 1/\mathcal{F}_{aa}$, one can easily obtain the following corollary.

Corollary 3.1.2. *The total variance is bounded as*

$$\sum_a \mathrm{var}(\hat{x}_a, \{\Pi_y\}) \geqslant \frac{1}{n}\mathrm{Tr}\left(\mathcal{F}^{-1}\right) \geqslant \sum_a \frac{1}{n\mathcal{F}_{aa}}. \tag{102}$$

The second inequality can only be attained when $\mathcal{F}$ *is diagonal. Similarly,*

$$\sum_a \mathrm{var}(\hat{x}_a, \{\Pi_y\}) \geqslant \frac{1}{n}\mathrm{Tr}\left(\mathcal{I}^{-1}(\{\Pi_y\})\right) \geqslant \sum_a \frac{1}{n\mathcal{I}_{aa}(\{\Pi_y\})}. \tag{103}$$

The simplest example for the multi-parameter estimation is the case with two parameters. In this case, $\mathcal{F}^{-1}$ can be calculated analytically as

$$\mathcal{F}^{-1} = \frac{1}{\det(\mathcal{F})}\begin{pmatrix} \mathcal{F}_{bb} & -\mathcal{F}_{ab} \\ -\mathcal{F}_{ab} & \mathcal{F}_{aa} \end{pmatrix}. \tag{104}$$

Here $\det(\cdot)$ denotes the determinant. With this equation, the corollary above can reduce to the following form.

Corollary 3.1.3. *For two-parameter quantum estimation, corollary 3.1.1 reduces to*

$$\sum_a \mathrm{var}(\hat{x}_a, \{\Pi_y\}) \geqslant \frac{1}{nI_{\mathrm{eff}}(\{\Pi_y\})} \geqslant \frac{1}{nF_{\mathrm{eff}}}, \tag{105}$$

where $I_{\mathrm{eff}}(\{\Pi_y\}) = \det(\mathcal{I})/\mathrm{Tr}(\mathcal{I})$ *and* $F_{\mathrm{eff}} = \det(\mathcal{F})/\mathrm{Tr}(\mathcal{F})$ *can be treated as effective classical and quantum Fisher information.*

In statistics, the mean error given by $\sum_a \mathrm{var}(\hat{x}_a, \{\Pi_y\})$ *is not the only way for the characterization of mean error. Recently Lu et al [129] considered the generalized-mean, including the geometric and harmonic means, and provided the corresponding multiparameter Cramér–Rao bounds.*

3.1.2. Attainability. Attainability is a crucial problem in parameter estimation. An unattainable bound usually means the given precision limit is too optimistic to be realized in physics. In classical statistical estimations, the classical Cramér–Rao bound can be attained by the maximum likelihood estimator in the asymptotic limit, i.e. $\lim_{n\to\infty} n\mathrm{cov}(\hat{\vec{x}}_{\mathrm{m}}(n)) = \mathcal{I}^{-1}$, where $\hat{\vec{x}}_{\mathrm{m}}(n)$ is the local maximum likelihood estimator and a function of repetition or sample number, which is unbiased in the asymptotic limit. Because of this, the parameter estimation based on Cramér–Rao bound is an asymptotic theory and requires infinite samples or repetition of the experiment. For a finite sample case, the maximum likelihood estimator is not unbiased and the Cramér–Rao bound may not be attainable as well. Therefore, the true attainability in quantum parameter

estimation should also be considered in the sense of asymptotic limit since the attainability of quantum Cramér–Rao bound usually requires the QFIM equals the CFIM first. The general study of quantum parameter estimation from the asymptotic aspect is not easy, and the recent progress can be found in [90] and references therein. Here in the following, the attainability majorly refers to that if the QFIM coincides with the CFIM in theory. Besides, another thing that needs to emphasize is that the maximum likelihood estimator is optimal in a local sense [129], i.e. the estimated value is very close to the true value, and a locally unbiased estimator only attains the bound locally but not globally in the parameter space, thus, the attainability and optimal measurement discussed below are referred to the local ones.

For the single-parameter quantum estimations, the quantum Cramér–Rao bound can be attained with a theoretical optimal measurement. However, for multi-parameter quantum estimation, different parameters may have different optimal measurements, and these optimal measurements may not commute with each other. Thus there may not be a common measurement that is optimal for the estimation for all the unknown parameters. The quantum Cramér–Rao bound for the estimation of multiple parameters is then not necessary attainable, which is a major obstacle for the utilization of this bound in many years. In 2002, Matsumoto [131] first provided the necessary and sufficient condition of attainability for pure states. After this, its generalization to mixed states was discussed in several specific scenarios [28, 132–134] and rigorously proved via the Holevo bound firstly with the theory of local asymptotic normality [135] and then the direct minimization of one term in Holevo bound [136]. We first show this condition in the following theorem.

Theorem 3.2. *The necessary and sufficient condition for the saturation of the quantum multiparameter Cramér–Rao bound is*

$$\mathrm{Tr}\left(\rho[L_a, L_b]\right) = 0, \ \forall\, a, b. \tag{106}$$

For a pure parameterized state $|\psi\rangle := |\psi(\vec{x})\rangle$*, this condition reduces to*

$$\langle\psi|[L_a, L_b]|\psi\rangle = 0, \ \forall\, a, b, \tag{107}$$

which is equivalent to the form

$$\mathrm{Im}(\langle\partial_a\psi|\partial_b\psi\rangle) = 0. \tag{108}$$

When this condition is satisfied, the Holevo bound is also attained and equivalent to the Cramér–Rao bound [135, 136]. Recall that the Berry curvature introduced in section 2.4.3 is of the form

$$\begin{aligned}\Upsilon_{ab} &= \mathrm{i}\partial_a(\langle\psi|\partial_b\psi\rangle) - \mathrm{i}\partial_b(\langle\psi|\partial_a\psi\rangle)\\ &= -2\mathrm{Im}(\langle\partial_a\psi|\partial_b\psi\rangle).\end{aligned} \tag{109}$$

Hence, the above condition can also be expressed as following.

Corollary 3.2.1. *The multi-parameter quantum Cramér–Rao bound for a pure parameterized state can be saturated if and only if*

$$\Upsilon = 0, \tag{110}$$

i.e. the matrix of Berry curvature is a null matrix.

For a unitary process U with a pure probe state $|\psi_0\rangle$, this condition can be expressed with the operator $\mathcal{H}_a$ and $\mathcal{H}_b$, as shown in the following corollary [48].

Corollary 3.2.2. *For a unitary process U with a pure probe state $|\psi_0\rangle$, the necessary and sufficient condition for the attainability of quantum multiparameter Cramér–Rao bound is*

$$\langle\psi_0|\left[\mathcal{H}_a, \mathcal{H}_b\right]|\psi_0\rangle = 0, \ \forall\, a, b. \tag{111}$$

Here $\mathcal{H}_a$ was introduced in section 2.3.4.

3.1.3. Optimal measurements. The satisfaction of attainability condition theoretically guarantees the existence of some CFIM that can reach the QFIM. However, it still requires an optimal measurement. The search of practical optimal measurements is always a core mission in quantum metrology, and it is for the best that the optimal measurement is independent of the parameter to be estimated. The most well studied measurement strategies nowadays include the individual measurement, adaptive measurement and collective measurement, as shown in figure 3. The individual measurement refers to the measurement on a single copy (figure 3(a)) or local systems (black lines in figure 3(d)), and can be easily extend the sequential scenario (figure 3(c)), which is the most common scheme for controlled quantum metrology. The collective measurement, or joint measurement, is the one performed simultaneously on multi-copies or on the global system (orange lines in figure 3(d)) in parallel schemes. A typical example for collective measurement is the Bell measurement. The adaptive measurement (figure 3(b)) usually uses some known tunable operations to adjust the outcome. A well-studied case is the optical Mach–Zehnder interferometer with a tunable path in one arm. The Mach–Zehnder interferometer will be thoroughly introduced in the next section.

For the single parameter case, a possible optimal measurement can be constructed with the eigenstates of the SLD operator. Denote $\{|l_i\rangle\langle l_i|\}$ as the set of eigenstates of L_a, if we choose the set of POVM as the projections onto these eigenstates, then the probability for the ith measurement result is $\langle l_i|\rho|l_i\rangle$. In the case where $|l_i\rangle$ is independent of x_a, the CFI then reads

$$\mathcal{I}_{aa} = \sum_i \frac{\langle l_i|\partial_a\rho|l_i\rangle^2}{\langle l_i|\rho|l_i\rangle}. \tag{112}$$

Due to the equation $2\partial_a\rho = \rho L_a + L_a\rho$, the equation above reduces to

$$\mathcal{I}_{aa} = \sum_i l_i^2\langle l_i|\rho|l_i\rangle = \mathrm{Tr}(\rho L_a^2) = \mathcal{F}_{aa}, \tag{113}$$

which means the POVM $\{|l_i\rangle\langle l_i|\}$ is the optimal measurement to attain the QFI. However, if the eigenstates of the SLD are dependent on x_a, it is no longer the optimal measurement. In the case with a high prior information, the CFI with respect to $\{|l_i(\hat{x}_a)\rangle\langle l_i(\hat{x}_a)|\}$ ($\hat{x}_a$ is the estimated value of x_a) may be very close to the QFI. In practice, this measurement has to be used adaptively. Once we obtain a new estimated value $\hat{x}_a$ via the measurement, we need to update the measurement with the new estimated value and then perform the next round of measurement. For a non-full rank parameterized density matrix, the SLD operator is not unique, as discussed in section 2.3.1, which means the optimal measurement constructed via the eigenbasis of SLD operator is not unique. Thus, finding a realizable and simple optimal measurement is always the core mission in quantum metrology. Update to date, only known states in single-parameter estimation that own parameter-independent optimal measurement is the so-called quantum exponential family [27, 90], which is of the form

$$\rho = \mathrm{e}^{\frac{1}{2}\left(\int_0^x c(x')\mathrm{d}x' O - \int_0^x x' c(x')\mathrm{d}x'\right)}\rho_0\mathrm{e}^{\frac{1}{2}\left(\int_0^x c(x')\mathrm{d}x' O - \int_0^x x' c(x')\mathrm{d}x'\right)}, \tag{114}$$

where $c(x)$ is a function of the unknown parameter x, ρ_0 is a parameter-independent density matrix, and O is an unbiased observable of x, i.e. $\langle O\rangle = x$. For this family of states, the SLD is $L_x = c(x)(O - x)$ and the optimal measurement is the eigenstates of O.

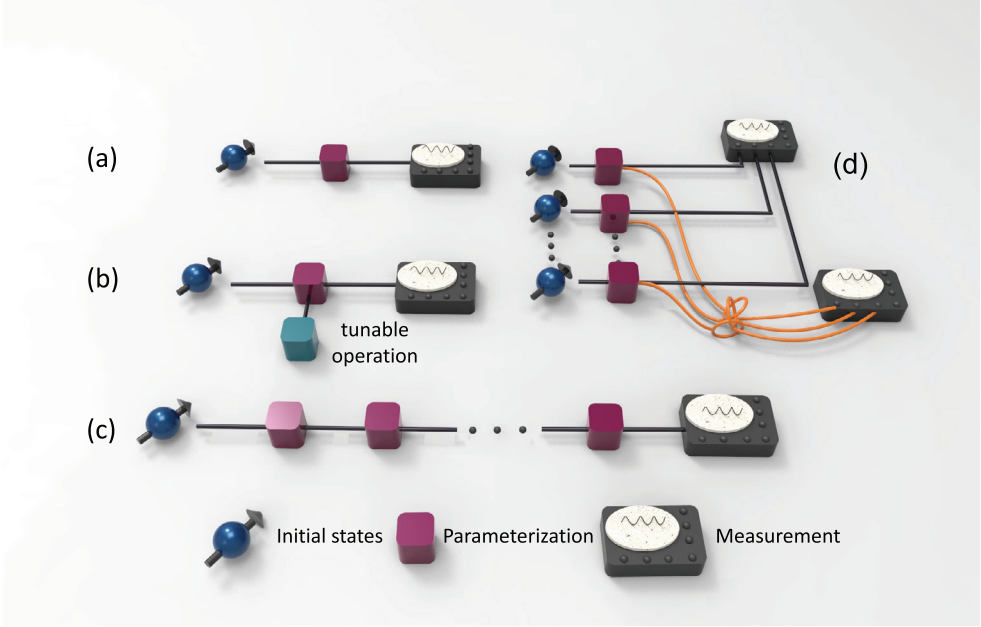

Figure 3. Schematics for basic measurement schemes in quantum metrology, including individual measurment, adaptive measurement and collective measurement.

For multiparameter estimation, the SLD operators for different parameters may not share the same eigenbasis, which means $\{|l_i(\hat{x}_a)\rangle\langle l_i(\hat{x}_a)|\}$ is no longer an optimal choice for the estimation of all unknown parameters, even with the adaptive strategy. Currently, most of the studies in multiparameter estimation focus on the construction of the optimal measurements for a pure parameterized state $|\psi\rangle$. In 2013, Humphreys *et al* [152] proposed a method to construct the optimal measurement, a complete set of projectors containing the operator $|\psi_{\vec{x}_{\rm true}}\rangle\langle\psi_{\vec{x}_{\rm true}}|$ ($\vec{x}_{\rm true}$ is the true value of $\vec{x}$). Here $|\psi_{\vec{x}_{\rm true}}\rangle$ equals the value of $|\psi\rangle$ by taking $\vec{x} = \vec{x}_{\rm true}$. All the other projectors can be constructed via the Gram–Schmidt process. In practice, since the true value is unknown, the measurement has to be performed adaptively with the estimated values $\hat{\vec{x}}$, similar as the single parameter case. Recently, Pezzè *et al* [137] provided the specific conditions this set of projectors should satisfy to be optimal, which is organized in the following three theorems.

Theorem 3.3. *Consider a parameterized pure state* $|\psi\rangle$. $|\psi_{\vec{x}_{\rm true}}\rangle := |\psi(\vec{x} = \vec{x}_{\rm true})\rangle$ *with* $\vec{x}_{\rm true}$ *the true value of* $\vec{x}$. *The set of projectors* $\{|m_k\rangle\langle m_k|, |m_0\rangle = |\psi_{\vec{x}_{\rm true}}\rangle\}$ *is an optimal measurement to let the CFIM reach QFIM if and only if [137]*

$$\lim_{\vec{x}\to\vec{x}_{\rm true}} \frac{{\rm Im}(\langle\partial_a\psi|m_k\rangle\langle m_k|\psi\rangle)}{|\langle m_k|\psi\rangle|} = 0,\ \forall x_a \text{ and } k \neq 0, \tag{115}$$

which is equivalent to

$${\rm Im}(\langle\partial_a\psi|m_k\rangle\langle m_k|\partial_b\psi\rangle) = 0,\ \forall x_a, x_b \text{ and } k \neq 0. \tag{116}$$

The proof is given in appendix I. This theorem shows that if the quantum Cramér–Rao bound can be saturated then it is always possible to construct the optimal measurement with

the projection onto the probe state itself at the true value and a suitable choice of vectors on the orthogonal subspace [137].

Theorem 3.4. *For a parameterized state* $|\psi\rangle$*, the set of projectors* $\{|m_k\rangle\langle m_k|, \langle\psi|m_k\rangle \neq 0\ \forall k\}$ *is an optimal measurement to let the CFIM reach QFIM if and only if [137]*

$$\mathrm{Im}(\langle\partial_a\psi|m_k\rangle\langle m_k|\psi\rangle) = |\langle\psi|m_k\rangle|^2\mathrm{Im}(\langle\partial_a\psi|\psi\rangle),\ \forall k, x_a. \tag{117}$$

For the most general case that some projectors are vertical to $|\psi\rangle$ and some not, we have following theorem.

Theorem 3.5. *For a parameterized pure state* $|\psi\rangle$*, assume a set of projectors* $\{|m_k\rangle\langle m_k|\}$ *include two subsets* $A = \{|m_k\rangle\langle m_k|, \langle\psi|m_k\rangle = 0\ \forall k\}$ *and* $B = \{|m_k\rangle\langle m_k|, \langle\psi|m_k\rangle \neq 0\ \forall k\}$*, i.e.* $\{|m_k\rangle\langle m_k|\} = A \cup B$*, then it is an optimal measurement to let the CFIM to reach the QFIM if and nly if [137] equation (115) is fulfilled for all the projectors in set A and (117) is fulfilled for all the projectors in set B.*

Apart from the QFIM, the CFIM is also bounded by a measurement-dependent matrix with the abth entry $\sum_k \mathrm{Re}[\mathrm{Tr}(\rho L_a \Pi_k L_b)]$ [138], where $\{\Pi_k\}$ is a set of POVM. Recently, Yang *et al* [138] provided the attainable conditions for the CFIM to attain this bound by generalizing the approach in [30].

3.2. Phase estimation in the Mach–Zehnder interferometer

Mach–Zehnder interferometer (MZI) is one of the most important model in quantum technology. It was first proposed in 1890th as an optical interferometer, and its quantum description was given in 1986 [139]. With the development of quantum mechanics, now it is not only a model for optical interferometer, but can also be realized via other systems like spin systems and cold atoms. The recently developed gravitational wave detector GEO 600 can also be mapped as a MZI in the absence of noise [140]. It is a little bit more complicated when the noise is involved, for which a valid bound has been provided by Branford *et al* [141] and is attainable by a frequency-dependent homodyne detection. Phase estimation in MZI is the earliest case showing quantum advantages in metrology. In 1981, Caves [142] showed that there exists an unused port in the MZI due to quantum mechanics and the vacuum fluctuation in that port actually affects the phase precision and limit it to the standard quantum limit (also known as shot-noise limit), which is the ultimate limit for a classical apparatus. He continued to point out that injecting a squeezed state in the unused port can lead to a high phase precision beating the standard quantum limit. This pioneer work proved that quantum technologies can be powerful in the field of precision measure, which was experimentally confirmed in [143, 144]. Since then, quantum metrology has been seeing a rapid development and grown into a major topic in quantum technology.

MZI is a two-path interferometer, which generally consists of two beam splitters and a phase shift between them, as shown in figure 4(a). In theory, the beam splitters and phase shift are unitary evolutions. A 50:50 beam splitter can be theoretically expressed by $B = \exp(-\mathrm{i}\frac{\pi}{2}J_x)$ where $J_x = \frac{1}{2}(\hat{a}^\dagger\hat{b} + \hat{b}^\dagger\hat{a})$ is a Schwinger operator with $\hat{a}$, $\hat{b}$ ($\hat{a}^\dagger$, $\hat{b}^\dagger$) the annihilation (creation) operators for two paths. Other Schwinger operators are $J_y = \frac{1}{2i}(\hat{a}^\dagger\hat{b} - \hat{b}^\dagger\hat{a})$ and $J_z = \frac{1}{2}(\hat{a}^\dagger\hat{a} - \hat{b}^\dagger\hat{b})$. The Schwinger operators satisfy the commutation $[J_i, J_j] = \mathrm{i}\sum_k \epsilon_{ijk}J_k$ with ϵ_{ijk} the Levi-Civita symbol. The second beam splitter usually takes the form as $B^\dagger$. For the standard MZI, the phase shift can be modeled as $P = \exp(\mathrm{i}\theta J_z)$, which means the entire operation of MZI is $BPB^\dagger = \exp(-\mathrm{i}\theta J_y)$, which is a SU(2) rotation, thus, this type of MZI is

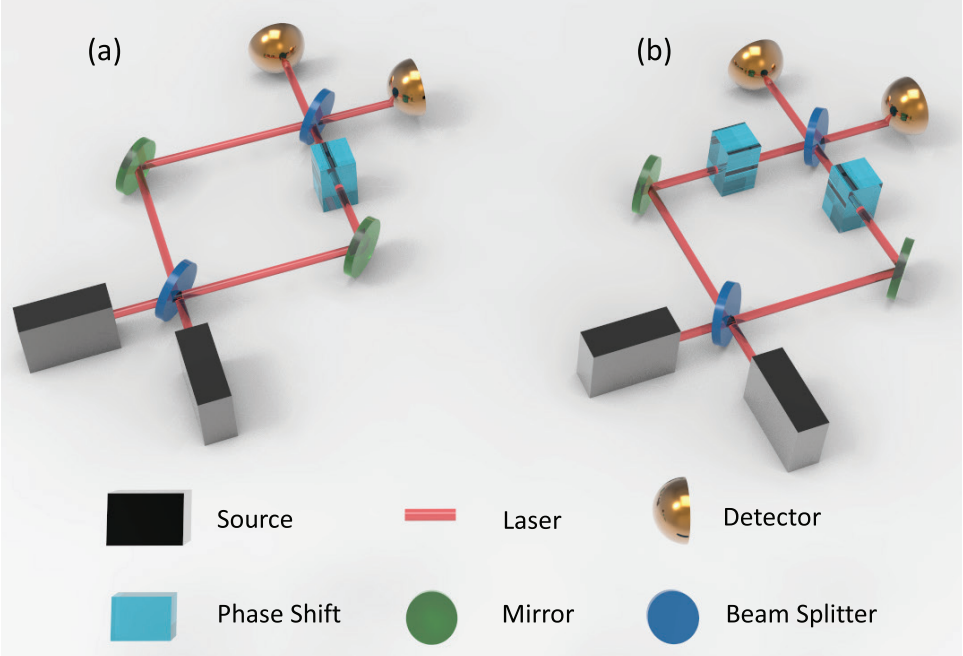

Figure 4. (a) Schematic for a standard Mach–Zehnder interferometer, which generally consists of two beam splitters and a phase shift; (b) schematic for a double phase Mach–Zehnder interferometer in which the phase shifts are put in all two paths. Here we emphasize that though the schematic is given in an optical setup, the MZI model can also be realized via other systems like spin systems and cold atoms.

also referred as SU(2) interferometer. If the input state is a pure state $|\psi_0\rangle$, the QFI for θ is just the variance of J_y with respect to $|\psi_0\rangle$, i.e. $\mathrm{var}_{|\psi_0\rangle}(J_y)$.

3.2.1. Double-phase estimation. A double-phase MZI consists of two beam splitters and a phase shift in each path, as shown in figure 4(b). In this setup, the operator of the two phase shifts is $P(\phi_a, \phi_b) = \exp(\mathrm{i}(\phi_a \hat{a}^\dagger \hat{a} + \phi_b \hat{b}^\dagger \hat{b}))$. According to proposition 2.1, the QFIM for the phases is not affected by the second beam splitter $B^\dagger$ since it is independent of the phases. Thus, the second beam splitter can be neglected for the calculation of QFIM. Now take $\phi_{\mathrm{tot}} = \phi_a + \phi_b$ and $\phi_{\mathrm{d}} = \phi_a - \phi_b$ as the parameters to be estimated. For a separable input state $|\alpha\rangle \otimes |\chi\rangle$ with $|\alpha\rangle$ as a coherent state, the entries of QFIM reads [145]

$$\mathcal{F}_{\phi_{\mathrm{tot}},\phi_{\mathrm{tot}}} = |\alpha|^2 + \mathrm{var}_{|\chi\rangle}(b^\dagger b), \tag{118}$$

$$\mathcal{F}_{\phi_{\mathrm{d}},\phi_{\mathrm{d}}} = 2|\alpha|^2 \mathrm{cov}_{|\chi\rangle}(b, b^\dagger) - 2\mathrm{Re}\left(\alpha^2 \mathrm{var}_{|\chi\rangle}(b^\dagger)\right) + \langle b^\dagger b\rangle, \tag{119}$$

$$\mathcal{F}_{\phi_{\mathrm{tot}},\phi_{\mathrm{d}}} = -\mathrm{i}\alpha^* \langle b\rangle - \mathrm{iIm}(\alpha^*(\langle b^\dagger b^2\rangle - \langle b^\dagger b\rangle\langle b\rangle)). \tag{120}$$

Focusing on the maximization of $\mathcal{F}_{\phi_{\mathrm{d}},\phi_{\mathrm{d}}}$ subject to a constraint of fixed mean photon number on b mode, Lang and Caves [145] proved that the squeezed vacuum state is the optimal choice for $|\chi\rangle$ which leads to the maximum sensitivity of ϕ_{d}.

Since Caves already pointed out that the vacuum fluctuation will affect the phase sensitivity [142], it is then interesting to ask the question that how bad the phase sensitivity could be if one input port keeps vacuum? Recently Takeoka *et al* [146] considered this question and gave the answer by proving a no-go theorem stating that in the double phase MZI, if one input port is the vacuum state, the sensitivity can never be better than the standard quantum limit regardless of the choice of quantum state in the other port and the detection scheme. However, this theorem does not hold for a single phase shift scenario in figure 4(a). Experimentally, Polino *et al* [147] recently demonstrated quantum-enhanced double-phase estimation with a photonic chip.

Besides the two-phase estimation, another practical two-parameter scenario in interometry is the joint measurement of phase and phase diffusion. In 2014, Vidrighin *et al* [132] provide a trade-off bound on the statistical variances for the joint estimation of phase and phase diffusion. Later in 2015, Altorio *et al* [148] addressed the usefulness of weak measurements in this case and in 2018 Hu *et al* [149] discussed the SU(1,1) interferometry in the presence of phase diffusion. In the same year, Roccia *et al* [150] experimentally showed that some collective measurement, like Bell measurement, can benefit the joint estimation of phase and phase diffusion.

3.2.2. Multi-phase estimation. Apart from double phase estimation, multi-phase estimation is also an important scenario in multiparameter estimation. The multi-phase estimation is usually considered in the multi-phase interferometer shown in figure 5(a). Another recent review on this topic is [16]. In this case, the total variance of all phases is the major concern, which is bounded by $\frac{1}{n}\mathrm{Tr}(\mathcal{F}^{-1})$ according to corollary 3.1.1. For multiple phases, the probe state undergoes the parameterization, which can be represented by $U = \exp(\mathrm{i}\sum_j x_j H_j)$ where H_j is the generator of the jth mode. In the optical scenario, this operation can be chosen as $\exp(\mathrm{i}\sum_j x_j a_j^\dagger a_j)$ with $a_j^\dagger$ (a_j) as the creation (annihilation) operator for the jth mode. For a separable state $\sum_k p_k \bigotimes_{i=0}^{d} \rho_k^{(i)}$ where $\rho_k^{(i)}$ is a state of the ith mode, and p_k is the weight with $p_k > 0$ and $\sum_k p_k = 1$, the QFI satisfies $\mathcal{F}_{jj} \leqslant d(h_{j,\max} - h_{j,\min})^2$ [151] with $h_{j,\max}$ ($h_{j,\min}$) as the maximum (minimum) eigenvalue of H_j. From corollary 3.1.2, the total variance is then bounded by [151]

$$\sum_j \mathrm{var}(\hat{x}_j, \{\Pi_y\}) \geqslant \frac{1}{d}\sum_{j=1}^{d} \frac{1}{(h_{j,\max} - h_{j,\min})^2}. \tag{121}$$

This bound indicates that the entanglement is crucial in the multi-phase estimation to beat the standard quantum limit.

N00N state is a well known entangled state in quantum metrology which can saturate the Heisenberg limit. In 2013, Humphreys *et al* [152] discussed a generalized $(d+1)$-mode N00N state in the form $c_0|N_0\rangle + c_1\sum_i |N_i\rangle$ where $|N_i\rangle = |0...0N0...0\rangle$ is the state in which only the ith mode corresponds to a Fock state and all other modes are left vacuum. c_0 and c_1 are real coefficients satisfying $c_0^2 + dc_1^2 = 1$. The 0-mode is the reference mode and the parametrization process is $\exp(\mathrm{i}\sum_{j=1}^{d} x_j a_j^\dagger a_j)$. The generation of this state has been proposed in [153]. Since this process is unitary, the QFIM can be calculated via corollary 2.7.1 with $\mathcal{H}_j = -a_j^\dagger a_j$. It is then easy to see that the entry of QFIM reads [152] $\mathcal{F}_{ij} = 4N^2(\delta_{ij}c_1^2 - c_1^4)$, which further gives

$$\min_{c_1} \mathrm{Tr}(\mathcal{F}^{-1}) = \frac{(1+\sqrt{d})^2 d}{4N^2}, \tag{122}$$

where the optimal c_1 is $1/\sqrt{d+\sqrt{d}}$.

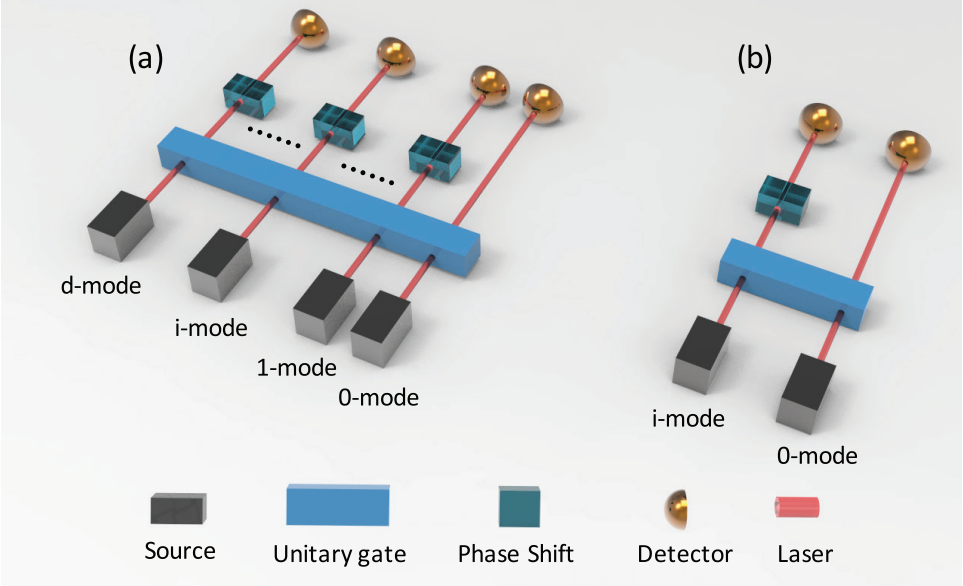

Figure 5. Schematics of (a) simultaneous multi-phase estimation and (b) independent estimation of multiple phases. 0-mode light is the reference mode. In the independent estimation, the phase in the ith mode is estimated via the MZI consisting of 0-mode and i-mode lights.

Apart from the scheme in figure 5(a) with the simultaneous estimation, the multi-phase estimation can also be performed by estimating the phases independently, using the ith mode and the reference mode, as shown in figure 5(b). In this scheme, the phases are estimated one by one with the N00N state, which provides the total precision limit d^3/N^2 [152]. Thus, the simultaneous estimation scheme in figure 5(a) shows a $\mathcal{O}(d)$ advantage compared to the independent scheme in figure 5(b). However, the performance of the simultaneous estimation may be strongly affected by the noise [154, 155] and the $\mathcal{O}(d)$ advantage may even disappear under the photon loss noise [156].

In the single phase estimation, it is known that the entangled coherent state $\mathcal{N}(|0\alpha\rangle + |\alpha 0\rangle)$ ($|\alpha\rangle$ is a coherent state and $\mathcal{N}$ is the normalization) can provide a better precision limit than the N00N state [157]. Hence, it is reasonable to think the generalization of entangled coherent state may also outperform the generalized N00N state. This result was theoretically confirmed in [158]. For a generalized entangled coherent state written in the form $c_0|\alpha_0\rangle + c_1 \sum_{j=1}^{d} |\alpha_j\rangle$ with $|\alpha_j\rangle = |0...0\alpha 0...0\rangle$, the QFIM is $\mathcal{F}_{ij} = 4|c_1|^2|\alpha|^2[\delta_{ij}(1+|\alpha|^2) - |c_1|^2|\alpha|^2]$ [158]. For most values of d and $|\alpha|$, the minimum $\mathrm{Tr}(\mathcal{F}^{-1})$ can be written as

$$\min_{c_1} \mathrm{Tr}(\mathcal{F}^{-1}) = \frac{(1+\sqrt{d})^2 d}{4(1+|\alpha|^2)^2}, \tag{123}$$

which is smaller than the counterpart of the generalized N00N state, indicating the performance of the generalized entangled coherent state is better than the generalized N00N state. For a large $|\alpha|$, the total particle number $\sim|\alpha|^2$ and the performances of both states basically coincide. With respect to the independent scheme, the generalized entangled coherent also shows a $\mathcal{O}(d)$ advantage in the absence of noise.

In 2017, Zhang *et al* [159] considered a general balanced state $c\sum_j|\psi_j\rangle$ with $|\psi_j\rangle = |0...0\psi 0...0\rangle$. c is the normalization coefficient. Four specific balanced states: N00N state, entangled coherent state, entangled squeezed vacuum state and entangled squeezed coherent state, were calculated and they found that the entangled squeezed vacuum state shows the best performance, and the balanced type of this state outperforms the unbalanced one in some cases.

A linear network is another common structure for multi-phase estimation [160, 161]. Different with the structure in figure 5(a), a network requires the phase in each arm can be detected independently, meaning that each arm needs a reference beam. The calculation of Cramér–Rao bound in this case showed [161] that the linear network for miltiparameter metrology behaves classically even though endowed with well-distributed quantum resources. It can only achieve the Heisenberg limit when the input photons are concentrated in a small number of input modes. Moreover, the performance of a mode-separable state $\mathcal{N}(|N\rangle + v|0\rangle)$ may also shows a high theoretical precision limit in this case if $v \propto \sqrt{d}$.

Recently, Gessner [162] considered a general case for multi-phase estimation with multi-mode interferometers. The general Hamiltonian is $H = \sum_{j=1}^{N} h_k^{(j)}$ with $h_k^{(j)}$ a local Hamiltonian for the ith particle in the kth mode. For the particle-separable states, the maximum QFIM is a diagonal matrix with the ith diagonal entry $\langle n_i\rangle$ being the ith average particle number (n_i is the ith particle number operator). This bound could be treated as the shot-noise limit for the multi-phase estimation. For the mode-separable states, the maximum QFIM is also diagonal, with the ith entry $\langle n_i^2\rangle$, which means the maximum QFIM for mode-separable state is larger than the particle-separate counterpart. Taking into account both the particle and mode entanglement, the maximum QFIM is in the form $\mathcal{F}_{ij} = \mathrm{sgn}(\langle n_i\rangle)\mathrm{sgn}(\langle n_j\rangle)\sqrt{\langle n_i^2\rangle\langle n_j^2\rangle}$, which gives the Heisenberg limit in this case.

The comparison among the performances of different strategies usually requires the same amount of resources, like the same sensing time, same particle number and so on. Generally speaking, the particle number here usually refers to the average particle number, which is also used to define the standard quantum limit and Heisenberg limit in quantum optical metrology. Although the Heisenberg limit is usually treated as a scaling behavior, people still attempt to redefine it as an ultimate bound given via quantum mechanics by using the expectation of the square of number operator to replace the square of average particle number [163], i.e. the variance should be involved in the Heisenberg limit [163, 164] and be treated as a resource.

3.3. Waveform estimation

In many practical problems, like the detection of gravitational waves [141] or the force detection [165], what needs to be estimated is not a parameter, but a time-varing signal. The QFIM also plays an important role in the estimation of such signals, also known as waveform estimation [166]. By discretizing time into small enough intervals, the estimation of a time-continuous signal $x(t)$ becomes the estimation of multiparameters x_j's. The prior information of the waveform has to be taken into account in the estimation problem, e.g. restricting the signal to a finite bandwidth, in order to make the estimation error well-defined. The estimation-error covariance matrix Σ is then given by

$$\Sigma_{jk} = \int [\hat{x}_j(y) - x_j][\hat{x}_k(y) - x_k]\,\mathrm{d}y\mathrm{d}\vec{x}, \tag{124}$$

where $\mathrm{d}\vec{x} = \prod_j \mathrm{d}x_j$ and y denotes the measurement outcome. Tsang proved the most general form of Bayesian quantum Cramér-Rao bound

$$\Sigma \geqslant \left(\mathcal{F}^{(\mathrm{C})} + \mathcal{F}^{(\mathrm{Q})}\right)^{-1}, \tag{125}$$

where the classical part

$$\mathcal{F}^{(\mathrm{C})}_{ab} = \int [\partial_a \ln p(\vec{x})][\partial_b \ln p(\vec{x})] p(\vec{x}) \mathrm{d}x \tag{126}$$

depends only on the prior information about the vector parameter $\vec{x}$ and the quantum part [29, 166]

$$\mathcal{F}^{(\mathrm{Q})}_{ab} = \int \mathrm{Re}\left[\mathrm{Tr}(\tilde{L}^\dagger_a \tilde{L}_b \rho)\right] p(\vec{x}) \mathrm{d}\vec{x} \tag{127}$$

depends on the parametric family ρ of density operators with $\tilde{L}_a$ being determined via

$$\partial_a \rho = \frac{1}{2}\left(\tilde{L}_a \rho + \rho \tilde{L}^\dagger_a\right). \tag{128}$$

Note that $\tilde{L}_a$ is an extended version of SLD and is not necessary to be Hermitian. When all $\tilde{L}_a$'s are Hermitian, $\mathcal{F}^{(\mathrm{Q})}$ is the average of the QFIM over the prior distribution of $\vec{x}$. $\tilde{L}_a$ can also be anti-Hermiaition [29]. In this case, the corresponding bound is equivalent to the SLD one for pure states but a potentially looser one for mixed states. For a unitary evolution, the entire operator U can be discretized into $U = U_m U_{m-1} \cdots U_1 U_0$, where $U_a = \exp(-iH(x_a)\delta t)$. Denote $h_a = U_0^\dagger U_1^\dagger \cdots U_a^\dagger (\partial_a H) U_a \cdots U_1 U_0$ and $\Delta h_a = h_a - \mathrm{Tr}(\rho_0 h_a)$ with ρ_0 the probe state, the quantum part in equation (127) reads [166]

$$\mathcal{F}^{(Q)}_{ab} = 2(\delta t)^2 \int \mathrm{Tr}\left(\{\Delta h_a, \Delta h_b\}\, \rho_0\right) p(\vec{x}) \mathrm{d}\vec{x}. \tag{129}$$

Taking the continuous-time limit, it can be rewritten as [166]

$$\mathcal{F}^{(Q)}(t, t') = 2 \int \mathrm{Tr}\left(\{\Delta h(t), \Delta h(t')\}\, \rho_0\right)\, p(\vec{x}) \mathrm{d}\vec{x}. \tag{130}$$

Together with $\mathcal{F}^{(C)}(t, t')$, the fundamental quantum limit to waveform estimation based on QFIM is established [166]. The waveform estimation can also be solved with other tools, like the Bell–Ziv–Zakai lower bounds [167].

3.4. Control-enhanced multiparameter estimation

The dynamics of many artificial quantum systems, like the Nitrogen-vacancy center, trapped ion and superconducting circuits, can be precisely altered by control. Hence, control provides another freedom for the enhancement of the precision limit in these apparatuses. It is already known that quantum control can help to improve the QFI to the Heisenberg scaling with the absence of noise in some scenarios [54, 169–170]. However, like other resources, this improvement could be sensitive to the noise, and the performance of optimal control may strongly depend on the type of noise [171, 172]. In general, the master equation for a noisy quantum system is described by

$$\partial_t \rho = \mathcal{E}_{\vec{x}} \rho. \tag{131}$$

Here $\mathcal{E}_{\vec{x}}$ is a $\vec{x}$-dependent superoperator. For the Hamiltonian estimation under control, the dynamics is

$$\mathcal{E}_{\vec{x}}\rho = -\mathrm{i}[H_0(\vec{x}) + H_\mathrm{c}, \rho] + \mathcal{L}\rho, \tag{132}$$

where $H_\mathrm{c} = \sum_{k=1}^{p} V_k(t)H_k$ is the control Hamiltonian with H_k the kth control and $V_k(t)$ the corresponding time-dependent control amplitude. For a general Hamiltonian, the optimal control can only be tackled via numerical methods. One choice for this problem is the Gradient ascent pulse engineering algorithm.

Gradient ascent pulse engineering (GRAPE) algorithm is a gradient-based algorithm, which was originally developed to search the optimal control for the design of nuclear magnetic resonance pulse sequences [173], and now is extended to the scenario of quantum parameter estimation [171, 172]. As a gradient-based method, GRAPE requires an objective function and analytical expression of the corresponding gradient. For quantum single-parameter estimation, the QFI is a natural choice for the objective function. Of course, in some specific systems the measurement methods might be very limited, which indicates the CFI is a proper objective function in such cases. For quantum multiparameter estimation, especially those with a large parameter number, it is difficult or even impossible to take into account the error of every parameter, and thus the total variance $\sum_a \mathrm{var}(\hat{x}_a, \{\Pi_y\})$ which represents the average error of all parameters, is then a good index to show system precision. According to corollary 3.1.1, $\mathrm{Tr}(\mathcal{F}^{-1})$ and $\mathrm{Tr}(\mathcal{I}^{-1})$ (for fixed measurement) could be proper objective functions for GRAPE if we are only concern with the total variance. For two-parameter estimation, $\mathrm{Tr}(\mathcal{F}^{-1})$ and $\mathrm{Tr}(\mathcal{I}^{-1})$ reduce to the effective QFI F_eff and CFI I_eff according to corollary 3.1.3. However, as the parameter number increases, the inverse matrix of QFIM and CFIM are difficult to obtain analytically, and consequently superseded objective functions are required. $(\sum_a \mathcal{I}_{aa})^{-1}$ or $(\sum_a \mathcal{F}_{aa})^{-1}$, based on corollary 3.1.2, is then a possible superseded objective function for fixed measurement. However, the use of $(\sum_a \mathcal{F}_{aa})^{-1}$ should be very cautious since $\mathrm{Tr}(\mathcal{F}^{-1})$ cannot always be achievable. The specific expressions of gradients for these objective functions in Hamiltonian estimation are given in appendix J.

The flow of the algorithm, shown in figure 6, is formulated as follows [171, 172]:

(i) Guess a set of initial values for $V_k(j)$ ($V_k(j)$ is the kth control at the jth time step).
(ii) Evolve the dynamics with the controls.
(iii) Calculate the objective function. For single-parameter estimation, the objective function can be chosen as QFI $\mathcal{F}_{aa}$ or CFI $\mathcal{I}_{aa}$ (for mixed measurement). For two-parameter estimation, it can be chosen as I_eff or F_eff. For large parameter number, it can be chosen as $f_0 = \frac{1}{\sum_a \mathcal{I}_{aa}^{-1}}$ or $\frac{1}{\sum_a \mathcal{F}_{aa}^{-1}}$.
(iv) Calculate the gradient.
(v) Update $V_k(j)$ to $V_k(j) + \epsilon \cdot \mathrm{gradient}$ (ϵ is a small quantity) for all j simultaneously.
(vi) Go back to step (ii) until the objective function converges.

In step (v), all $V_k(j)$ are updated simultaneously in each time of iteration [173], as shown in figure 7(a), which could improve the speed of convergence in some cases. However, this parallel update method does not promise the monotonicity of convergence, and the choice of initial guess of $V_k(j)$ is then important for a convergent result. The specific codes for this algorithm can be found in the package QuanEstimation[14].

Krotov's method is another gradient-based method in quantum control, which promises the monotonicity of convergence during the iteration [174]. Different from GRAPE, only one

[14] QuanEstimation package: https://github.com/LiuJPhys/QuanEstimation.

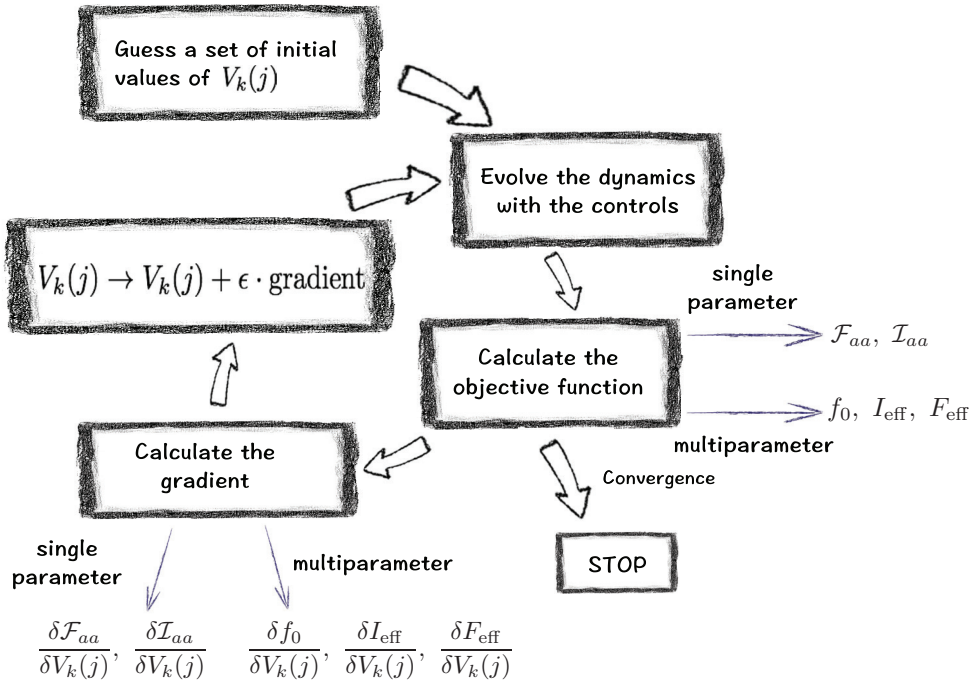

Figure 6. Flow chart of GRAPE algorithm for controlled single-parameter and multiparameter estimation. Reprinted figure with permission from [171, 172]. Copyright (2019) by the American Physical Society.

$V_k(j)$ is updated in each iteration in Krotov's method, as shown in figure 7(b). This method can also be extended to quantum parameter estimation with the aim of searching the optimal control for a high precision limit. It is known that the gradient-based methods can only harvest the local extremals. Thus, it is also useful to involve gradient-free methods, including Monte Carlo method and particle swarm optimization, into the quantum parameter estimation, or apply a hybrid method combining gradient-based and gradient-free methods as discussed in [175].

3.5. Estimation of a magnetic field

Measurement of the magnetic fields is an important application of quantum metrology, as it promises better performances than the classical counterparts. Various physical systems have been used as quantum magnetometers, including but not limited to nitrogen-vacancy centers [176, 177], optomechanical systems [178], and cold atoms [179].

A magnetic field can be represented as a vector, $\vec{B} = B(\cos\theta\cos\phi, \cos\theta\sin\phi, \sin\phi)$, in the spherical coordinates, where B is the amplitude, and θ, ϕ define the direction of the field. Therefore, the estimation of a magentic field is in general a three-parameter estimation problem. The estimation of the amplitude with known angles is the most widely-studied case in quantum metrology, both in theory and experiments. For many quantum systems, it is related to the estimation of the strength of system-field coupling. In the case where one angle, for example ϕ is known, the estimation of the field becomes a two-parameter estimation problem. The simplest quantum detector for this case is a single-spin system [48, 53]. An example of the interaction Hamiltonian is $H = -B\vec{n}_0 \cdot \vec{\sigma}$ with $n_0 = (\cos\theta, 0, \sin\theta)$ and $\vec{\sigma} = (\sigma_x, \sigma_y, \sigma_z)$. The QFIM can then be obtained by making use of the expressions of $\mathcal{H}$ operators [48, 53]

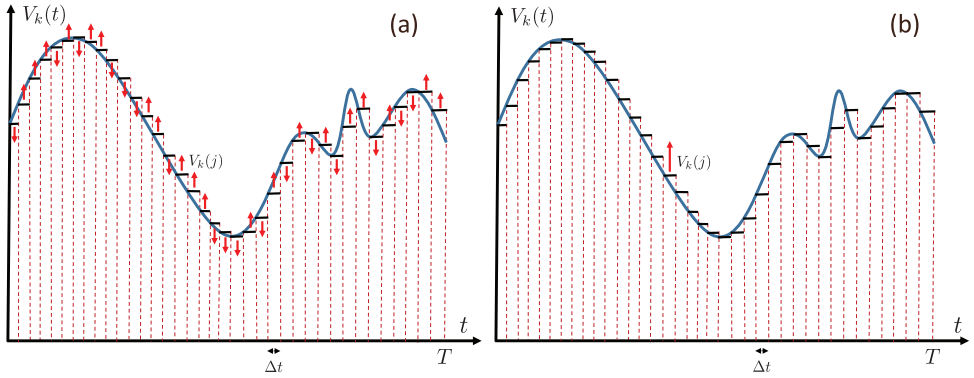

Figure 7. (a) In GRAPE, the entire evolution time T is cut into m parts with time interval Δt, i.e. $m\Delta t = T$. $V_k(t)$ within the jth time interval is denoted as $V_k(j)$ and is assumed to be a constant. All the $V_k(j)$ are simultaneously updated in each iteration. (b) Krotov's method updates one $V_k(j)$ in each iteration.

$$\mathcal{H}_B = t\vec{n}_0 \cdot \vec{\sigma},\ \mathcal{H}_\theta = -\frac{1}{2}\sin(Bt)\vec{n}_1 \cdot \vec{\sigma}, \tag{133}$$

where $n_1 = (\cos(Bt)\sin\theta, \sin(Bt), -\cos(Bt)\cos\theta)$. The entries of QFIM then read

$$\mathcal{F}_{\theta\theta} = \sin^2(Bt)[1 - (\vec{n}_1 \cdot \vec{r}_{\text{in}})^2], \tag{134}$$

$$\mathcal{F}_{BB} = 4t^2[1 - (\vec{n}_0 \cdot \vec{r}_{\text{in}})^2], \tag{135}$$

$$\mathcal{F}_{B\theta} = 2t\sin(Bt)(\vec{n}_0 \cdot \vec{r}_{\text{in}})(\vec{n}_1 \cdot \vec{r}_{\text{in}}), \tag{136}$$

where $\vec{r}_{\text{in}}$ is the Bloch vector of the probe state. The maximal values of $\mathcal{F}_{\theta\theta}$ and $\mathcal{F}_{BB}$ can be attained when $\vec{r}_{\text{in}}$ is vertical to both $\vec{n}_0$ and $\vec{n}_1$. However, as a two-parameter estimation problem, we have to check the value of $\langle\psi_0|[\mathcal{H}_B, \mathcal{H}_\theta]|\psi_0\rangle$ due to corollary 3.2.2. Specifically, for a pure probe state it reads $\langle\psi_0|[\mathcal{H}_B, \mathcal{H}_\theta]|\psi_0\rangle = -\sin(Bt)(\vec{n}_0 \times \vec{n}_1) \cdot \vec{\sigma}$. For the time $t = n\pi/B$ ($n = 1, 2, 3...$), the expression above vanishes. However, another consequence of this condition is that $\mathcal{F}_{\theta\theta}$ also vanishes. Thus, single-qubit probe may not be an ideal magnetometer when at least one angle is unknown. One possible candidate is a collective spin system, in which the $\mathcal{H}$ operator and QFIM are provided in [180]. Another simple and practical-friendly candidate is a two-qubit system. One qubit is the probe and the other one is an ancilla, which does not interact with the field. Consider the Hamiltonian $H = -\vec{B} \cdot \vec{\sigma}$, the maximal QFIM in this case is (in the basis $\{B, \theta, \phi\}$) [84]

$$\max \mathcal{F} = 4\begin{pmatrix} t^2 & 0 & 0 \\ 0 & \sin^2(Bt) & 0 \\ 0 & 0 & \sin^2(Bt)\cos^2\theta \end{pmatrix}, \tag{137}$$

which can be attained by any maximally entangled state and the Bell measurement as the optimal measurement. With the assistance of an ancilla, all three parameters B, θ, ϕ of the field can be simultaneously estimated. However, $\mathcal{F}_{\theta\theta}$ and $\mathcal{F}_{\phi\phi}$ are only proportional to $\sin^2(Bt)$, indicating that unlike the estimation of the amplitude, a longer evolution time does not always lead to a better precision for the estimation of θ or ϕ.

In 2016, Baumgratz and Datta [181] provided a framework for the estimation of a multidimensional field with noncommuting unitary generators. Analogous to the optical multi-phase estimation, simultaneous estimation shows a better performance than separate and individual estimation.

To improve the performance of the probe system, additional control could be employed. For unitary evolution [84], showed that the performance can be significantly enhanced by inserting the anti-evolution operator as the control. Specifically if after each evolution of a period of δt, we insert a control which reverses the evolution as $U_c = U^\dagger(\delta t) = \mathrm{e}^{\mathrm{i}H(\vec{B})\delta t}$, the QFIM can reach

$$\mathcal{F} = 4N^2 \begin{pmatrix} (\delta t)^2 & 0 & 0 \\ 0 & \sin^2(B\delta t) & 0 \\ 0 & 0 & \sin^2(B\delta t)\cos^2\theta \end{pmatrix}, \tag{138}$$

where N is the number of the injected control pulses, and $N\delta t = t$. In practice the control needs to be applied adaptively as $U_c = \mathrm{e}^{\mathrm{i}H(\hat{\vec{B}})\delta t}$ with $\hat{\vec{B}}$ as the estimated value obtained from previous measurement results. In the controlled scheme, the number of control pulses becomes a resource for the estimation of all three parameters. For the amplitude, the precision limit is the same as non-controlled scheme. But for the angles, the precision limit is significantly improved, especially when N is large. When $\delta t \to 0$, the QFIM becomes

$$\mathcal{F} = 4 \begin{pmatrix} t^2 & 0 & 0 \\ 0 & B^2t^2 & 0 \\ 0 & 0 & B^2t^2\cos^2\theta \end{pmatrix}, \tag{139}$$

which reaches the highest precision for the estimation of B, θ and ϕ simultaneously. Recently, Hou *et al* [182] demonstrated this scheme up to eight controls in an optical platform and demonstrate a precision near the Heisenberg limit.

Taking into account the effect of noise, the optimal control for the estimation of the magnetic field is then hard to obtain analytically. The aforementioned numerical methods like GRAPE or Krotov's method could be used in this case to find the optimal control. The performance of the controlled scheme relies on the specific form of noise [171, 172], which could be different for different magnetometers.

In practice, the magnetic field may not be a constant field in space. In this case, the gradient of the field also needs to be estimated. The corresponding theory for the estimation of gradients based on Cramér–Rao bound has been established in [183, 184].

3.6. Other applications and alternative mathematical tools

Apart from the aforementioned cases, quantum multiparameter estimation is also studied in other scenarios, including the spinor systems [186], unitary photonic systems [187], networked quantum sensors [188], and the quantum thermometry [189]. In the case of noise estimation, the simultaneous estimation of loss parameters has been studied in [190].

In 2016, Tsang *et al* [191] used quantum multiparameter estimation for a quantum theory of superresolution for two incoherent optical point sources. With weak-source approximation, the density operator for the optical field in the imaging plane can be expressed as $\rho = (1-\epsilon)|\mathrm{vac}\rangle\langle\mathrm{vac}| + \frac{\epsilon}{2}(|\psi_1\rangle\langle\psi_1| + |\psi_2\rangle\langle\psi_2|)$, with ϵ the average photon number in a temporal mode, $|\mathrm{vac}\rangle$ the vacuum state, $|\psi_j\rangle = \int \mathrm{d}y\, \psi_{x_j}(y)|y\rangle$ the quantum state of an arrival photon from the point source located at x_j of the object plane, $\psi_{x_j}(y)$ the wave function in the

image plane, and $|y\rangle$ the photon image-plane position eigenstate. Taking the position coordinates to be one-dimensional, the parameters to be estimated are x_1 and x_2. The performance of the underlying quantum measurement can be assessed by the CFIM and its fundamental quantum limit can be revealed by the QFIM. In this case, the QFIM is analytically calculated in the 4-dimensional Hilbert subspace spanned by $|\psi_1\rangle, |\psi_2\rangle, |\partial_1\psi_1\rangle$, and $|\partial_2\psi_2\rangle$. For convenience, the two parameters x_1 and x_2 can be transformed to the centriod $\theta_1 = (x_1 + x_2)/2$ and the separation $\theta_2 = x_2 - x_1$. Assuming the imaging system is spatially invariant such that the point-spread function of the form $\psi_{x_j}(y) = \psi(y - x_j)$ with real-valued $\psi(y)$, the QFIM with respect to θ_1 and θ_2 is then given by

$$\mathcal{F} = \begin{pmatrix} 4\epsilon(\Delta k^2 - \gamma^2) & 0 \\ 0 & \epsilon\Delta k^2 \end{pmatrix}, \tag{140}$$

where $\Delta k^2 = \int_{-\infty}^{\infty} [\partial\psi(y)/\partial y]^2 \,\mathrm{d}y$ and $\gamma = \int_{-\infty}^{\infty} \psi(y - \theta_2)\partial\psi(y)/\partial y \,\mathrm{d}y$ [191]. With this result, it has been shown that direct imaging performs poorly for estimating small separations and other elaborate methods like spatial-mode demultiplexing and image inversion interferometry can be used to achieve the quantum limit [191, 192].

The design of enhanced schemes for quantum parameter estimation would inevitably face optimization processes, including the optimization of probe states, the parameterization trajectories, the measurement and so on. If control is involved, one would also need to harvest the optimal control. Therefore, the stochastic optimization methods, including convex optimization, Monte Carlo method and machine learning, could be used in quantum parameter estimation.

Machine learning is one of the most promising and cutting-edge methods nowadays. In recent years, it has been applied to condensed matter physics for phase transitions [193, 194], design of a magneto-optical trap [195] and other aspects [196]. With respect to quantum parameter estimation, in 2010, Hentschel and Sanders [197] applied the particle swarm optimization algorithm [198] in the adaptive phase estimation to determine the best estimation strategy, which was experimentally realized by Lumino *et al* [199] in 2018. Meanwhile, in 2017, Greplova *et al* [200] proposed to use neural networks to estimate the rates of coherent and incoherent processes in quantum systems with continuous measurement records. In the case of designing controlled schemes, similar to gradient-based methods, machine learning could also help use to find the optimal control protocal in order to achieve the best precision limit [185]. In particular, for quantum multiparameter estimation, there still lacks of systematic research on the role of machine learning. For instance, we are not assured if there exists different performance compared to single-parameter estimation.

As a mathematical tool, quantum Cramér–Rao bound is not the only one for quantum multiparameter estimation. Bayesian approach [203–207], including Ziv–Zakai family [167, 168, 201] and Weiss–Weinstein family [166, 208], and some other tools [208–210] like Holevo bound [2, 28, 202], have also shown their validity in various multiparameter scenarios. These tools beyond the Cramér–Rao bound will be thoroughly reviewed by Guţă *et al* [211] in the same special issue and hence we do not discuss them in this paper. Please see [211] for further reading of this topic. In some scenarios in quantum parameter estimations, there may exist some parameters that not of interest but affect the precision of estimating other parameters of interest, which is usually referred to as the nuisance parameters. Suzuki *et al* [212] has thoroughly reviewed the quantum state estimation with nuisance parameters in the same special issue. Please see [212] for further reading.

4. Conclusion and outlook

Quantum metrology has been recognized as one of the most promising quantum technologies and has seen a rapid development in the past few decades. Quantum Cramér–Rao bound is the most studied mathematical tool for quantum parameter estimation, and as the core quantity of quantum Cramér–Rao bound, the QFIM has drawn plenty of attentions. It is now well-known that the QFIM is not only a quantity to quantify the precision limit, but also closely connected to many different subjects in quantum physics. This makes it an important and fundamental concept in quantum mechanics.

In recent years, many quantum multiparameter estimation schemes have been proposed and discussed with regard to various quantum systems, and some of them have shown theoretical advances compared to single-parameter schemes. However, there are still many open problems, such as the design of optimal measurement, especially simple and practical measurement which are independent of the unknown parameters, as well as the robustness of precision limit against the noises and imperfect controls. We believe that some of the issues will be solved in the near future. Furthermore, quantum multiparameter metrology will then go deeply into the field of applied science and become a basic technology for other aspects of sciences.

Acknowledgments

The authors thank Zibo Miao, Christiane Koch, Rafał Demkowicz-Dobrzański, Yanming Che, Dominic Branford, Dominik Šafránek, Jasminder Sidhu, Wenchao Ge, Jesus Rubio, Wojciech Rzadkowski, Marco Genoni, Haggai Landa and two anonymous referees for for helpful discussions and suggestions. JL particularly thanks Yanyan Shao and Jinfeng Qin for the assistance on drawing some of the schematics. JL acknowledges the support from National Natural Science Foundation of China (Grant No. 11805073) and the startup grant of HUST. HY acknowledges the support from the Research Grants Council of Hong Kong (GRF No. 14207717). XML acknowledges the support from the National Natural Science Foundation of China (Grant Nos. 61871162 and 11805048), and Zhejiang Provincial Natural Science Foundation of China (Grant No. LY18A050003). XW acknowledges the support from National Key Research and Development Program of China (Grant Nos. 2017YFA0304202 and 2017YFA0205700), the National Natural Science Foundation of China (Grant Nos. 11935012 and 11875231), and the Fundamental Research Funds for the Central Universities (Grant No. 2017FZA3005).

Appendix A. Derivation of traditional form of QFIM

The traditional calculation of QFIM usually assume a full rank density matrix, of which the spectral decompostion is in the form

$$\rho = \sum_{i=0}^{\dim \rho - 1} \lambda_i |\lambda_i\rangle\langle\lambda_i|, \tag{A.1}$$

where λ_i and $|\lambda_i\rangle$ are ith eigenvalue and eigenstate of ρ. $\dim \rho$ is the dimension of ρ. $|\lambda_i\rangle$ satisfies $\sum_{i=0}^{\dim \rho - 1} |\lambda_i\rangle\langle\lambda_i| = \mathbb{1}$ with $\mathbb{1}$ the identity matrix. Substituting equation (A.1) into the equation of SLD (∂_{x_a} is the abbreviation of ∂/∂_{x_a})

$$\partial_{x_a}\rho = \frac{1}{2}\left(\rho L_{x_a} + L_{x_a}\rho\right), \tag{A.2}$$

and taking $\langle\lambda_i|\cdot|\lambda_j\rangle$ on both sides of above equation, one can obtain

$$\langle\lambda_i|L_{x_a}|\lambda_j\rangle = \frac{2\langle\lambda_i|\partial_{x_a}\rho|\lambda_j\rangle}{\lambda_i+\lambda_j}. \tag{A.3}$$

Next, utlizing equation (A.1), the QFIM

$$\mathcal{F}_{ab} = \frac{1}{2}\mathrm{Tr}\left(\rho\{L_{x_a}, L_{x_b}\}\right) \tag{A.4}$$

can be rewritten as

$$\mathcal{F}_{ab} = \frac{1}{2}\sum_{i=0}^{\dim\rho-1}\lambda_i\left(\langle\lambda_i|L_{x_a}L_{x_b}|\lambda_i\rangle + \langle\lambda_i|L_{x_b}L_{x_a}|\lambda_i\rangle\right). \tag{A.5}$$

Inserting the equation $\mathbb{1} = \sum_{i=0}^{\dim\rho-1}|\lambda_i\rangle\langle\lambda_i|$ into above equation, one can obtain

$$\mathcal{F}_{ab} = \sum_{i,j=0}^{\dim\rho-1}\lambda_i\mathrm{Re}(\langle\lambda_i|L_{x_a}|\lambda_j\rangle\langle\lambda_j|L_{x_b}|\lambda_i\rangle). \tag{A.6}$$

Substituting equation (A.3) into this equation, one has

$$\mathcal{F}_{ab} = \sum_{i,j=0}^{\dim\rho-1}4\lambda_i\frac{\mathrm{Re}(\langle\lambda_i|\partial_{x_a}\rho|\lambda_j\rangle\langle\lambda_j|\partial_{x_b}\rho|\lambda_i\rangle)}{(\lambda_i+\lambda_j)^2}. \tag{A.7}$$

Exchange subscripts i and j, the traditional form of QFIM is obtained as below

$$\mathcal{F}_{ab} = \sum_{i,j=0}^{\dim\rho-1}\frac{2\mathrm{Re}(\langle\lambda_i|\partial_{x_a}\rho|\lambda_j\rangle\langle\lambda_j|\partial_{x_b}\rho|\lambda_i\rangle)}{\lambda_i+\lambda_j}. \tag{A.8}$$

Appendix B. Derivation of QFIM for arbitrary-rank density matrices

In this appendix we show the detailed derivation of QFIM for arbitrary-rank density matrices. Here the spectral decompostion of ρ is

$$\rho = \sum_{i=0}^{N-1}\lambda_i|\lambda_i\rangle\langle\lambda_i|, \tag{B.1}$$

where λ_i and $|\lambda_i\rangle$ are ith eigenvalue and eigenstate of ρ. Notice N here is the dimension of ρ 's support. For a full-rank density matrix, N equals to $\dim\rho$, the dimension of ρ, and for a non-full rank density matrix, $N < \dim\rho$, and $\sum_{i=0}^{N-1}|\lambda_i\rangle\langle\lambda_i| \neq \mathbb{1}$ ($\mathbb{1}$ is the identity matrix and $\mathbb{1} = \sum_{i=0}^{\dim\rho-1}|\lambda_i\rangle\langle\lambda_i|$). Furthermore, $\lambda_i \neq 0$ for $i \in [0, N-1]$. With these notations, $\mathcal{F}_{ab}$ can be expressed by

$$\begin{aligned}\mathcal{F}_{ab} = &\sum_{i=0}^{N-1}\frac{(\partial_{x_a}\lambda_i)(\partial_{x_b}\lambda_i)}{\lambda_i} + \sum_{i=0}^{N-1}4\lambda_i\mathrm{Re}\left(\langle\partial_{x_a}\lambda_i|\partial_{x_b}\lambda_i\rangle\right)\\ &-\sum_{i,j=0}^{N-1}\frac{8\lambda_i\lambda_j}{\lambda_i+\lambda_j}\mathrm{Re}(\langle\partial_{x_a}\lambda_i|\lambda_j\rangle\langle\lambda_j|\partial_{x_b}\lambda_i\rangle).\end{aligned} \tag{B.2}$$

Followings are the detailed proof of this equation.

Based on the equation of SLD (∂_{x_a} is the abbreviation of $\partial/\partial x_a$)

$$\partial_{x_a}\rho = \frac{1}{2}\left(\rho L_{x_a} + L_{x_a}\rho\right), \tag{B.3}$$

one can easily obtain

$$\langle\lambda_i|\partial_{x_a}\rho|\lambda_j\rangle = \frac{1}{2}\langle\lambda_i|L_{x_a}|\lambda_j\rangle\left(\lambda_i + \lambda_j\right). \tag{B.4}$$

The derivative of ρ reads $\partial_{x_a}\rho = \sum_{i=0}^{N-1}\partial_{x_a}\lambda_i|\lambda_i\rangle\langle\lambda_i| + \lambda_i|\partial_{x_a}\lambda_i\rangle\langle\lambda_i| + \lambda_i|\lambda_i\rangle\langle\partial_{x_a}\lambda_i|$, which gives $\langle\lambda_i|\partial_{x_a}\rho|\lambda_j\rangle = \partial_{x_a}\lambda_i\delta_{ij} + \lambda_j\langle\lambda_j|\partial_{x_a}\lambda_i\rangle + \lambda_i\langle\partial_{x_a}\lambda_j|\lambda_i\rangle$. δ_{ij} is the Kronecker delta function ($\delta_{ij} = 1$ for $i = j$ and zero otherwise). Substituting this expression into above equation, $\langle\lambda_i|L_{x_a}|\lambda_j\rangle$ can be calculated as

$$\langle\lambda_i|L_{x_a}|\lambda_j\rangle = \begin{cases} \delta_{ij}\frac{\partial_{x_a}\lambda_i}{\lambda_i} + \frac{2(\lambda_j-\lambda_i)}{\lambda_i+\lambda_j}\langle\lambda_i|\partial_{x_a}\lambda_j\rangle, & i\,\text{or}\,j\in[0,N-1]; \\ \text{arbitrary value}, & i,j\in[N,\dim\rho-1]. \end{cases} \tag{B.5}$$

With the solution of SLD, we can now further calculate the QFIM. Utlizing equation (B.1), the QFIM can be rewritten into

$$\mathcal{F}_{ab} = \frac{1}{2}\sum_{i=0}^{N-1}\lambda_i\left(\langle\lambda_i|L_{x_a}L_{x_b}|\lambda_i\rangle + \langle\lambda_i|L_{x_b}L_{x_a}|\lambda_i\rangle\right). \tag{B.6}$$

Inserting the equation $\mathbb{1} = \sum_{i=0}^{\dim\rho-1}|\lambda_i\rangle\langle\lambda_i|$ into above equation, one can obtain

$$\mathcal{F}_{ab} = \sum_{i=0}^{N-1}\sum_{j=0}^{\dim\rho-1}\lambda_i\text{Re}(\langle\lambda_i|L_{x_a}|\lambda_j\rangle\langle\lambda_j|L_{x_b}|\lambda_i\rangle). \tag{B.7}$$

In this equation, it can be seen that the arbitrary part of $\langle\lambda_i|L_{x_a}|\lambda_j\rangle$ does not affect the value of QFIM since it is not involved in above equation, but it provides a freedom for the optimal measurements, which will be further discussed later. Substituting equation (B.5) into above equation, we have

$$\begin{aligned}\mathcal{F}_{ab} = &\sum_{i,j=0}^{N-1}\delta_{ij}\frac{(\partial_{x_a}\lambda_i)(\partial_{x_b}\lambda_i)}{\lambda_i} + \frac{4\lambda_i(\lambda_i-\lambda_j)^2}{(\lambda_i+\lambda_j)^2}\text{Re}\left(\langle\lambda_i|\partial_{x_a}\lambda_j\rangle\langle\partial_{x_b}\lambda_j|\lambda_i\rangle\right) \\ &+\sum_{i=0}^{N-1}\sum_{j=N}^{\dim\rho-1}4\lambda_i\text{Re}\left(\langle\partial_{x_a}\lambda_i|\lambda_j\rangle\langle\lambda_j|\partial_{x_b}\lambda_i\rangle\right),\end{aligned} \tag{B.8}$$

where the fact $\langle\lambda_i|\partial_{x_a}\lambda_j\rangle = -\langle\partial_{x_a}\lambda_i|\lambda_j\rangle$ has been applied. The third term in above equation can be further calculated as

$$\begin{aligned}
&\sum_{i=0}^{N-1}\sum_{j=N}^{\dim\rho-1} 4\lambda_i \mathrm{Re}\left(\langle\partial_{x_a}\lambda_i|\lambda_j\rangle\langle\lambda_j|\partial_{x_b}\lambda_i\rangle\right)\\
&=\sum_{i=0}^{N-1} 4\lambda_i \mathrm{Re}\left(\langle\partial_{x_a}\lambda_i|\left(\sum_{j=N}^{\dim\rho-1}|\lambda_j\rangle\langle\lambda_j|\right)|\partial_{x_b}\lambda_i\rangle\right)\\
&=\sum_{i=0}^{N-1} 4\lambda_i \mathrm{Re}\left(\langle\partial_{x_a}\lambda_i|\left(\mathbb{1}-\sum_{j=0}^{N-1}|\lambda_j\rangle\langle\lambda_j|\right)|\partial_{x_b}\lambda_i\rangle\right)\\
&=\sum_{i=0}^{N-1} 4\lambda_i \mathrm{Re}\left(\langle\partial_{x_a}\lambda_i|\partial_{x_b}\lambda_i\rangle-\sum_{j=0}^{N-1}\langle\partial_{x_a}\lambda_i|\lambda_j\rangle\langle\lambda_j|\partial_{x_b}\lambda_i\rangle\right).
\end{aligned} \tag{B.9}$$

Therefore equation (B.8) can be rewritten into

$$\begin{aligned}
\mathcal{F}_{ab}=&\sum_{i,j=0}^{N-1}\delta_{ij}\frac{(\partial_{x_a}\lambda_i)(\partial_{x_b}\lambda_i)}{\lambda_i}+\frac{4\lambda_i(\lambda_i-\lambda_j)^2}{(\lambda_i+\lambda_j)^2}\mathrm{Re}\left(\langle\lambda_i|\partial_{x_a}\lambda_j\rangle\langle\partial_{x_b}\lambda_j|\lambda_i\rangle\right)\\
&+\sum_{i=0}^{N-1}4\lambda_i\mathrm{Re}\left(\langle\partial_{x_a}\lambda_i|\partial_{x_b}\lambda_i\rangle\right)-\sum_{i,j=0}^{N-1}4\lambda_i\mathrm{Re}\left(\langle\partial_{x_a}\lambda_i|\lambda_j\rangle\langle\lambda_j|\partial_{x_b}\lambda_i\rangle\right).
\end{aligned}$$

Exchange the subscripts i and j in the second and fourth terms of above equation, it reduces into a symmetric form as shown in equation (B.2).

Appendix C. QFIM in Bloch representation

Bloch representation is a well-used representation of quantum states in quantum mechanics and quantum information theory. For a d-dimensional quantum state ρ, it can be expressed by

$$\rho=\frac{1}{d}\left(\mathbb{1}+\sqrt{\frac{d(d-1)}{2}}\vec{r}\cdot\vec{\kappa}\right), \tag{C.1}$$

where $\vec{r}=(r_1,r_2...,r_k,...)^{\mathrm{T}}$ is the Bloch vector ($|\vec{r}|^2\leqslant 1$) and $\vec{\kappa}$ is a (d^2-1)-dimensional vector of $\mathfrak{su}(d)$ generator satisfying $\mathrm{Tr}(\kappa_i)=0$ and

$$\{\kappa_i,\kappa_j\}=\frac{4}{d}\delta_{ij}\mathbb{1}+\sum_{m=1}^{d^2-1}\mu_{ijm}\kappa_m, \tag{C.2}$$

$$[\kappa_i,\kappa_j]=\mathrm{i}\sum_{m=1}^{d^2-1}\epsilon_{ijm}\kappa_m, \tag{C.3}$$

where δ_{ij} is the Kronecker delta function. μ_{ijm} and ϵ_{ijm} are the symmetric and antisymmetric structure constants, which can be calculated via the following equations

$$\mu_{ijl}=\frac{1}{2}\mathrm{Tr}\left(\{\kappa_i,\kappa_j\}\kappa_l\right), \tag{C.4}$$

$$\epsilon_{ijl} = -\frac{\mathrm{i}}{2}\mathrm{Tr}\left([\kappa_i, \kappa_j]\kappa_l\right). \tag{C.5}$$

It is easy to find $\mathrm{Tr}(\kappa_i\kappa_j) = 2\delta_{ij}$ and μ_{ijl} keeps still for any order of ijl, which will be used in the following.

Now we express the SLD operator with the $\mathfrak{su}(d)$ generators as [43, 44]

$$L_{x_a} = z_a\mathbb{1} + \vec{y}_a \cdot \vec{\kappa}, \tag{C.6}$$

where z_a is a number and $\vec{y}_a$ is a vector. In the following we only use z and $\vec{y}$ for convenience. From the equation $\partial_{x_a}\rho = \frac{1}{2}(\rho L + L\rho)$, one can find

$$c\partial_{x_a}\vec{r}\cdot\vec{\kappa} = \frac{z}{d}\mathbb{1} + \frac{1}{d}\vec{y}\cdot\vec{\kappa} + cz\vec{r}\cdot\vec{\kappa} + \frac{c}{2}\{\vec{r}\cdot\vec{\kappa}, \vec{y}\cdot\vec{\kappa}\}, \tag{C.7}$$

where $c = \sqrt{(d-1)/(2d)}$. Furthermore,

$$\frac{c}{2}\{\vec{r}\cdot\vec{\kappa}, \vec{y}\cdot\vec{\kappa}\} = \sum_{ij} r_i y_j \frac{c}{2}\{\kappa_i, \kappa_j\} = \frac{2c}{d}\vec{y}\cdot\vec{r}\mathbb{1} + \frac{c}{2}\sum_{ijm} r_i y_j \mu_{ijm}\kappa_m. \tag{C.8}$$

The coefficients of $\mathbb{1}$ in equation (C.7) from both sides have to be the same, which gives

$$z = -2c\vec{y}\cdot\vec{r} = -2c\vec{y}^{\mathrm{T}}\vec{r}, \tag{C.9}$$

which can also be obtained from the equation $\mathrm{Tr}(\rho L_{x_a}) = 0$. Similarly, the coefficients of κ_i in equation (C.7) from both sides have to be the same, which gives

$$c\partial_{x_a} r_i = \frac{y_i}{d} + czr_i + \frac{c}{2}\sum_{jm}\mu_{jmi}y_m r_j. \tag{C.10}$$

This can also be obtained by multipling κ_i on both sides of equation (C.7) and then taking the trace. Now we introduce the matrix G with the entry

$$G_{ij} = \frac{1}{2}\mathrm{Tr}(\rho\{\kappa_i, \kappa_j\}). \tag{C.11}$$

It is easy to see G is real symmetric. Substituting equation (C.2) into the equation above, it can be further written into

$$G_{ij} = \frac{2}{d}\delta_{ij} + c\sum_m \mu_{ijm}r_m. \tag{C.12}$$

Hence, the last term in equation (C.10) can be rewritten into

$$\begin{aligned}\frac{c}{2}\sum_{jm}\mu_{jmi}y_m r_j &= \frac{c}{2}\sum_m y_m \sum_j \mu_{jmi}r_j \\ &= \frac{1}{2}\sum_m y_m\left(G_{im} - \frac{2}{d}\delta_{im}\right) \\ &= \frac{1}{2}\sum_m G_{im}y_m - \frac{y_i}{d}.\end{aligned} \tag{C.13}$$

Substituting this equation into equation (C.10), one has $c\partial_{x_a}r_i = czr_i + \frac{1}{2}\sum_m G_{im}y_m$, which immediately leads to

$$c\partial_{x_a}\vec{r} = cz\vec{r} + \frac{1}{2}G\vec{y}. \tag{C.14}$$

Futhermore, one can check that

$$(\vec{r}\,\vec{r}^{\mathrm{T}})\vec{y} = \left(\vec{y}^{\mathrm{T}}\vec{r}\right)\vec{r} = -\frac{1}{2c}z\vec{r}. \tag{C.15}$$

Utilizing this equation, equation (C.14) reduces to

$$c\partial_{x_a}\vec{r} = -2c^2\left(\vec{r}\,\vec{r}^{\mathrm{T}}\right)\vec{y} + \frac{1}{2}G\vec{y}. \tag{C.16}$$

Therefore,

$$\vec{y} = \left(\frac{1}{2c}G - 2c\,\vec{r}\,\vec{r}^{\mathrm{T}}\right)^{-1}\partial_{x_a}\vec{r}. \tag{C.17}$$

Next, we calculate the entry of QFIM and we will use the full notation z_a and $\vec{y}_a$ instead of z, $\vec{y}$. The entry of QFIM reads

$$\begin{aligned}\mathcal{F}_{ab} &= \frac{1}{2}\mathrm{Tr}(\rho\{L_a, L_b\}) \\ &= z_a z_b + 2c(z_a\vec{y}_b\cdot\vec{r} + z_b\vec{y}_a\cdot\vec{r}) + \frac{1}{2}\sum_{ij} y_{a,i}y_{b,j}\mathrm{Tr}\left(\rho\{\kappa_i,\kappa_j\}\right) \\ &= -z_a z_b + \vec{y}_a^{\mathrm{T}}G\vec{y}_b.\end{aligned} \tag{C.18}$$

Based on equations (C.9) and (C.14), one can obtain

$$c\vec{y}_a^{\mathrm{T}}\partial_{x_b}\vec{r} = cz_b\vec{y}_a^{\mathrm{T}}\vec{r} + \frac{1}{2}\vec{y}_a^{\mathrm{T}}G\vec{y}_b = -\frac{1}{2}z_a z_b + \frac{1}{2}\vec{y}_a^{\mathrm{T}}G\vec{y}_b. \tag{C.19}$$

Hence, the QFIM can be written as

$$\mathcal{F}_{ab} = 2c\vec{y}_a^{\mathrm{T}}\partial_{x_b}\vec{r} = 2c(\partial_{x_b}\vec{r})^{\mathrm{T}}\vec{y}_a. \tag{C.20}$$

Utilizing equation (C.17), the QFIM can be finally written into

$$\begin{aligned}\mathcal{F}_{ab} &= 2c(\partial_{x_b}\vec{r})^{\mathrm{T}}\left(\frac{1}{2c}G - 2c\,\vec{r}\,\vec{r}^{\mathrm{T}}\right)^{-1}\partial_{x_a}\vec{r} \\ &= (\partial_{x_b}\vec{r})^{\mathrm{T}}\left(\frac{1}{4c^2}G - \vec{r}\,\vec{r}^{\mathrm{T}}\right)^{-1}\partial_{x_a}\vec{r} \\ &= (\partial_{x_b}\vec{r})^{\mathrm{T}}\left(\frac{d}{2(d-1)}G - \vec{r}\,\vec{r}^{\mathrm{T}}\right)^{-1}\partial_{x_a}\vec{r}.\end{aligned} \tag{C.21}$$

The theorem has been proved.

The simplest case here is single-qubit systems. The corresponding density matrix is $\rho = \frac{1}{2}(\mathbb{1}_2 + \vec{r}\cdot\vec{\sigma})$ with $\vec{\sigma} = (\sigma_1, \sigma_2, \sigma_3)$ the vector of Pauli matrices and $\mathbb{1}_2$ is the 2 by 2 identity matrix. In this case, $G = \mathbb{1}_3$ ($\mathbb{1}_3$ is the 3 by 3 identity matrix) due to the fact $\{\sigma_i, \sigma_j\} = 2\delta_{ij}\mathbb{1}_2$. Equation (C.21) then reduces to

$$\mathcal{F}_{ab} = (\partial_{x_b}\vec{r})^{\mathrm{T}}\left(\mathbb{1}_3 - \vec{r}\,\vec{r}^{\mathrm{T}}\right)^{-1}\partial_{x_a}\vec{r}. \tag{C.22}$$

It can be checked that

$$\left(\mathbb{1}_3 - \vec{r}\,\vec{r}^{\mathrm{T}}\right)^{-1} = \mathbb{1}_3 + \frac{1}{1-|\vec{r}|^2}\vec{r}\,\vec{r}^{\mathrm{T}}. \tag{C.23}$$

The QFIM then reads

$$\mathcal{F}_{ab} = (\partial_{x_b}\vec{r})^{\mathrm{T}}(\partial_{x_a}\vec{r}) + \frac{\left[(\partial_{x_a}\vec{r})^{\mathrm{T}}\vec{r}\right]\left[(\partial_{x_b}\vec{r})^{\mathrm{T}}\vec{r}\right]}{1-|\vec{r}|^2}, \tag{C.24}$$

or equivalently,

$$\mathcal{F}_{ab} = (\partial_{x_a}\vec{r})\cdot(\partial_{x_b}\vec{r}) + \frac{(\vec{r}\cdot\partial_{x_a}\vec{r})(\vec{r}\cdot\partial_{x_b}\vec{r})}{1-|\vec{r}|^2}. \tag{C.25}$$

Appendix D. One-qubit basis-independent expression of QFIM

This appendix shows the proof of theorem 2.6. We first prove that the QFIM for one-qubit mixed state can be written as [46]

$$\mathcal{F}_{ab} = \mathrm{Tr}\left[(\partial_{x_a}\rho)(\partial_{x_b}\rho)\right] + \frac{1}{\det\rho}\mathrm{Tr}\left[(\partial_{x_a}\rho-\rho\partial_{x_a}\rho)(\partial_{x_b}\rho-\rho\partial_{x_b}\rho)\right]. \tag{D.1}$$

Utilizing the spectral decomposition $\rho = \lambda_0|\lambda_0\rangle\langle\lambda_0| + \lambda_1|\lambda_1\rangle\langle\lambda_1|$, the first term reads

$$\begin{aligned}\mathrm{Tr}[(\partial_{x_a}\rho)(\partial_{x_b}\rho)] = {}& \langle\lambda_0|\partial_{x_a}\rho|\lambda_0\rangle\langle\lambda_0|\partial_{x_b}\rho|\lambda_0\rangle + \langle\lambda_1|\partial_{x_a}\rho|\lambda_1\rangle\langle\lambda_1|\partial_{x_b}\rho|\lambda_1\rangle \\ & + 2\mathrm{Re}(\langle\lambda_0|\partial_{x_a}\rho|\lambda_1\rangle\langle\lambda_1|\partial_{x_b}\rho|\lambda_0\rangle).\end{aligned} \tag{D.2}$$

The second term

$$\begin{aligned}&\frac{1}{\det\rho}\mathrm{Tr}\left[(\partial_{x_a}\rho-\rho\partial_{x_a}\rho)(\partial_{x_b}\rho-\rho\partial_{x_b}\rho)\right] \\ &= \frac{1}{\det\rho}\mathrm{Tr}\left[(\partial_{x_a}\rho)(\partial_{x_b}\rho) + \rho(\partial_{x_a}\rho)\rho(\partial_{x_b}\rho) - \rho\{\partial_{x_a}\rho,\partial_{x_b}\rho\}\right].\end{aligned} \tag{D.3}$$

Since

$$\begin{aligned}&\frac{1}{\det\rho}\mathrm{Tr}\left[\rho(\partial_{x_a}\rho)\rho(\partial_{x_b}\rho)\right] \\ &= \frac{\lambda_0}{\lambda_1}\langle\lambda_0|\partial_{x_a}\rho|\lambda_0\rangle\langle\lambda_0|\partial_{x_b}\rho|\lambda_0\rangle + \frac{\lambda_1}{\lambda_0}\langle\lambda_1|\partial_{x_a}\rho|\lambda_1\rangle\langle\lambda_1|\partial_{x_b}\rho|\lambda_1\rangle \\ &+ 2\mathrm{Re}(\langle\lambda_0|\partial_{x_a}\rho|\lambda_1\rangle\langle\lambda_1|\partial_{x_b}\rho|\lambda_0\rangle),\end{aligned} \tag{D.4}$$

and

$$\begin{aligned}&-\frac{1}{\det\rho}\mathrm{Tr}\left[\rho\{\partial_{x_a}\rho,\partial_{x_b}\rho\}\right] \\ &= -\frac{2}{\lambda_1}\langle\lambda_0|\partial_{x_a}\rho|\lambda_0\rangle\langle\lambda_0|\partial_{x_b}\rho|\lambda_0\rangle - \frac{2}{\lambda_0}\langle\lambda_1|\partial_{x_a}\rho|\lambda_1\rangle\langle\lambda_1|\partial_{x_b}\rho|\lambda_1\rangle \\ &- \frac{2}{\lambda_0\lambda_1}\mathrm{Re}(\langle\lambda_0|\partial_{x_a}\rho|\lambda_1\rangle\langle\lambda_1|\partial_{x_b}\rho|\lambda_0\rangle),\end{aligned} \tag{D.5}$$

one can finally obtain

$$\begin{aligned}&\mathrm{Tr}\left[(\partial_{x_a}\rho)(\partial_{x_b}\rho)\right] + \frac{1}{\det\rho}\mathrm{Tr}\left[(\partial_{x_a}\rho-\rho\partial_{x_a}\rho)(\partial_{x_b}\rho-\rho\partial_{x_b}\rho)\right] \\ &= \frac{1}{\lambda_0}\langle\lambda_0|\partial_{x_a}\rho|\lambda_0\rangle\langle\lambda_0|\partial_{x_b}\rho|\lambda_0\rangle + \frac{1}{\lambda_1}\langle\lambda_1|\partial_{x_a}\rho|\lambda_1\rangle\langle\lambda_1|\partial_{x_b}\rho|\lambda_1\rangle \\ &+ 4\mathrm{Re}(\langle\lambda_0|\partial_{x_a}\rho|\lambda_1\rangle\langle\lambda_1|\partial_{x_b}\rho|\lambda_0\rangle),\end{aligned} \tag{D.6}$$

which coincides with the traditional formula of QFIM in theorem 2.1. Equation (D.1) is then proved. Furthermore, one may notice that $\langle\lambda_0|\partial_{x_a}\rho|\lambda_0\rangle = \partial_{x_a}\lambda_0$, $\langle\lambda_1|\partial_{x_a}\rho|\lambda_1\rangle = \partial_{x_a}\lambda_1$, and $\langle\lambda_0|\partial_{x_a}\rho|\lambda_1\rangle = \langle\partial_{x_a}\lambda_0|\lambda_1\rangle + \langle\lambda_0|\partial_{x_a}\lambda_1\rangle = 0$, which gives

$$\begin{aligned}&\mathrm{Tr}\left[(\partial_{x_a}\rho)(\partial_{x_b}\rho) - \rho\{\partial_{x_a}\rho, \partial_{x_b}\rho)\}\right]\\ &= (\partial_{x_a}\lambda_0)(\partial_{x_b}\lambda_0) - \lambda_0(\partial_{x_a}\lambda_0)(\partial_{x_b}\lambda_0) - \lambda_1(\partial_{x_a}\lambda_1)(\partial_{x_b}\lambda_1)\\ &= 0,\end{aligned} \tag{D.7}$$

namely, the equality $\mathrm{Tr}\left[(\partial_{x_a}\rho)(\partial_{x_b}\rho)\right] = \mathrm{Tr}\left(\rho\{\partial_{x_a}\rho, \partial_{x_b}\rho)\}\right)$ holds for single-qubit mixed states. Thus, equation (D.1) can further reduce to

$$\mathcal{F}_{ab} = \mathrm{Tr}\left[(\partial_{x_a}\rho)(\partial_{x_b}\rho)\right] + \frac{1}{\det\rho}\mathrm{Tr}\left[(\rho(\partial_{x_a}\rho)\rho(\partial_{x_b}\rho)\right]. \tag{D.8}$$

The theorem has been proved.

Appendix E. Derivation of SLD operator for Gaussian states

E.1. SLD operator for multimode Gaussian states

The derivation in this appendix is majorly based on the calculation in [62, 67]. Let us first recall the notations before the derivation. The vector of quadrature operators are defined as $\vec{R} = (\hat{q}_1, \hat{p}_1, ..., \hat{q}_m, \hat{p}_m)^{\mathrm{T}}$. Ω is a symplectic matrix $\Omega = \mathrm{i}\sigma_y^{\oplus m}$. $\chi(\vec{s})$ is the characteristic function. Furthermore, denote $d = \langle\vec{R}\rangle$. To keep the calculation neat, we use χ, ρ, L instead of $\chi(\vec{s})$, ρ, L_{x_a} in this appendix. Some other notations are $\langle\cdot\rangle = \mathrm{Tr}(\rho\cdot)$ and $\dot{A} = \partial_{x_a}A$.

The characteristic function $\chi = \langle D\rangle$, where $D = \mathrm{e}^{\mathrm{i}\vec{R}^{\mathrm{T}}\Omega\vec{s}}$ with $\vec{s}\in\mathbb{R}^{2m}$. Substituting D into the equation $\partial_{x_a}\rho = \frac{1}{2}(\rho L + L\rho)$ and taking the trace, we obtain

$$\partial_{x_a}\chi = \frac{1}{2}\langle\{L, D\}\rangle. \tag{E.1}$$

Next, assume the SLD operator is in the following form

$$L = L^{(0)}\mathbb{1} + \vec{L}^{(1),\mathrm{T}}\vec{R} + \vec{R}^{\mathrm{T}}G\vec{R}, \tag{E.2}$$

where $L^{(0)}$ is a real number, $\vec{L}^{(1)}$ is a $2m$-dimensional real vector and G is a $2m$-dimensional real symmetric matrix. These conditions promise the Hermiticity of SLD. With this ansatz, equation (E.1) can then be rewritten into

$$\partial_{x_a}\chi = L^{(0)}\chi + \frac{1}{2}\sum_i L_i^{(1)}\langle\{R_i, D\}\rangle + \frac{1}{4}\sum_{ij} G_{ij}\langle\{\{R_i, R_j\}, D\}\rangle. \tag{E.3}$$

Now we calculate $\langle\{R_i, D\}\rangle$ in equation (E.3). Denote $[A, \cdot] = A^{\times}(\cdot)$, one can have

$$\begin{aligned}
\partial_{s_k} D &= \sum_i \mathrm{i}\Omega_{ik} \int_0^1 \mathrm{e}^{\mathrm{i}y\vec{R}^{\mathrm{T}}\Omega\vec{s}} R_i \mathrm{e}^{-\mathrm{i}y\vec{R}^{\mathrm{T}}\Omega\vec{s}} \mathrm{d}y D \\
&= \sum_i \mathrm{i}\Omega_{ik} \int_0^1 \sum_n \frac{(\mathrm{i}y\vec{R}^{\mathrm{T}}\Omega\vec{s})^{\times,n}}{n!} R_i \mathrm{d}y D \\
&= \sum_i \mathrm{i}\Omega_{ik} \int_0^1 R_i + y\left[\mathrm{i}\vec{R}^{\mathrm{T}}\Omega\vec{s}, R_i\right] \mathrm{d}y D \\
&= \sum_i \mathrm{i}\Omega_{ik} \left(R_i + \frac{1}{2}\sum_{jl} \Omega_{ij}\Omega_{jl} s_l\right) D \\
&= \mathrm{i}\sum_i \Omega_{ki} \left(\frac{1}{2} s_i - R_i\right) D,
\end{aligned} \tag{E.4}$$

where we have used the fact $\Omega_{ij} = -\Omega_{ji}$ and $\sum_j \Omega_{ij}\Omega_{jk} = -\delta_{ik}$ which come from the equation $\Omega^2 = -\mathbb{1}_{2m}$. Substituting the equation

$$\int_0^1 \mathrm{e}^{\mathrm{i}y\vec{R}^{\mathrm{T}}\Omega\vec{s}} R_i \mathrm{e}^{-\mathrm{i}y\vec{R}^{\mathrm{T}}\Omega\vec{s}} \mathrm{d}y D = D \int_0^1 \mathrm{e}^{-\mathrm{i}y\vec{R}^{\mathrm{T}}\Omega\vec{s}} R_i \mathrm{e}^{\mathrm{i}y\vec{R}^{\mathrm{T}}\Omega\vec{s}} \mathrm{d}y, \tag{E.5}$$

into the first line of equation (E.4) and repeat the calculation, one can obtain $\partial_{s_k} D = -\mathrm{i}\sum_i \Omega_{ki} D\left(\frac{1}{2} s_i + R_i\right)$. Combining this equation with equation (E.4), $\partial_{s_k} D$ can be finally written as

$$\partial_{s_k} D = -\frac{\mathrm{i}}{2}\sum_i \Omega_{ki}\{R_i, D\}, \tag{E.6}$$

which further gives $\langle\partial_{s_k} D\rangle = -\frac{\mathrm{i}}{2}\sum_i \Omega_{ki}\langle\{R_i, D\}\rangle$. Based on this equation, it can be found $\sum_k \Omega_{jk}\langle\partial_{s_k} D\rangle = -\frac{\mathrm{i}}{2}\sum_{ik} \Omega_{jk}\Omega_{ki}\langle\{R_i, D\}\rangle$. Again since $\sum_k \Omega_{jk}\Omega_{ki} = -\delta_{ij}$, it reduces to

$$\langle\{R_j, D\}\rangle = -\mathrm{i}2\sum_k \Omega_{jk}\langle\partial_{s_k} D\rangle = -\mathrm{i}2\sum_k \Omega_{jk}\partial_{s_k}\chi. \tag{E.7}$$

Next, continue to take the derivative on $\partial_{s_k} D$, we have

$$\partial_{s_{k'}}\partial_{s_k} D = -\frac{\mathrm{i}}{2}\sum_i \Omega_{ki}\{R_i, \partial_{s_{k'}} D\} - \frac{1}{4}\sum_{ij} \Omega_{k'j}\Omega_{ki}\{R_i, \{R_j, D\}\}. \tag{E.8}$$

Due to the Baker–Campbell–Hausdorff formula, $D^{\dagger} R_i D = R_i + [-\mathrm{i}\vec{R}^{\mathrm{T}}\Omega\vec{s}, R_i] = R_i + s_i$, the commutation between R_i and D can be obtained as $[R_i, D] = s_i D$, which further gives $\{R_i, \{R_j, D\}\} = \{\{R_i, R_j\}, D\} - s_i s_j D$. Then equation (E.8) can be rewritten into

$$\partial_{s_{k'}}\partial_{s_k} D = -\frac{1}{4}\sum_{ij} \Omega_{k'j}\Omega_{ki}\{\{R_i, R_j\}, D\} + \frac{1}{4}\sum_{ij} \Omega_{k'j}\Omega_{ki} s_i s_j D. \tag{E.9}$$

And one can finally obtain

$$\begin{aligned}
\langle\{R_i, \{R_j, D\}\}\rangle &= -4\sum_{kk'} \Omega_{ik}\Omega_{jk'}\langle\partial_{s_{k'}}\partial_{s_k} D\rangle + s_i s_j \chi \\
&= -4\sum_{kk'} \Omega_{ik}\Omega_{jk'}\left(\partial_{s_{k'}}\partial_{s_k}\chi\right) + s_i s_j \chi.
\end{aligned} \tag{E.10}$$

With equations (E.7) and (E.10), equation (E.3) can be expressed by

$$\partial_{x_a}\chi = \left(L^{(0)} + \frac{1}{4}\sum_{ij} G_{ij}s_i s_j\right)\chi - \mathrm{i}\sum_{ik} L_i^{(1)}\Omega_{ik}(\partial_{s_k}\chi) - \sum_{ijkk'} G_{ij}\Omega_{ik}\Omega_{jk'}(\partial_{s_{k'}}\partial_{s_k}\chi). \tag{E.11}$$

On the other hand, from the expression of characteristic function

$$\chi = \mathrm{e}^{-\frac{1}{2}\vec{s}^{\mathrm{T}}\Omega C\Omega^{\mathrm{T}}\vec{s} - \mathrm{i}(\Omega d)^{\mathrm{T}}\vec{s}} \tag{E.12}$$

it can be found that

$$\partial_{x_a}\chi = \left[-\frac{1}{2}\vec{s}^{\mathrm{T}}\Omega\dot{C}\Omega^{\mathrm{T}}\vec{s} - \mathrm{i}(\Omega\dot{d})^{\mathrm{T}}\vec{s}\right]\chi, \tag{E.13}$$

and

$$\begin{aligned}
\partial_{s_k}\chi &= -\sum_{ijl}\Omega_{kl}\Omega_{ij}C_{jl}s_i\chi - \mathrm{i}\sum_i \Omega_{ki}d_i\chi,\\
\partial_{s_{k'}}\partial_{s_k}\chi &= -\sum_{i_1j_1}\Omega_{ki_1}\Omega_{k'j_1}C_{i_1j_1}\chi - \sum_{i_1j_1}\Omega_{ki_1}\Omega_{k'j_1}d_{i_1}d_{j_1}\chi\\
&\quad + \sum_{i_1j_1l_1i_2j_2l_2}\Omega_{kl_1}\Omega_{k'l_2}\Omega_{i_1j_1}\Omega_{i_2j_2}C_{j_1l_1}C_{j_2l_2}s_{i_1}s_{i_2}\chi\\
&\quad + \mathrm{i}\sum_{i_1j_1l_1i_2}\left(\Omega_{ki_2}\Omega_{k'l_1} + \Omega_{k'i_2}\Omega_{kl_1}\right)\Omega_{i_1j_1}C_{j_1l_1}s_{i_1}d_{i_2}\chi.
\end{aligned}$$

Then we have $-\mathrm{i}\sum_{ik} L_i^{(1)}\Omega_{ik}(\partial_{s_k}\chi) = \sum_i L_i^{(1)}\left(-\mathrm{i}\sum_{jk}\Omega_{kj}C_{ij}s_k + d_i\right)\chi$, and

$$\begin{aligned}
&-\sum_{ijkk'} G_{ij}\Omega_{ik}\Omega_{jk'}(\partial_{s_{k'}}\partial_{s_k}\chi)\\
&= \sum_{ij} G_{ij}\left(C_{ij} + d_i d_j\right)\chi - \sum_{iji_1j_1i_2j_2} G_{ij}\Omega_{i_1j_1}\Omega_{i_2j_2}C_{ij_1}C_{jj_2}s_{i_1}s_{i_2}\chi\\
&\quad - \mathrm{i}\sum_{iji_1j_1} G_{ij}\Omega_{i_1j_1}s_{i_1}\left(C_{jj_1}d_i + C_{ij_1}d_j\right)\chi.
\end{aligned}$$

Substituting these equations into equation (E.11), $\partial_{x_a}\chi$ can be expressed by

$$\begin{aligned}
\partial_{x_a}\chi &= \left(L^{(0)} + \frac{1}{4}\sum_{ij} G_{ij}s_i s_j\right)\chi + \sum_i L_i^{(1)}\left(-\mathrm{i}\sum_{jk}\Omega_{kj}C_{ij}s_k + d_i\right)\chi\\
&\quad + \sum_{ij} G_{ij}\left(C_{ij} + d_i d_j\right)\chi - \sum_{iji_1j_1i_2j_2} G_{ij}\Omega_{i_1j_1}\Omega_{i_2j_2}C_{ij_1}C_{jj_2}s_{i_1}s_{i_2}\chi\\
&\quad - \mathrm{i}\sum_{iji_1j_1} G_{ij}\Omega_{i_1j_1}s_{i_1}\left(C_{jj_1}d_i + C_{ij_1}d_j\right)\chi.
\end{aligned} \tag{E.14}$$

This equation can be written into a more compact way as below

$$\begin{aligned}\partial_{x_a}\chi = L^{(0)}\chi + \vec{L}^{(1),\mathrm{T}}\mathrm{d}\chi + \mathrm{Tr}(GC)\chi + d^{\mathrm{T}}G\mathrm{d}\chi \\ + \mathrm{i}\vec{L}^{(1),\mathrm{T}}C\Omega\vec{s}\chi + \mathrm{i}2d^{\mathrm{T}}GC\Omega\vec{s}\chi + \vec{s}^{\mathrm{T}}\Omega CGC\Omega\vec{s}\chi + \frac{1}{4}\vec{s}^{\mathrm{T}}G\vec{s}\chi.\end{aligned} \tag{E.15}$$

Compare this equation with equation (E.13), it can be found that

$$L^{(0)} + L^{(1),\mathrm{T}}d + \mathrm{Tr}(GC) + d^{\mathrm{T}}Gd = 0, \tag{E.16}$$

$$\vec{L}^{(1),\mathrm{T}}C\Omega + 2d^{\mathrm{T}}GC\Omega = -\dot{d}^{\mathrm{T}}\Omega^{\mathrm{T}}, \tag{E.17}$$

$$\frac{1}{4}G + \Omega CGC\Omega = -\frac{1}{2}\Omega\dot{C}\Omega^{\mathrm{T}}. \tag{E.18}$$

From the second equation above, one can obtain

$$\vec{L}^{(1)} = C^{-1}\dot{d} - 2Gd. \tag{E.19}$$

Using this equation and the equation (E.16), it can be found that

$$L^{(0)} = d^{\mathrm{T}}Gd - \dot{d}^{\mathrm{T}}C^{-1}d - \mathrm{Tr}(GC). \tag{E.20}$$

Once we obtain the expression of G, $L^{(0)}$ and $\vec{L}^{(1)}$ can be obtained correspondingly, which means we need to solve equation (E.18), which can be rewritten into following form

$$\Omega G\Omega + 4CGC = 2\dot{C}. \tag{E.21}$$

Since $C = SC_{\mathrm{d}}S^{\mathrm{T}}$ and $S\Omega S^{\mathrm{T}} = \Omega$, above equation can be rewritten into

$$\Omega G_{\mathrm{s}}\Omega + 4C_{\mathrm{d}}G_{\mathrm{s}}C_{\mathrm{d}} = 2S^{-1}\dot{C}\left(S^{\mathrm{T}}\right)^{-1}, \tag{E.22}$$

where $G_{\mathrm{s}} = S^{\mathrm{T}}GS$. Denote the map $\mathcal{E}(G_{\mathrm{s}}) := \Omega G_{\mathrm{s}}\Omega + 4C_{\mathrm{d}}G_{\mathrm{s}}C_{\mathrm{d}}$, then $G_{\mathrm{s}} = \mathcal{E}^{-1}(\mathcal{E}(G_{\mathrm{s}}))$. The map $\mathcal{E}(G_{\mathrm{s}})$ can be decomposed via the generators $\{A_l^{(jk)}\}$ $(j,k = 1,...,m)$, where

$$A_l^{(jk)} = \frac{1}{\sqrt{2}}\mathrm{i}\sigma_y^{(jk)},\ \frac{1}{\sqrt{2}}\sigma_z^{(jk)},\ \frac{1}{\sqrt{2}}\mathbb{1}_2^{(jk)},\ \frac{1}{\sqrt{2}}\sigma_x^{(jk)} \tag{E.23}$$

for $l = 0,1,2,3$. $\sigma_i^{(jk)}$ is a $2m$-dimensional matrix with all the entries zero expect the 2×2 block shown as below

$$\sigma_i^{(jk)} = \begin{pmatrix} & 1\mathrm{st} & \cdots & k\mathrm{th} & \cdots \\ 1\mathrm{st} & 0_{2\times 2} & 0_{2\times 2} & 0_{2\times 2} & 0_{2\times 2} \\ \vdots & 0_{2\times 2} & \vdots & \vdots & \vdots \\ j\mathrm{th} & 0_{2\times 2} & \cdots & \sigma_i & \cdots \\ \vdots & \vdots & \vdots & \vdots & \vdots \end{pmatrix}, \tag{E.24}$$

where $0_{2\times 2}$ represents a 2 by 2 block with zero entries. $\mathbb{1}_2^{(jk)}$ is similar to $\sigma_i^{(jk)}$ but replace the block σ_i with $\mathbb{1}_2$. $A_l^{(jk)}$ satisfies the orthogonal relation $\mathrm{Tr}(A_l^{(jk)}A_{l'}^{(j'k')}) = \delta_{jj'}\delta_{kk'}\delta_{ll'}$. Recall that $C_{\mathrm{d}} = \bigoplus_{k=1}^{m} c_k\mathbb{1}_2$, it is easy to check that

$$\Omega A_l^{(jk)}\Omega = (-1)^{l+1}A_l^{(jk)}, \tag{E.25}$$

$$C_{\mathrm{d}}A_l^{(jk)}C_{\mathrm{d}} = c_jc_kA_l^{(jk)}. \tag{E.26}$$

Next decompose $S^{-1}\dot{C}(S^{\mathrm{T}})^{-1}$ with $\{A_l^{(jk)}\}$ as

$$S^{-1}\dot{C}(S^{\mathrm{T}})^{-1} = \sum_{jkl} g_l^{(jk)} A_l^{(jk)}, \tag{E.27}$$

where $g_l^{(jk)} = \mathrm{Tr}[S^{-1}\dot{C}(S^{\mathrm{T}})^{-1}A_l^{(jk)}]$. Decomposing G_{s} as $G_{\mathrm{s}} = \sum_{jkl}\tilde{g}_l^{(jk)}A_l^{(jk)}$, and substituting it into equation (E.22), we have

$$\sum_{jkl} g_l^{(jk)} \left(\Omega A_l^{(jk)}\Omega + 4C_{\mathrm{d}}A_l^{(jk)}C_{\mathrm{d}}\right) = \sum_{jkl} g_l^{(jk)} A_l^{(jk)}. \tag{E.28}$$

Utilizing equations (E.25) and (E.26), above equation reduces to

$$\sum_{jkl} \tilde{g}_l^{(jk)} \left[4c_jc_k + (-1)^{l+1}\right] A_l^{(jk)} = \sum_{jkl} g_l^{(jk)} A_l^{(jk)}, \tag{E.29}$$

which indicates

$$\tilde{g}_l^{(jk)} = \frac{g_l^{(jk)}}{4c_jc_k + (-1)^{l+1}}. \tag{E.30}$$

Thus, $G = (S^{\mathrm{T}})^{-1}G_{\mathrm{s}}S^{-1}$ can be solved as below

$$G = \sum_{jkl} \frac{g_l^{(jk)}}{4c_jc_k + (-1)^{l+1}} \left(S^{\mathrm{T}}\right)^{-1} A_l^{(jk)} S^{-1}. \tag{E.31}$$

In summary, the SLD can be expressed by

$$L = L^{(0)}\mathbb{1} + \vec{L}^{(1),\mathrm{T}}\vec{R} + \vec{R}^{\mathrm{T}}G\vec{R}, \tag{E.32}$$

where

$$G = \sum_{j,k=1}^{m}\sum_{l=0}^{3} \frac{g_l^{(jk)}}{4c_jc_k + (-1)^{l+1}} \left(S^{\mathrm{T}}\right)^{-1} A_l^{(jk)} S^{-1} \tag{E.33}$$

with

$$A_l^{(jk)} = \frac{1}{\sqrt{2}}\mathrm{i}\sigma_y^{(jk)},\ \frac{1}{\sqrt{2}}\sigma_z^{(jk)},\ \frac{1}{\sqrt{2}}\mathbb{1}_2^{(jk)},\ \frac{1}{\sqrt{2}}\sigma_x^{(jk)} \tag{E.34}$$

for $l = 0, 1, 2, 3$ and $g_l^{(jk)} = \mathrm{Tr}[S^{-1}\dot{C}(S^{\mathrm{T}})^{-1}A_l^{(jk)}]$. And

$$\vec{L}^{(1)} = C^{-1}\dot{d} - 2Gd, \tag{E.35}$$

$$L^{(0)} = d^{\mathrm{T}}Gd - \dot{d}^{\mathrm{T}}C^{-1}d - \mathrm{Tr}(GC). \tag{E.36}$$

E.2. SLD operator for single-mode Gaussian state

For a single-mode case, a 2 by 2 symplectic S matrix satisfies $\det S = 1$. Based on the equation $C = SC_{\mathrm{d}}S^{\mathrm{T}} = cSS^{\mathrm{T}}$ (c is the symplectic value), the following equations can be obtained

$$C_{00} = c(S_{00}^2 + S_{01}^2), \tag{E.37}$$

$$C_{11} = c(S_{10}^2 + S_{11}^2),$$

$$C_{01} = c(S_{00}S_{10} + S_{01}S_{11}). \tag{E.38}$$

Together with the equation $\det S = S_{00}S_{11} - S_{01}S_{10} = 1$, the symplectic value c can be solved as $c = \sqrt{\det C}$. Assume the form

$$S_{00} = \sqrt{\frac{C_{00}}{c}}\cos\theta, \quad S_{01} = \sqrt{\frac{C_{00}}{c}}\sin\theta, \tag{E.39}$$

$$S_{10} = \sqrt{\frac{C_{11}}{c}}\cos\phi, \quad S_{11} = \sqrt{\frac{C_{11}}{c}}\sin\phi. \tag{E.40}$$

Substituting above expressions into equation (E.37), it can be found θ, ϕ need to satisfy

$$\cos(\phi-\theta) = \frac{C_{01}}{\sqrt{C_{00}C_{11}}}, \ \sin(\phi-\theta) = \frac{c}{\sqrt{C_{00}C_{11}}}. \tag{E.41}$$

Since there is only four constrains for these five variables, one of them is free. We take $\theta = \pi/2 - \phi$, and the symplectic matrix reduces to

$$S = \frac{1}{\sqrt{c}}\begin{pmatrix}\sqrt{C_{00}}\sin\phi & \sqrt{C_{00}}\cos\phi \\ \sqrt{C_{11}}\cos\phi & \sqrt{C_{11}}\cos\phi\end{pmatrix}, \tag{E.42}$$

where ϕ satisfies $\sin(2\phi) = \frac{C_{01}}{\sqrt{C_{00}C_{11}}}$ and $\cos(2\phi) = -\frac{c}{\sqrt{C_{00}C_{11}}}$. Based on theorem 2.9, we obtain

$$g_0 = 0, \tag{E.43}$$

$$g_1 = \frac{1}{\sqrt{2C_{00}C_{11}}}C_{11}\dot{C}_{00} - C_{00}\dot{C}_{11}, \tag{E.44}$$

$$g_2 = \sqrt{2}\dot{c}, \tag{E.45}$$

$$g_3 = \frac{\sqrt{2}(c\dot{C}_{01} - \dot{c}C_{01})}{\sqrt{C_{00}C_{11}}}, \tag{E.46}$$

where $\dot{C}$, $\dot{c}$ are short for $\partial_{x_a}C$ and $\partial_{x_a}c$. Meanwhile, we have

$$(S^{\mathrm{T}})^{-1}A_1S^{-1} = \frac{\sqrt{2C_{00}C_{11}}}{2}\begin{pmatrix}\frac{1}{C_{00}} & 0 \\ 0 & -\frac{1}{C_{11}}\end{pmatrix}, \tag{E.47}$$

$$(S^{\mathrm{T}})^{-1}A_2S^{-1} = \frac{1}{\sqrt{2}c}\begin{pmatrix}C_{11} & -C_{01} \\ -C_{01} & C_{00}\end{pmatrix}, \tag{E.48}$$

$$(S^{\mathrm{T}})^{-1}A_3S^{-1} = \frac{\sqrt{C_{00}C_{11}}}{\sqrt{2}c}\begin{pmatrix}-\frac{C_{01}}{C_{00}} & 1 \\ 1 & -\frac{C_{01}}{C_{11}}\end{pmatrix}. \tag{E.49}$$

These expressions immediately give G_{x_a} as below

$$\begin{aligned}[G_{x_a}]_{00} &= \frac{1}{4c^2+1}\left[\frac{C_{11}\dot{C}_{00} - C_{00}\dot{C}_{11}}{2C_{00}} - \frac{C_{01}}{C_{00}}(\dot{C}_{01} - \frac{\dot{c}}{c}C_{01})\right] + \frac{1}{4c^2-1}\frac{\dot{c}}{c}C_{11} \\ &= \frac{1}{4c^2+1}\left(\frac{\dot{c}}{c}C_{11} - \dot{C}_{11}\right) + \frac{1}{4c^2-1}\frac{\dot{c}}{c}C_{11} \\ &= -\frac{1}{16c^4-1}\left[(4c^2-1)C_{11} - 8c\dot{c}C_{11}\right].\end{aligned} \tag{E.50}$$

Define a matrix

$$J := \frac{1}{4c^2-1}C, \tag{E.51}$$

$[G_{x_a}]_{00}$ can be rewritten into

$$[G_{x_a}]_{00} = -\frac{4c^2-1}{4c^2+1}\partial_{x_a}J_{11}. \tag{E.52}$$

Similarly, one can obtain

$$[G_{x_a}]_{11} = -\frac{4c^2-1}{4c^2+1}\partial_{x_a}J_{00}, \tag{E.53}$$

and

$$[G_{x_a}]_{01} = [G_{x_a}]_{10} = \frac{4c^2-1}{4c^2+1}\partial_{x_a}J_{01}. \tag{E.54}$$

These expressions indicate

$$G_{x_a} = \frac{4c^2-1}{4c^2+1}\Omega(\partial_{x_a}J)\Omega, \tag{E.55}$$

with

$$\Omega = \begin{pmatrix} 0 & 1 \\ -1 & 0 \end{pmatrix}. \tag{E.56}$$

Appendix F. QFIM and Bures metric

The Bures distance between two quantum states ρ_1 and ρ_2 is defined as

$$D_{\mathrm{B}}^2(\rho_1,\rho_2) = 2 - 2f(\rho_1,\rho_2), \tag{F.1}$$

where $f(\rho_1,\rho_2) = \mathrm{Tr}\sqrt{\sqrt{\rho_1}\rho_2\sqrt{\rho_1}}$ is the quantum fidelity. Now we calcuate the fidelity for two close quantum states $\rho(\vec{x})$ and $\rho(\vec{x}+\mathrm{d}\vec{x})$. The Taylor series of $\rho(\vec{x}+\mathrm{d}\vec{x})$ (up to the second order) reads

$$\rho(\vec{x}+\mathrm{d}\vec{x}) = \rho(\vec{x}) + \sum_a \partial_{x_a}\rho(\vec{x})\mathrm{d}x_a + \frac{1}{2}\sum_{ab}\frac{\partial^2\rho(\vec{x})}{\partial x_a\partial x_b}\mathrm{d}x_a\mathrm{d}x_b. \tag{F.2}$$

In the following ρ will be used as the abbreviation of $\rho(\vec{x})$. Utilizing the equation above, one can obtain

$$\begin{aligned}&\sqrt{\rho}\rho(\vec{x}+\mathrm{d}\vec{x})\sqrt{\rho}\\ &= \rho^2 + \sum_a \sqrt{\rho}\partial_{x_a}\rho\sqrt{\rho}\mathrm{d}x_a + \frac{1}{2}\sum_{ab}\left(\sqrt{\rho}\frac{\partial^2\rho}{\partial x_a\partial x_b}\sqrt{\rho}\right)\mathrm{d}x_a\mathrm{d}x_b.\end{aligned} \tag{F.3}$$

Now we assume

$$\sqrt{\sqrt{\rho}\rho(\vec{x}+\mathrm{d}\vec{x})\sqrt{\rho}} = \rho + \sum_a W_a\mathrm{d}x_a + \sum_{ab}Y_{ab}\mathrm{d}x_a\mathrm{d}x_b. \tag{F.4}$$

Taking the square of above equation and compare it to equation (F.3), one can obtain

$$\sqrt{\rho}\partial_{x_a}\rho\sqrt{\rho} = \rho W_a + W_a\rho, \tag{F.5}$$

$$\frac{1}{2}\sqrt{\rho}\partial^2\rho\sqrt{\rho} = \rho Y_{ab} + Y_{ab}\rho + \frac{1}{2}\{W_a, W_b\}, \tag{F.6}$$

where $\partial^2\rho$ is short for $\frac{\partial^2\rho}{\partial x_a\partial x_b}$. $\frac{1}{2}\{W_a, W_b\}$ (not W_aW_b) is used to make sure the equation is unchanged when the subscripts a and b exchange. Meawhile, from equation (F.4), the Bures metric $D_{\mathrm{B}}(\rho(\vec{x}), \rho(\vec{x}+\mathrm{d}\vec{x}))$ (the abbreviation D_{B} will bu used below) can be calculated as

$$D_{\mathrm{B}}^2 = -2\sum_a(\mathrm{Tr}W_a)\mathrm{d}x_a - 2\sum_{ab}(\mathrm{Tr}Y_{ab})\mathrm{d}x_a\mathrm{d}x_b. \tag{F.7}$$

As long as we obtain the specific expressions of W_a and Y_{ab} from equations (F.5) and (F.6), D_{B} can be obtained immediately. To do that, we utilize the spectral decomposition $\rho = \sum_i \lambda_i|\lambda_i\rangle\langle\lambda_i|$. In the basis $\{|\lambda_i\rangle\}$, the matrix entries ($[\cdot]_{ij} = \langle\lambda_i|\cdot|\lambda_j\rangle$) read

$$[\sqrt{\rho}\partial_{x_a}\rho\sqrt{\rho}]_{ij} = \sqrt{\lambda_i\lambda_j}[\partial_{x_a}\rho]_{ij}, \tag{F.8}$$

$$\left[\sqrt{\rho}\partial^2\rho\sqrt{\rho}\right]_{ij} = \sqrt{\lambda_i\lambda_j}\left[\partial^2\rho\right]_{ij}. \tag{F.9}$$

Here $[\partial_{x_a}\rho]_{ij} = \delta_{ij}\partial_{x_a}\lambda_i - (\lambda_i-\lambda_j)\langle\lambda_i|\partial_{x_a}\lambda_j\rangle$, and

$$\begin{aligned}\left[\partial^2\rho\right]_{ij} = {}& \partial^2\lambda_i\delta_{ij} + \lambda_i\langle\partial^2\lambda_i|\lambda_j\rangle + \lambda_j\langle\lambda_i|\partial^2\lambda_j\rangle \\ & + (\partial_{x_a}\lambda_j - \partial_{x_a}\lambda_i)\langle\lambda_i|\partial_{x_b}\lambda_j\rangle + (\partial_{x_b}\lambda_j - \partial_{x_b}\lambda_i)\langle\lambda_i|\partial_{x_a}\lambda_j\rangle \\ & + \sum_k \lambda_k(\langle\lambda_i|\partial_{x_a}\lambda_k\rangle\langle\partial_{x_b}\lambda_k|\lambda_j\rangle + \langle\lambda_i|\partial_{x_b}\lambda_k\rangle\langle\partial_{x_a}\lambda_k|\lambda_j\rangle),\end{aligned} \tag{F.10}$$

where $\partial^2\lambda_i$ and $|\partial^2\lambda_i\rangle$ are short for $\frac{\partial^2\lambda_i}{\partial x_a\partial x_b}$ and $\frac{\partial^2}{\partial x_a\partial x_b}|\lambda_i\rangle$. Now we denote ρ's dimension as N and $\lambda_i \in \mathcal{S}$ for $i = 0, 1, 2..., M-1$. Under the assumption that the support $\mathcal{S}$ is not affected by the values of $\vec{x}$, i.e. the rank of $\rho(\vec{x})$ equals to that of $\rho(\vec{x}+\mathrm{d}\vec{x})$, $\sqrt{\rho}\partial_{x_a}\rho\sqrt{\rho}$ and $\sqrt{\rho}\partial^2\rho\sqrt{\rho}$ are both block diagonal. Based on equation (F.5), the ijth matrix entry of W_a can be calculated as

$$[W_a]_{ij} = \frac{\left[\sqrt{\rho}\partial_{x_a}\rho\sqrt{\rho}\right]_{ij}}{\lambda_i+\lambda_j} = \frac{1}{2}\partial_{x_a}\lambda_i\delta_{ij} - \frac{\sqrt{\lambda_i\lambda_j}(\lambda_i-\lambda_j)}{\lambda_i+\lambda_j}\langle\lambda_i|\partial_{x_a}\lambda_j\rangle, \tag{F.11}$$

for $i, j \in [0, M-1]$ and $[W_a]_{ij} = 0$ for others. One can observe that W_a is a Hermitian matrix, and

$$\mathrm{Tr}W_a = \sum_{ii}[W_a]_{ii} = \frac{1}{2}\sum_i \partial_{x_a}\lambda_i = 0, \tag{F.12}$$

which means there is no first order term in Bures metric. With respect to the second order term, we need to know the value of $[Y_{ab}]_{ii}$. From equation (F.6), one can obtain

$$\mathrm{Tr}Y_{ab} = \frac{1}{4}\sum_i[\partial^2\rho]_{ii} - \sum_{ik}\frac{1}{2\lambda_i}\mathrm{Re}\left([W_a]_{ik}[W_b]_{ki}\right). \tag{F.13}$$

Due to the fact $\langle\partial^2\lambda_i|\lambda_i\rangle + \langle\lambda_i|\partial^2\lambda_i\rangle = -2\mathrm{Re}(\langle\partial_{x_a}\lambda_i|\partial_{x_b}\lambda_i\rangle)$, one can have

$$[\partial^2\rho]_{ii} = \partial^2\lambda_i - 2\lambda_i\mathrm{Re}(\langle\partial_{x_a}\lambda_i|\partial_{x_b}\lambda_i\rangle) + \sum_k 2\lambda_k\mathrm{Re}(\langle\lambda_i|\partial_{x_a}\lambda_k\rangle\langle\partial_{x_b}\lambda_k|\lambda_i\rangle), \tag{F.14}$$

which further gives

$$\frac{1}{4}\sum_i[\partial^2\rho]_{ii} = -\frac{1}{2}\sum_i \lambda_i \mathrm{Re}(\langle\partial_{x_a}\lambda_i|\partial_{x_b}\lambda_i\rangle) + \sum_{ik}\frac{1}{4}(\lambda_i+\lambda_k)\mathrm{Re}(\langle\lambda_i|\partial_{x_a}\lambda_k\rangle\langle\partial_{x_b}\lambda_k|\lambda_i\rangle), \tag{F.15}$$

where the fact $\sum_i \partial^2\lambda_i = 0$ has been applied. Next, from equation (F.11) one can obtain

$$[W_a]_{ik}[W_b]_{ki} = \frac{1}{4}(\partial_{x_a}\lambda_i)(\partial_{x_b}\lambda_i) + \sum_k \frac{\lambda_i\lambda_k(\lambda_i-\lambda_k)^2}{(\lambda_i+\lambda_k)^2}\langle\lambda_i|\partial_{x_a}\lambda_k\rangle\langle\partial_{x_b}\lambda_k|\lambda_i\rangle,$$

which means

$$\begin{aligned}
&\sum_{ik}\frac{1}{2\lambda_i}\mathrm{Re}([W_a]_{ik}[W_b]_{ki}) \\
&= \sum_i \frac{1}{8\lambda_i}(\partial_{x_a}\lambda_i)(\partial_{x_b}\lambda_i) + \sum_{ik}\frac{\lambda_k(\lambda_i-\lambda_k)^2}{2(\lambda_i+\lambda_k)^2}\mathrm{Re}(\langle\lambda_i|\partial_{x_a}\lambda_k\rangle\langle\partial_{x_b}\lambda_k|\lambda_i\rangle) \\
&= \sum_i \frac{1}{8\lambda_i}(\partial_{x_a}\lambda_i)(\partial_{x_b}\lambda_i) + \sum_{ik}\frac{(\lambda_i-\lambda_k)^2}{4(\lambda_i+\lambda_k)}\mathrm{Re}(\langle\lambda_i|\partial_{x_a}\lambda_k\rangle\langle\partial_{x_b}\lambda_k|\lambda_i\rangle).
\end{aligned}$$

Thus, $\mathrm{Tr}Y_{ab}$ can then be expressed by

$$\begin{aligned}
\mathrm{Tr}Y_{ab} &= -\frac{1}{8}\left[\sum_i \frac{(\partial_{x_a}\lambda_i)(\partial_{x_b}\lambda_i)}{\lambda_i} + \sum_i 4\lambda_i\mathrm{Re}(\langle\partial_{x_a}\lambda_i|\partial_{x_b}\lambda_i\rangle)\right. \\
&\quad \left. - \sum_{ik}\frac{8\lambda_i\lambda_k}{\lambda_i+\lambda_k}\mathrm{Re}\langle\lambda_i|\partial_{x_a}\lambda_k\rangle\langle\partial_{x_b}\lambda_k|\lambda_i\rangle\right] \\
&= -\frac{1}{8}\mathcal{F}_{ab}.
\end{aligned} \tag{F.16}$$

With this equation, we finally obtain

$$D_{\mathrm{B}}(\rho(\vec{x}),\rho(\vec{x}+\mathrm{d}\vec{x})) = \sum_{ab}\frac{1}{4}\mathcal{F}_{ab}\mathrm{d}x_a x_b. \tag{F.17}$$

One should notice that this proof shows that this relation is established for density matrices with any rank as long as the rank of $\rho(\vec{x})$ is unchanged with the varying of $\vec{x}$. In the case the rank can change, a thorough discussion can be found in [87].

Appendix G. Relation between QFIM and cross-correlation functions

This appendix gives the thorough calculation of the relation between QFIM and dynamic susceptibility in [109]. Consider the unitary parameterization $U = \exp(\mathrm{i}\sum_a x_a O_a)$ with a thermal state $\rho = \frac{1}{Z}\mathrm{e}^{-\beta H}$. Here $Z = \mathrm{Tr}(\mathrm{e}^{-\beta H})$ is the partition function. O_a is a Hermitian generator for x_a. In the following we set $k_B = 1$ and assume all O_a are commutative, i.e. $[O_a, O_b] = 0$ for any a and b. Denote $O_a(t) = \mathrm{e}^{\mathrm{i}Ht}O_a\mathrm{e}^{-\mathrm{i}Ht}$, and $\langle\cdot\rangle = \mathrm{Tr}(\rho\cdot)$, the symmetric cross-correlation spectrum in this case reads

$$S_{ab}(\omega) = \frac{1}{2}\int_{-\infty}^{\infty} \langle\{Q_a(t), O_b\}\rangle \mathrm{e}^{\mathrm{i}\omega t}\mathrm{d}t. \tag{G.1}$$

Utilizing the energy basis $\{|E_i\rangle\}$ (with E_i the ith energy), it can be rewritten into

$$S_{ab}(\omega) = \frac{1}{2Z}\sum_{ij}(\mathrm{e}^{-\beta E_i} + \mathrm{e}^{-\beta E_j})\langle E_i|O_a|E_j\rangle\langle E_j|O_b|E_i\rangle \int_{-\infty}^{\infty} \mathrm{e}^{\mathrm{i}(\omega+E_i-E_j)}\mathrm{d}t.$$

Further use the equation $\int_{-\infty}^{\infty} \mathrm{e}^{\mathrm{i}(\omega+E_i-E_j)}\mathrm{d}t = 2\pi\delta(\omega + E_i - E_j)$, $S_{ab}(\omega)$ can reduce to

$$S_{ab}(\omega) = \frac{\pi}{Z}\sum_{ij}(\mathrm{e}^{-\beta E_i} + \mathrm{e}^{-\beta E_j})\delta(\omega + E_i - E_j)\langle E_i|O_a|E_j\rangle\langle E_j|O_b|E_i\rangle. \tag{G.2}$$

With this expression, one can find

$$\begin{aligned}
&\int_{-\infty}^{\infty} \tanh^2\left(\frac{\omega}{2T}\right) \mathrm{Re}(S_{ab}(\omega))\mathrm{d}\omega \\
&= \sum_{ij}\int_{-\infty}^{\infty} \tanh^2\left(\frac{\omega}{2T}\right)\delta(\omega + E_i - E_j)\mathrm{d}\omega \\
&\times \frac{\pi}{Z}(\mathrm{e}^{-\beta E_i} + \mathrm{e}^{-\beta E_j})\mathrm{Re}(\langle E_i|O_a|E_j\rangle\langle E_j|O_b|E_i\rangle) \\
&= \sum_{ij} \tanh^2\left(\frac{E_j - E_i}{2T}\right)\frac{\pi}{Z}(\mathrm{e}^{-\beta E_i} + \mathrm{e}^{-\beta E_j})\mathrm{Re}(\langle E_i|O_a|E_j\rangle\langle E_j|O_b|E_i\rangle).
\end{aligned}$$

Since

$$\begin{aligned}
\tanh\left(\frac{E_i - E_j}{2T}\right) &= \frac{[\mathrm{e}^{\frac{1}{2}\beta(E_i-E_j)} - \mathrm{e}^{-\frac{1}{2}\beta(E_i-E_j)}]\mathrm{e}^{-\frac{1}{2}\beta(E_i+E_j)}}{[\mathrm{e}^{\frac{1}{2}\beta(E_i-E_j)} + \mathrm{e}^{-\frac{1}{2}\beta(E_i-E_j)}]\mathrm{e}^{-\frac{1}{2}\beta(E_i+E_j)}} \\
&= \frac{\mathrm{e}^{-\beta E_j} - \mathrm{e}^{-\beta E_i}}{\mathrm{e}^{-\beta E_i} + \mathrm{e}^{-\beta E_j}},
\end{aligned} \tag{G.3}$$

one can obtain

$$\int_{-\infty}^{\infty} \tanh^2\left(\frac{\omega}{2T}\right) \mathrm{Re}(S_{ab}(\omega))\mathrm{d}\omega \tag{G.4}$$

$$= \pi\sum_{ij}\frac{\left(\frac{1}{Z}\mathrm{e}^{\beta E_i} - \frac{1}{Z}\mathrm{e}^{-\beta E_j}\right)^2}{\frac{1}{Z}\mathrm{e}^{-\beta E_i} + \frac{1}{Z}\mathrm{e}^{-\beta E_j}}\mathrm{Re}(\langle E_i|O_a|E_j\rangle\langle E_j|O_b|E_i\rangle). \tag{G.5}$$

From the expression of QFIM, it can be found that

$$\mathcal{F}_{ab} = \frac{4}{\pi}\int_{-\infty}^{\infty} \tanh^2\left(\frac{\omega}{2T}\right) \mathrm{Re}(S_{ab}(\omega))\mathrm{d}\omega. \tag{G.6}$$

It can also be checked that

$$\mathrm{Re}(S_{ab}(\omega)) = \frac{1}{2}\int_{-\infty}^{\infty} \langle Q_a(t)O_b + O_b(t)O_a\rangle \mathrm{e}^{\mathrm{i}\omega t}\mathrm{d}t. \tag{G.7}$$

In the mean time, the asymmetric cross-correlation spectrum is in the form

$$\begin{aligned}\chi_{ab}(\omega) &= \frac{\mathrm{i}}{2}\int_{-\infty}^{\infty} \mathrm{e}^{\mathrm{i}\omega t}\langle[O_a(t), O_b]\rangle \mathrm{d}t \\ &= i\frac{\pi}{Z}\sum_{ij}\delta(\omega + E_i - E_j)(\mathrm{e}^{-\beta E_i} - \mathrm{e}^{-\beta E_j})\langle E_i|O_a|E_j\rangle\langle E_j|O_b|E_i\rangle,\end{aligned}$$

which directly gives the relation between χ_{ab} and S_{ab} as below

$$\begin{aligned}\mathrm{Im}(\chi_{ab}(\omega)) &= \frac{\pi}{Z}\sum_{ij}\tanh\left(\frac{E_j - E_i}{2T}\right)(\mathrm{e}^{-\beta E_i} + \mathrm{e}^{-\beta E_j})\delta(\omega + E_i - E_j) \\ &\quad \times \mathrm{Re}(\langle E_i|O_a|E_j\rangle\langle E_j|O_b|E_i\rangle) \\ &= \frac{\pi}{Z}\tanh\left(\frac{\omega}{2T}\right)\sum_{ij}(\mathrm{e}^{-\beta E_i} + \mathrm{e}^{-\beta E_j})\delta(\omega + E_i - E_j) \\ &\quad \times \mathrm{Re}(\langle E_i|O_a|E_j\rangle\langle E_j|O_b|E_i\rangle) \\ &= \tanh\left(\frac{\omega}{2T}\right)\mathrm{Re}(S_{ab}(\omega)),\end{aligned} \tag{G.8}$$

namely,

$$\mathrm{Im}(\chi_{ab}(\omega)) = \tanh\left(\frac{\omega}{2T}\right)\mathrm{Re}(S_{ab}(\omega)), \tag{G.9}$$

which is just the fluctuation-dissipation theorem. Using this relation, one can further obtain the result in [109] as below

$$\mathcal{F}_{ab} = \frac{4}{\pi}\int_{-\infty}^{\infty}\tanh\left(\frac{\omega}{2T}\right)\mathrm{Im}(\chi_{ab}(\omega))\mathrm{d}\omega. \tag{G.10}$$

Appendix H. Derivation of quantum multiparameter Cramér–Rao bound

The derivation of quantum multiparameter Cramér–Rao bound is based on the Cauchy–Schwarz inequality below

$$\mathrm{Tr}(X^\dagger X)\mathrm{Tr}(Y^\dagger Y) \geqslant \frac{1}{4}|\mathrm{Tr}(X^\dagger Y + XY^\dagger)|^2, \tag{H.1}$$

which comes from the complete form

$$\mathrm{Tr}(X^\dagger X)\mathrm{Tr}(Y^\dagger Y) \geqslant \frac{1}{4}|\mathrm{Tr}(X^\dagger Y + XY^\dagger)|^2 + \frac{1}{4}|\mathrm{Tr}(X^\dagger Y - XY^\dagger)|^2. \tag{H.2}$$

Define X and Y as

$$X := \sum_m f_m L_m\sqrt{\rho}, \tag{H.3}$$

$$Y := \sum_m g_m(O_m - \langle O_m\rangle)\sqrt{\rho}, \tag{H.4}$$

where f_m, g_m are real numbers for any m, and $\langle\cdot\rangle = \mathrm{Tr}(\cdot\rho)$. Here O_m is an observable defined as

$$O_m := \sum_k \hat{x}_m(k)\Pi_k. \tag{H.5}$$

$\hat{x}_m(k)$ is the estimator of x_m and is the function of kth result. Based on equation (H.3), it can be calculated that $\mathrm{Tr}(X^\dagger X) = \sum_{ml} f_m f_l \mathrm{Tr}(L_m L_l \rho)$, which can be symmetrized into $\mathrm{Tr}(X^\dagger X) = \frac{1}{2}\sum_{ml} f_m f_l \mathrm{Tr}(\{L_m, L_l\}\rho) = \sum_{ml} f_m f_l \mathcal{F}_{ab}$. Define $\vec{f} = (f_0, f_1, ..., f_m, ...)^{\mathrm{T}}$, $\mathrm{Tr}(X^\dagger X)$ can be further rewritten into

$$\mathrm{Tr}(X^\dagger X) = \vec{f}^{\,\mathrm{T}} \mathcal{F} \vec{f}. \tag{H.6}$$

Similarly, define $\vec{g} = (g_0, g_1, ..., g_m, ...)^{\mathrm{T}}$ and through some algebra, $\mathrm{Tr}(Y^\dagger Y)$ can be calculated as

$$\mathrm{Tr}(Y^\dagger Y) = \vec{g}^{\,\mathrm{T}} C \vec{g}, \tag{H.7}$$

where C is the covariance matrix for $\{O_m\}$, and is defined as $C_{ml} = \frac{1}{2}\langle\{O_m, O_l\}\rangle - \langle O_m\rangle\langle O_l\rangle$. Furthermore, one can also obtain

$$\frac{1}{2}\mathrm{Tr}(X^\dagger Y + X Y^\dagger) = \vec{f}^{\,\mathrm{T}} B \vec{g}, \tag{H.8}$$

where the entry of B is defined as $B_{ml} = \frac{1}{2}\mathrm{Tr}(\rho\{L_m, \Pi_l\}) = \frac{1}{2}\mathrm{Tr}(\{\rho, L_m\}O_l)$. Utilizing $\partial_{x_a}\rho = \frac{1}{2}\{\rho, L_m\}$, B_{ml} reduces to $B_{ml} = \mathrm{Tr}(\Pi_l \partial_{x_m}\rho)$. Since we consider unbiased estimators, i.e. $\langle O_m\rangle = \sum_m \hat{x}_m \mathrm{Tr}(\rho\Pi_k) = x_m$, B_{ml} further reduces to $B_{ml} = \partial_{x_m}\langle O_l\rangle = \delta_{ml}$, with δ_{ml} the Kronecker delta function. Hence, for unbiased estimators B is actually the identity matrix $\mathbb{1}$.

Now substituting equations (H.6)–(H.8) into the Cauchy–Schwarz inequality (H.1), one can obtain

$$\vec{f}^{\,\mathrm{T}} \mathcal{F} \vec{f} \vec{g}^{\,\mathrm{T}} C \vec{g} \geqslant \left(\vec{f}^{\,\mathrm{T}} \vec{g}\right)^2. \tag{H.9}$$

Assuming $\mathcal{F}$ is invertable, i.e. it is positive-definite, and taking $\vec{f} = \mathcal{F}^{-1}\vec{g}$, above inequality reduces to $\vec{g}^{\,\mathrm{T}}\mathcal{F}^{-1}\vec{g}\vec{g}^{\,\mathrm{T}} C\vec{g} \geqslant \left(\vec{g}^{\,\mathrm{T}}\mathcal{F}^{-1}\vec{g}\right)^2$. Since $\mathcal{F}$ is positive-definite, $\mathcal{F}^{-1}$ is also positive-definite, which means $\vec{g}^{\,\mathrm{T}}\mathcal{F}^{-1}\vec{g}$ is a positive number, thus, the above equation can further reduce to $\vec{g}^{\,\mathrm{T}} C\vec{g} \geqslant \vec{g}^{\,\mathrm{T}}\mathcal{F}^{-1}\vec{g}$, namely,

$$C \geqslant \mathcal{F}^{-1}. \tag{H.10}$$

Next we discuss the relation between C and $\mathrm{cov}(\hat{\vec{x}}, \{\Pi_k\})$. Utilizing the defintion of O_m, C_{ml} can be written as

$$\begin{aligned} C_{ml} = &\sum_{kk'} \hat{x}_m(k)\hat{x}_l(k')\frac{1}{2}\mathrm{Tr}(\rho\{\Pi_k, \Pi_{k'}\}) \\ &- \left[\sum_k \hat{x}_m \mathrm{Tr}(\rho\Pi_k)\right]\left[\sum_k \hat{x}_l \mathrm{Tr}(\rho\Pi_k)\right], \end{aligned} \tag{H.11}$$

and $\mathrm{cov}(\hat{\vec{x}}, \{\Pi_k\})$ for unbiased estimators reads

$$\mathrm{cov}(\hat{\vec{x}}, \{\Pi_k\}) = \sum_k \hat{x}_m \hat{x}_l \mathrm{Tr}(\rho\Pi_k) - x_m x_l. \tag{H.12}$$

If $\{\Pi_k\}$ is a set of projection operators, it satisfies $\Pi_k\Pi_{k'} = \Pi_k\delta_{kk'}$. For unbiased estimators, $\sum_k \hat{x}_{m(l)}\mathrm{Tr}(\rho\Pi_k) = x_{m(l)}$, which gives $C_{ml} = \sum_k \hat{x}_m\hat{x}_l\mathrm{Tr}(\rho\Pi_k) - x_m x_l$, i.e.

$$C = \mathrm{cov}(\hat{\vec{x}}, \{\Pi_k\}). \tag{H.13}$$

If $\{\Pi_k\}$ is a set of POVM, one can see

$$\begin{aligned}\vec{g}^{\mathrm{T}}\mathrm{cov}(\hat{\vec{x}}, \{\Pi_k\})\vec{g} &= \sum_k \sum_{ml} g_m g_l \hat{x}_m \hat{x}_l \mathrm{Tr}(\rho\Pi_k) - \sum_{ml} g_m g_l x_m x_l \\ &= \sum_k \left(\sum_m g_m \hat{x}_m\right)^2 \mathrm{Tr}(\rho\Pi_k) - \sum_{ml} g_m g_l x_m x_l. \end{aligned} \tag{H.14}$$

In the mean time,

$$\vec{g}^{\mathrm{T}} C \vec{g} = \frac{1}{2}\sum_{ml} g_m g_l \mathrm{Tr}\left(\rho O_m O_l + \rho O_l O_m\right) - \sum_{ml} g_m g_l x_m x_l. \tag{H.15}$$

Now define $\mathcal{B}_k := \sqrt{\Pi_k}\left(\sum_m g_m \hat{x}_m - \sum_m g_m O_m\right)$. Based on the Cauchy–Schwarz inequality $\mathrm{Tr}(A^\dagger A) \geqslant 0$, which is valid for any operator A, one can immediately obtain $\mathrm{Tr}(\rho\mathcal{B}_k^\dagger \mathcal{B}_k) = \mathrm{Tr}(\sqrt{\rho}\mathcal{B}_k^\dagger \mathcal{B}_k \sqrt{\rho}) \geqslant 0$, which further gives $\sum_k \mathrm{Tr}(\rho\mathcal{B}_k^\dagger \mathcal{B}_k) \geqslant 0$. Through some calculations, the expression of $\sum_k \mathrm{Tr}(\rho\mathcal{B}_k^\dagger \mathcal{B}_k)$ is in the form

$$\sum_k \mathrm{Tr}(\rho\mathcal{B}_k^\dagger \mathcal{B}_k) = \sum_k \left(\sum_m g_m \hat{x}_m\right)^2 \mathrm{Tr}(\rho\Pi_k) - \sum_{ml} g_m g_l \mathrm{Tr}(\rho O_m O_l). \tag{H.16}$$

Now taking the difference of equations (H.14) and (H.15), it can be found

$$\sum_k \mathrm{Tr}(\rho\mathcal{B}_k^\dagger \mathcal{B}_k) = \vec{g}^{\mathrm{T}}\left(\mathrm{cov}(\hat{\vec{x}}, \{\Pi_k\}) - C\right)\vec{g}. \tag{H.17}$$

Finally, we obtain the following inequality $\vec{g}^{\mathrm{T}}(\mathrm{cov}(\hat{\vec{x}}, \{\Pi_k\}) - C)\vec{g} \geqslant 0$, namely, for any POVM measurement,

$$\mathrm{cov}(\hat{\vec{x}}, \{\Pi_k\}) \geqslant C. \tag{H.18}$$

Based on inequality (H.10) and the property of quadratic form, we finally obtain $\mathrm{cov}(\hat{\vec{x}}, \{\Pi_k\}) \geqslant \mathcal{F}^{-1}$. Consider the repetition of experiments (denoted as n), above bound needs to add a factor of $1/n$. Hence the quantum multiparameter Cramér–Rao bound can be finally expressed by

$$\mathrm{cov}(\hat{\vec{x}}, \{\Pi_k\}) \geqslant \frac{1}{n}\mathcal{F}^{-1}. \tag{H.19}$$

Appendix I. Construction of optimal measurement for pure states

Assume the true values of the vector of unknown parameters $\vec{x}$ is $\vec{x}_{\mathrm{true}}$, we now provide the proof that for a pure parameterized state $|\psi\rangle$, a set of projectors containing the state $|\psi_{\vec{x}_{\mathrm{true}}}\rangle := |\psi(\vec{x} = \vec{x}_{\mathrm{true}})\rangle$, i.e. $\{|m_k\rangle\langle m_k|, |m_0\rangle = |\psi_{\vec{x}_{\mathrm{true}}}\rangle\}$ is possible to be an optimal measurement to attain the quantum Cramér–Rao bound, as shown in [137, 152]. The calculation in this appendix basically coincides with the appendix in [137].

Since $\{|m_k\rangle\langle m_k|\}$ contains the information of the true value, in practice one need to use the estimated value of $\vec{x}$ (denoted as $\hat{\vec{x}}$) to construct $|m_0\rangle = |\psi(\hat{\vec{x}})\rangle$ to perform this measurement, then improve the accuracy of $\hat{\vec{x}}$ adaptively. Thus, it is reasonable to assume

$|\psi_{\vec{x}_{\rm true}}\rangle = |m_0\rangle + \sum_{x_a} \delta x_a |\partial_{x_a}\psi\rangle|_{\vec{x}=\hat{\vec{x}}}$. The probability for $|m_k\rangle\langle m_k|$ is $p_k = |\langle\psi|m_k\rangle|^2$, which gives the CFIM as below

$$\mathcal{I}_{ab}(\hat{\vec{x}}) = \sum_k \frac{4{\rm Re}(\langle m_k|\partial_{x_a}\psi\rangle\langle\psi|m_k\rangle){\rm Re}(\langle m_k|\partial_{x_b}\psi\rangle\langle\psi|m_k\rangle)}{|\langle\psi|m_k\rangle|^2}. \tag{I.1}$$

At the limit $\hat{\vec{x}} \to \vec{x}_{\rm true}$, it is

$$\mathcal{I}_{ab}(\vec{x}_{\rm true}) = \lim_{\hat{\vec{x}}\to\vec{x}_{\rm true}} \sum_k \frac{4{\rm Re}(\langle m_k|\partial_{x_a}\psi\rangle\langle\psi|m_k\rangle){\rm Re}(\langle m_k|\partial_{x_b}\psi\rangle\langle\psi|m_k\rangle)}{|\langle\psi|m_k\rangle|^2}. \tag{I.2}$$

For the $k = 0$ term,

$$\begin{aligned}\lim_{\hat{\vec{x}}\to\vec{x}_{\rm true}} {\rm Re}(\langle m_0|\partial_{x_a}\psi\rangle\langle\psi|m_0\rangle) &= {\rm Re}(\langle\psi_{\vec{x}_{\rm true}}|\partial_{x_a}\psi\rangle) \\ &= {\rm Re}(\langle\psi|\partial_{x_a}\psi\rangle)|_{\vec{x}=\vec{x}_{\rm true}} = 0,\end{aligned} \tag{I.3}$$

and $\lim_{\vec{x}\to\vec{x}_{\rm true}}\langle\psi|m_0\rangle = 1$. Thus, the CFIM is

$$\mathcal{I}_{ab}(\vec{x}_{\rm true}) = \lim_{\hat{\vec{x}}\to\vec{x}_{\rm true}} \sum_{k\neq 0} \frac{4{\rm Re}(\langle m_k|\partial_{x_a}\psi\rangle\langle\psi|m_k\rangle){\rm Re}(\langle m_k|\partial_{x_b}\psi\rangle\langle\psi|m_k\rangle)}{|\langle\psi|m_k\rangle|^2}. \tag{I.4}$$

Due to the fact

$$\begin{aligned}&4{\rm Re}(\langle m_k|\partial_{x_a}\psi\rangle\langle\psi|m_k\rangle){\rm Re}(\langle m_k|\partial_{x_b}\psi\rangle\langle\psi|m_k\rangle) \\ &= 2{\rm Re}(\langle\partial_{x_a}\psi|m_k\rangle\langle m_k|\partial_{x_b}\psi\rangle)|\langle\psi|m_k\rangle|^2 \\ &\quad + 2{\rm Re}(\langle m_k|\partial_{x_a}\psi\rangle\langle m_k|\partial_{x_b}\psi\rangle\langle\psi|m_k\rangle^2),\end{aligned} \tag{I.5}$$

one can have

$$\mathcal{I}_{ab}(\vec{x}_{\rm true}) = \mathcal{F}_{ab}(\vec{x}_{\rm true}) - Q_{ab}, \tag{I.6}$$

where

$$\begin{aligned}Q_{ab} &:= \lim_{\hat{\vec{x}}\to\vec{x}_{\rm true}} \sum_{k\neq 0} \frac{2{\rm Re}(\langle m_k|\partial_{x_a}\psi\rangle\langle\partial_{x_b}\psi|m_k\rangle)|\langle\psi|m_k\rangle|^2}{|\langle\psi|m_k\rangle|^2} \\ &\quad - \frac{2{\rm Re}(\langle m_k|\partial_{x_a}\psi\rangle\langle m_k|\partial_{x_b}\psi\rangle\langle\psi|m_k\rangle^2)}{|\langle\psi|m_k\rangle|^2} \\ &= \lim_{\hat{\vec{x}}\to\vec{x}_{\rm true}} \sum_{k\neq 0} \frac{4{\rm Im}(\langle\partial_{x_a}\psi|m_k\rangle\langle m_k|\psi\rangle){\rm Im}(\langle\partial_{x_b}\psi|m_k\rangle\langle m_k|\psi\rangle)}{|\langle\psi|m_k\rangle|^2}.\end{aligned} \tag{I.7}$$

To let $\mathcal{I}(\vec{x}_{\rm true}) = \mathcal{F}(\vec{x}_{\rm true})$, Q has to be a zero matrix. Since the diagonal entry

$$Q_{aa} = \lim_{\hat{\vec{x}}\to\vec{x}_{\rm true}} \sum_{k\neq 0} \frac{4{\rm Im}^2(\langle\partial_{x_a}\psi|m_k\rangle\langle m_k|\psi\rangle)}{|\langle\psi|m_k\rangle|^2}, \tag{I.8}$$

in which all the terms within the summation are non-negative. Therefore, its value is zero if and only if

$$\lim_{\hat{\vec{x}}\to\vec{x}_{\rm true}} \frac{{\rm Im}(\langle\partial_{x_a}\psi|m_k\rangle\langle m_k|\psi\rangle)}{|\langle\psi|m_k\rangle|} = 0,\ \forall x_a, k \neq 0. \tag{I.9}$$

Furthermore, this condition simultaneously makes the non-diagonal entries of Q vanish. Thus, it is the necessary and sufficient condition for $Q = 0$, which means it is also the necessary and

sufficient condition for $\mathcal{I} = \mathcal{F}$ at the point of true value. One may notice that the limitation in equation (I.9) is a 0/0 type. Thus, we use the formula $|\psi_{\vec{x}_{\text{true}}}\rangle = |m_0\rangle + \sum_{x_j} \delta x_j |\partial_{x_j}\psi\rangle|_{\vec{x}=\hat{\vec{x}}}$ to further calculate above equation. With this formula, one has

$$\frac{\text{Im}(\langle\partial_{x_a}\psi|m_k\rangle\langle m_k|\psi\rangle)}{|\langle\psi|m_k\rangle|} = \frac{\sum_j \delta x_j \text{Im}(\langle\partial_{x_a}\psi|m_k\rangle\langle m_k|\partial_{x_j}\psi\rangle)}{|\sum_j \delta x_j \langle\partial_{x_j}\psi|m_k\rangle|}. \tag{I.10}$$

$\langle\partial_{x_j}\psi|m_k\rangle$ cannot generally be zero for all x_j since all $\partial_{x_j}\psi\rangle$ are not orthogonal in general. Thus, equation (I.9) is equivalent to

$$\text{Im}(\langle\partial_{x_a}\psi|m_k\rangle\langle m_k|\partial_{x_b}\psi\rangle) = 0, \ \forall x_a, x_b, k \neq 0. \tag{I.11}$$

Appendix J. Gradient in GRAPE for Hamiltonian estimation

J.1. Gradient of CFIM

The core of GRAPE algorithm is to obtain the expression of gradient. The dynamics of the system is described by

$$\partial_t \rho = \mathcal{E}_{\vec{x}}\rho. \tag{J.1}$$

For the Hamiltonian estimation under control, the dynamics is

$$\partial_t \rho = -\text{i}[H_0(\vec{x}) + H_\text{c}, \rho] + \mathcal{L}\rho, \tag{J.2}$$

where $H_\text{c} = \sum_{k=1}^{p} V_k(t) H_k$ is the control Hamiltonian with H_k the kth control and $V_k(t)$ the corresponding time-dependent control amplitude. To perform the algorithm, the entire evolution time T is cut into m parts with time interval Δt, i.e. $m\Delta t = T$. $V_k(t)$ within the jth time interval is denoted as $V_k(j)$ and is assumed to be a constant.

For a set of probability distribution $p(y|\vec{x}) = \text{Tr}(\rho\Pi_y)$ with $\{\Pi_y\}$ a set of POVM. The gradient of $\mathcal{I}_{ab}$ at target time T reads [172]

$$\begin{aligned}\frac{\delta\mathcal{I}_{ab}(T)}{\delta V_k(j)} = {} & \Delta t \text{Tr}\left(\tilde{L}_{2,ab}\mathcal{M}_j^{(1)}\right) - \Delta^2 t \text{Tr}\left[\tilde{L}_{1,b}\left(\mathcal{M}_{j,a}^{(2)} + \mathcal{M}_{j,a}^{(3)}\right)\right] \\ & - \Delta^2 t \text{Tr}\left[\tilde{L}_{1,a}\left(\mathcal{M}_{j,b}^{(2)} + \mathcal{M}_{j,b}^{(3)}\right)\right],\end{aligned} \tag{J.3}$$

where

$$\tilde{L}_{1,a(b)} = \sum_y \left[\partial_{x_{a(b)}} \ln p(y|\vec{x})\right] \Pi_y, \tag{J.4}$$

$$\tilde{L}_{2,ab} = \sum_y \left[\partial_{x_a} \ln p(y|\vec{x})\right] \left[\partial_{x_b} \ln p(y|\vec{x})\right] \Pi_y, \tag{J.5}$$

and $\mathcal{M}_j^{(1)}$, $\mathcal{M}_{j,a(b)}^{(2)}$ and $\mathcal{M}_{j,a(b)}^{(3)}$ are Hermitian operators and can be expressed by

$$\mathcal{M}_j^{(1)} = \text{i}\mathcal{D}_{j+1}^m H_k^\times(\rho_j), \tag{J.6}$$

$$\mathcal{M}_{j,a(b)}^{(2)} = \sum_{i=1}^{j} \mathcal{D}_{j+1}^m H_k^\times \mathcal{D}_{i+1}^j (\partial_{x_{a(b)}} H_0)^\times(\rho_i), \tag{J.7}$$

$$\mathcal{M}^{(3)}_{j,a(b)} = (1-\delta_{jm})\sum_{i=j+1}^{m}\mathcal{D}^{m}_{i+1}(\partial_{x_{a(b)}}H_0)^{\times}\mathcal{D}^{i}_{j+1}H_k^{\times}(\rho_j). \tag{J.8}$$

The notation $A^{\times}(\cdot) := [A,\cdot]$ is a superoperator. δ_{jm} is the Kronecker delta function. $D_j^{j'}$ is the propagating superoperator from the jth time point to the j'th time with the definition $D_j^{j'} := \prod_{i=j}^{j'}\exp(\Delta t\mathcal{E}_i)$ for $j \leqslant j'$. We define $D_j^{j'} = \mathbb{1}$ for $j > j'$. $\rho_j = D_1^j\rho(0)$ is the quantum state at jth time.

For a two-parameter case $\vec{x} = (x_0, x_1)$, the objective function can be chosen as $F_{\text{eff}}(T)$ according to corollary 3.1.3, and the corresponding gradient is

$$\frac{\delta\mathcal{F}_{\text{eff}}(T)}{\delta V_k(j)} = \frac{\mathcal{I}_{11}^2+\mathcal{I}_{01}^2}{(\mathcal{I}_{00}+\mathcal{I}_{11})^2}\frac{\delta\mathcal{I}_{00}}{\delta V_k(j)} + \frac{\mathcal{I}_{00}^2+\mathcal{I}_{01}^2}{(\mathcal{I}_{00}+\mathcal{I}_{11})^2}\frac{\delta\mathcal{I}_{11}}{\delta V_k(j)} - \frac{2\mathcal{I}_{01}}{\mathcal{I}_{00}+\mathcal{I}_{11}}\frac{\delta\mathcal{I}_{01}}{\delta V_k(j)}. \tag{J.9}$$

For the objective function

$$f_0(T) = \left(\sum_a \frac{1}{\mathcal{I}_{aa}(T)}\right)^{-1}, \tag{J.10}$$

the gradient reads

$$\frac{\delta f_0(T)}{\delta V_k(j)} = \sum_a\left(\frac{f_0}{\mathcal{I}_{aa}}\right)^2\frac{\delta\mathcal{I}_{aa}}{\delta V_k(j)}. \tag{J.11}$$

J.2. Gradient of QFIM

Now we calculate the gradient of the QFIM. Based on the equation

$$\partial_{x_a}\rho(T) = \frac{1}{2}(\rho(T)L_{x_a}(T) + L_{x_a}(T)\rho(T)), \tag{J.12}$$

we can obtain

$$\begin{aligned}\text{Tr}\left(\partial_{x_a}\frac{\delta\rho(T)}{\delta V_k(j)}L_{x_b}\right) = &\frac{1}{2}\text{Tr}\left(\frac{\delta\rho(T)}{\delta V_k(j)}\{L_{x_a}(T), L_{x_b}(T)\}\right)\\ &+\frac{1}{2}\text{Tr}\left(\frac{\delta L_{x_a}(T)}{\delta V_k(j)}\{\rho(T), L_{x_b}(T)\}\right).\end{aligned} \tag{J.13}$$

Similarly, we have

$$\begin{aligned}\text{Tr}\left(\partial_{x_b}\frac{\delta\rho(T)}{\delta V_k(j)}L_{x_a}\right) = &\frac{1}{2}\text{Tr}\left(\frac{\delta\rho(T)}{\delta V_k(j)}\{L_{x_a}(T), L_{x_b}(T)\}\right)\\ &+\frac{1}{2}\text{Tr}\left(\frac{\delta L_{x_b}(T)}{\delta V_k(j)}\{\rho(T), L_{x_a}(T)\}\right).\end{aligned} \tag{J.14}$$

Next, from the definition of QFIM, the gradient for $\mathcal{F}_{ab}$ at target time T reads [172]

$$\begin{aligned}\frac{\delta\mathcal{F}_{ab}(T)}{\delta V_k(j)} = &\frac{1}{2}\text{Tr}\left(\frac{\delta\rho(T)}{\delta V_k(j)}\{L_{x_a}(T), L_{x_b}(T)\}\right) + \frac{1}{2}\text{Tr}\left(\frac{\delta L_{x_a}(T)}{\delta V_k(j)}\{\rho(T), L_{x_b}(T)\}\right)\\ &+\frac{1}{2}\text{Tr}\left(\frac{\delta L_{x_b}(T)}{\delta V_k(j)}\{\rho(T), L_{x_a}(T)\}\right).\end{aligned} \tag{J.15}$$

Combing equations (J.13)–(J.15), one can obtain

$$\frac{\delta \mathcal{F}_{ab}(T)}{\delta V_k(j)} = \mathrm{Tr}\left(\partial_{x_a}\frac{\delta\rho(T)}{\delta V_k(j)}L_{x_b}(T)\right) + \mathrm{Tr}\left(\partial_{x_b}\frac{\delta\rho(T)}{\delta V_k(j)}L_{x_a}(T)\right) - \frac{1}{2}\mathrm{Tr}\left(\frac{\delta\rho(T)}{\delta V_k(j)}\left\{L_{x_a}(T), L_{x_b}(T)\right\}\right). \tag{J.16}$$

Substituing the specific expressions of $\frac{\delta\rho(T)}{\delta V_k(j)}$ given in [172], one can obtain the gradient of $\mathcal{F}_{ab}$ as below

$$\begin{aligned}\frac{\delta \mathcal{F}_{ab}(T)}{\delta V_k(j)} = &\frac{1}{2}\Delta t\mathrm{Tr}\left(\left\{L_{x_a}(T), L_{x_b}(T)\right\}\mathcal{M}_j^{(1)}\right)\\ &- \Delta^2 t\mathrm{Tr}\left[L_{x_b}(T)\left(\mathcal{M}_{j,a}^{(2)} + \mathcal{M}_{j,a}^{(3)}\right)\right]\\ &- \Delta^2 t\mathrm{Tr}\left[L_{x_a}(T)\left(\mathcal{M}_{j,b}^{(2)} + \mathcal{M}_{j,b}^{(3)}\right)\right].\end{aligned} \tag{J.17}$$

The gradient for the diagonal entry $\mathcal{F}_{aa}$ reduces to the form in [172], i.e.

$$\frac{\delta \mathcal{F}_{aa}(T)}{\delta V_k(j)} = \Delta t\mathrm{Tr}\left(L_{x_a}^2(T)\mathcal{M}_j^{(1)}\right) - 2\Delta^2 t\mathrm{Tr}\left[L_{x_a}(T)\left(\mathcal{M}_{j,a}^{(2)} + \mathcal{M}_{j,a}^{(3)}\right)\right]. \tag{J.18}$$

ORCID iDs

Jing Liu https://orcid.org/0000-0001-9944-4493
Xiao-Ming Lu https://orcid.org/0000-0001-9822-5387

References

[1] Helstrom C W 1976 *Quantum Detection and Estimation Theory* (New York: Academic)
[2] Holevo A S 1982 *Probabilistic and Statistical Aspects of Quantum Theory* (Amsterdam: North-Holland)
[3] Giovannetti V, Lloyd S and Maccone L 2004 Quantum-enhanced measurements: beating the standard quantum limit *Science* **306** 1330–6
[4] Giovannetti V, Lloyd S and Maccone L 2011 Advances in quantum metrology *Nat. Photon.* **5** 222–9
[5] Paris M G A 2009 Quantum estimation for quantum technology *Int. J. Quantum Inf.* **7** 125
[6] Tóth G and Apellaniz I 2014 Quantum metrology from a quantum information science perspective *J. Phys. A: Math. Theor.* **47** 424006
[7] Braun D, Adesso G, Benatti F, Floreanini R, Marzolino U, Mitchell M W and Pirandola S 2018 Quantum-enhanced measurements without entanglement *Rev. Mod. Phys.* **90** 035006
[8] Pezzè L, Smerzi A, Oberthaler M K, Schmied R and Treutlein P 2018 Quantum metrology with nonclassical states of atomic ensembles *Rev. Mod. Phys.* **90** 035005
[9] Huang J, Wu S, Zhong H and Lee C 2014 Chapter 7: quantum metrology with cold atoms *Annu. Rev. Cold Atoms Molecules* **2** 365–415
[10] Degen C L, Reinhard F and Cappellaro P 2017 Quantum sensing *Rev. Mod. Phys.* **89** 035002
[11] Pirandola S, Bardhan B R, Gehring T, Weedbrook C and Lloyd S 2018 Advances in photonic quantum sensing *Nat. Photon.* **12** 724–33
[12] Dowling J P 2008 Quantum optical metrology-the lowdown on high-N00N states *Contemp. Phys.* **49** 125
[13] Dowling J P and Seshadreesan K P 2015 Quantum optical technologies for metrology, sensing, and imaging *J. Lightwave Technol.* **33** 2359
[14] Demkowicz-Dobrzański R, Jarzyna M and Kołodyński J 2015 Quantum limits in optical interferometry *Prog. Opt.* **60** 345–435 (chapter 4)

[15] Sidhu J S and Kok P 2019 A geometric perspective on quantum parameter estimation (arXiv:1907.06628)
[16] Szczykulska M, Baumgratz T and Datta A 2016 Multi-parameter quantum metrology *Adv. Phys.* X **1** 621
[17] Petz D and Ghinea C 2011 Introduction to quantum Fisher information *Quantum Probab. White Noise Anal.* **27** 261–81
[18] Gu S J 2010 Fidelity approach to quantum phase transition *Int. J. Mod. Phys.* B **24** 4371
[19] Wang T-L, Wu L-N, Yang W, Jin G-R, Lambert N and Nori F 2014 Quantum Fisher information as a signature of the superradiant quantum phase transition *New J. Phys.* **16** 063039
[20] Marzolino U and Prosen T 2017 Fisher information approach to nonequilibrium phase transitions in a quantum XXZ spin chain with boundary noise *Phys. Rev.* B **96** 104402
[21] Hyllus P, Laskowski W, Krischek R, Schwemmer C, Wieczorek W, Weinfurter H, Pezzé L and Smerzi A 2012 Fisher information and multiparticle entanglement *Phys. Rev.* A **85** 022321
[22] Tóth G 2012 Multipartite entanglement and high-precision metrology *Phys. Rev.* A **85** 022322
[23] Venuti L C and Zanardi P 2007 Quantum critical scaling of the geometric tensors *Phys. Rev. Lett.* **99** 095701
[24] Amari S-I and Nagaoka H 2000 *Methods of Information Geometry* (Providence, RI: American Mathematical Society)
[25] Yuen H P and Lax M 1973 Multiple-parameter quantum estimation and measurement of nonselfadjoint observables *IEEE Trans. Inf. Theory* **19** 740–50
[26] Petz D 1996 Monotone metrics on matrix spaces *Linear Algebr. Appl.* **244** 81
[27] Petz D 2008 *Quantum Information Theory and Quantum Statistics* (*Theoretical and Mathematical Physics*) (Berlin: Springer)
[28] Suzuki J 2016 Explicit formula for the Holevo bound for two-parameter qubit-state estimation problem *J. Math. Phys.* **57** 042201
[29] Fujiwara A and Nagaoka H 1995 Quantum Fisher metric and estimation for pure state models *Phys. Lett.* A **201** 119–24
[30] Braunstein S L and Caves C M 1994 Statistical distance and the geometry of quantum states *Phys. Rev. Lett.* **72** 3439–43
[31] Liu J, Xiong H-N, Song F and Wang X 2014 Fidelity susceptibility and quantum Fisher information for density operators with arbitrary ranks *Physica* A **410** 167–73
[32] Knysh S, Smelyanskiy V N and Durkin G A 2011 Scaling laws for precision in quantum interferometry and the bifurcation landscape of the optimal state *Phys. Rev.* A **83** 021804
[33] Liu J, Jing X-X and Wang X 2013 Phase-matching condition for enhancement of phase sensitivity in quantum metrology *Phys. Rev.* A **88** 042316
[34] Zhang Y M, Li X W, Yang W and Jin G R 2013 Quantum Fisher information of entangled coherent states in the presence of photon loss *Phys. Rev.* A **88** 043832
[35] Jing X X, Liu J, Zhong W and Wang X 2014 Quantum Fisher information of entangled coherent states in a Lossy Mach–Zehnder interferometer *Commun. Theor. Phys.* **61** 115–20
[36] Liu J, Jing X-X, Zhong W and Wang X 2014 Q uantum Fisher information for density matrices with arbitrary ranks *Commun. Theor. Phys.* **61** 45–50
[37] Fujiwara A and Nagaoka H 1999 An estimation theoretical characterization of coherent states *J. Math. Phys.* **40** 4227
[38] Liu J, Chen J, Jing X-X and Wang X 2016 Quantum Fisher information and symmetric logarithmic derivative via anti-commutators *J. Phys. A: Math. Theor.* **49** 275302
[39] Šafránek D 2018 Simple expression for the quantum Fisher information matrix *Phys. Rev.* A **97** 042322
[40] Gilchrist A, Terno D R and Wood C J 2009 Vectorization of quantum operations and its use (arXiv:0911.2539)
[41] Wood C J, Biamonte J D and Cory D G 2015 Tensor networks and graphical calculus for open quantum systems *Quantum Inf. Comput.* **15** 759
[42] Havel T F 2003 Robust procedures for converting among Lindblad, Kraus and matrix representations of quantum dynamical semigroups *J. Math. Phys.* **44** 534
[43] Watanabe Y, Sagawa T and Ueda M 2010 Optimal measurement on noisy quantum systems *Phys. Rev. Lett.* **104** 020401
[44] Watanabe Y, Sagawa T and Ueda M 2011 Uncertainty relation revisited from quantum estimation theory *Phys. Rev.* A **84** 042121

[45] Watanabe Y 2014 *Formulation of Uncertainty Relation Between Error and Disturbance in Quantum Measurement by Using Quantum Estimation Theory* (Berlin: Springer)
[46] Dittmann J 1999 Explicit formulae for the Bures metric *J. Phys. A: Math. Gen.* **32** 2663
[47] Zhong W, Sun Z, Ma J, Wang X and Nori F 2013 Fisher information under decoherence in Bloch representation *Phys. Rev.* A **87** 022337
[48] Liu J, Jing X-X and Wang X 2015 Quantum metrology with unitary parametrization processes *Sci. Rep.* **5** 8565
[49] Taddei M M, Escher B M, Davidovich L and de Matos Filho R L 2013 Quantum speed limit for physical processes *Phys. Rev. Lett.* **110** 050402
[50] Boixo S, Flammia S T, Caves C M and Geremia J M 2007 Generalized limits for single-parameter quantum estimation *Phys. Rev. Lett.* **98** 090401
[51] Sidhu J S and Kok P 2017 Quantum metrology of spatial deformation using arrays of classical and quantum light emitters *Phys. Rev.* A **95** 063829
[52] Sidhu J S and Kok P 2018 Quantum Fisher information for general spatial deformations of quantum emitters (arXiv:1802.01601)
[53] Pang S and Brun T A 2014 Quantum metrology for a general Hamiltonian parameter *Phys. Rev.* A **90** 022117
[54] Pang S and Jordan A N 2017 Optimal adaptive control for quantum metrology with time-dependent Hamiltonians *Nat. Commun.* **8** 14695
[55] Scully M O and Zubairy M S 1997 *Quantum Optics* (Cambridge: Cambridge University Press)
[56] Braunstein S L and van Loock P 2005 Quantum information with continuous variables *Rev. Mod. Phys.* **77** 513
[57] Simon R, Mukunda N and Dutta B 1994 Quantum-noise matrix for multimode systems: U(n) invariance, squeezing, and normal forms *Phys. Rev.* A **49** 1567
[58] Weedbrook C, Pirandola S, García-Patrón R, Cerf N J, Ralph T C, Shapiro J H and Lloyd S 2012 Gaussian quantum information *Rev. Mod. Phys.* **84** 621
[59] Williamson J 1936 On the algebraic problem concerning the normal forms of linear dynamical systems *Am. J. Math.* **58** 141
[60] Adesso G, Ragy S and Lee A R 2014 Continuous variable quantum information: Gaussian states and beyond *Open Syst. Inf. Dyn.* **21** 1440001
[61] Wang X-B, Hiroshima T, Tomita A and Hayashi M 2007 Quantum information with Gaussian states *Phys. Rep.* **448** 1–111
[62] Monras A 2013 Phase space formalism for quantum estimation of Gaussian states (arXiv:1303.3682)
[63] Pinel O, Jian P, Treps N, Fabre C and Braun D 2013 Quantum parameter estimation using general single-mode Gaussian states *Phys. Rev.* A **88** 040102
[64] Gao Y and Lee H 2014 Bounds on quantum multiple-parameter estimation with Gaussian state *Eur. Phys. J.* D **68** 347
[65] Nichols R, Liuzzo-Scorpo P, Knott P A and Adesso G 2018 Multiparameter Gaussian quantum metrology *Phys. Rev.* A **98** 012114
[66] Šafránek D 2018 Estimation of Gaussian quantum states *J. Phys. A: Math. Theor.* **52** 035304
[67] Serafini A 2017 *Quantum Continuous Variables: a Primer of Theoretical Methods* (Oxford: Taylor and Francis)
[68] Pinel O, Fade J, Braun D, Jian P, Treps N and Fabre C 2012 Ultimate sensitivity of precision measurements with intense Gaussian quantum light: a multimodal approach *Phys. Rev.* A **85** 010101
[69] Šafránek D, Lee A R and Fuentes I 2015 Quantum parameter estimation using multi-mode Gaussian states *New J. Phys.* **17** 073016
[70] Marian P and Marian T A 2016 Quantum Fisher information on two manifolds of two-mode Gaussian states *Phys. Rev.* A **93** 052330
[71] Scutaru H 1998 Fidelity for displaced squeezed thermal states and the oscillator semigroup *J. Phys. A: Math. Gen.* **31** 3659
[72] Marian P and Marian T A 2012 Uhlmann fidelity between two-mode Gaussian states *Phys. Rev.* A **86** 022340
[73] Banchi L, Braunstein S L and Pirandola S 2015 Quantum fidelity for arbitrary Gaussian states *Phys. Rev. Lett.* **115** 260501
[74] Oh C, Lee C, Banchi L, Lee S-Y, Rockstuhl C and Jeong H 2019 Optimal measurements for quantum fidelity between Gaussian states and its relevance to quantum metrology *Phys. Rev.* A **100** 012323

[75] Matsubara T, Facchi P, Giovannetti V and Yuasa K 2019 Optimal Gaussian metrology for generic multimode interferometric circuit *New J. Phys.* **21** 033014
[76] Jiang Z 2014 Quantum Fisher information for states in exponential form *Phys. Rev.* A **89** 032128
[77] Gagatsos C N, Branford D and Datta A 2016 Gaussian systems for quantum-enhanced multiple phase estimation *Phys. Rev.* A **94** 042342
[78] Šafránek D and Fuentes I 2016 Optimal probe states for the estimation of Gaussian unitary channels *Phys. Rev.* A **94** 062313
[79] Facchi P, Kulkarni R, Man'ko V I, Marmo G, Sudarshan E C G and Ventriglia F 2010 Classical and quantum Fisher information in the geometrical formulation of quantum mechanics *Phys. Lett.* A **374** 4801–3
[80] Nielsen M A and Chuang I L 2000 *Quantum Computation and Quantum Information* (Cambridge: Cambridge University Press)
[81] Twamley J 1996 Bures and statistical distance for squeezed thermal states *J. Phys. A: Math. Gen.* **29** 3723–31
[82] Zanardi P, Venuti L C and Giorda P 2007 Bures metric over thermal state manifolds and quantum criticality *Phys. Rev.* A **76** 062318
[83] Zanardi P, Paris M G A and Venuti L C 2008 Quantum criticality as a resource for quantum estimation *Phys. Rev.* A **78** 042105
[84] Yuan H 2016 Sequential feedback scheme outperforms the parallel scheme for Hamiltonian parameter estimation *Phys. Rev. Lett.* **117** 160801
[85] Fŕerot I and Roscilde T 2018 Quantum critical metrology *Phys. Rev. Lett.* **121** 020402
[86] Rams M M, Sierant P, Dutta O, Horodecki P and Zakrzewski J 2018 At the limits of criticality-based quantum metrology: apparent super-Heisenberg scaling revisited *Phys. Rev.* X **8** 021022
[87] Šafránek D 2017 Discontinuities of the quantum Fisher information and the Bures metric *Phys. Rev.* A **95** 052320
[88] Seveso L, Albarelli F, Genoni M G and Paris M G A 2019 On the discontinuity of the quantum Fisher information for quantum statistical models with parameter dependent rank *J. Phys. A: Math. Theor.* (accepted) (https://doi.org/10.1088/1751-8121/ab599b)
[89] Morozova E A and Čencov N N 1991 Markov invariant geometry on manifolds of states *J. Sov. Math.* **56** 2648
[90] Hayashi M (ed) 2005 *Asymptotic Theory of Quantum Statistical Inference: Selected Papers* (Singapore: World Scientific)
[91] Bengtsson I and Zyczkowski K 2006 *Geometry of Quantum States: an Introduction to Quantum Entanglement* (Cambridge: Cambridge University Press)
[92] Sommers H J and Życzkowski K 2003 Bures volume of the set of mixed quantum states *J. Phys. A: Math. Gen.* **36** 10083–100
[93] Pires D P, Cianciaruso M, Céleri L C, Adesso G and Soares-Pinto D O 2016 Generalized geometric quantum speed limits *Phys. Rev.* X **6** 021031
[94] Shitara T and Ueda M 2016 Determining the continuous family of quantum Fisher information from linear-response theory *Phys. Rev.* A **94** 062316
[95] Provost J P and Vallee G 1980 Riemannian structure on manifolds of quantum states *Commun. Math. Phys.* **76** 289
[96] Shapere A and and Wilczek F (ed) 1989 *Geometric Phases in Physics* (Singapore: World Scientific)
[97] Berry M V 1984 Quantal phase factors accompanying adiabatic changes *Proc. R. Soc.* A **392** 45
[98] Guo W, Zhong W, Jing X-X, Fu L-B and Wang X 2016 Berry curvature as a lower bound for multiparameter estimation *Phys. Rev.* A **93** 042115
[99] Paris M G A 2016 Achieving the Landau bound to precision of quantum thermometry in systems with vanishing gap *J. Phys. A: Math. Theor.* **49** 03LT02
[100] Hofer P P, Brask J B and Brunner N 2019 Fundamental limits on low-temperature quantum thermometry *Quantum* **3** 161
[101] Zanardi P, Giorda P and Cozzini M 2007 Information-theoretic differential geometry of quantum phase transitions *Phys. Rev. Lett.* **99** 100603
[102] De Pasquale A, Rossini D, Fazio R and Giovannetti V 2016 Local quantum thermal susceptibility *Nat. Commun.* **7** 12782
[103] Kubo R, Toda M and Hashitsume N 1991 *Statistical Physics II, Nonequilibrium Statistical Mechanics* (*Springer Series on Solid State Sciences*) (Berlin: Springer)

[104] Petz D and Toth G 1993 The bogoliubov inner product in quantum statistics *Lett. Math. Phys.* **27** 205
[105] Petz D 1994 Geometry of canonical correlation on the state space of a quantum system *J. Math. Phys.* **35** 780
[106] Hayashi M 2002 Two quantum analogues of Fisher information from a large deviation viewpoint of quantum estimation *J. Phys. A: Math. Gen.* **35** 7689–727
[107] Balian R, Alhassid Y and Reinhardt H 1986 Dissipation in many-body systems: a geometric approach based on information theory *Phys. Rep.* **131** 1–146
[108] You W-L, Li Y-W and Gu S-J 2007 Fidelity, dynamic structure factor, and susceptibility in critical phenomena *Phys. Rev.* E **76** 022101
[109] Hauke P, Markus H, Tagliacozzo L and Zoller P 2016 Measuring multipartite entanglement through dynamic susceptibilities *Nat. Phys.* **12** 778–82
[110] Shirane G, Shapiro S M and Tranquada J M 2002 *Neutron Scattering with a Triple-Axis Spectrometer, Basic Techniques* (Cambridge: Cambridge University Press)
[111] Stöferle T, Moritz H, Schori C, Köhl M and Esslinger T 2004 Transition from a strongly interacting 1D superfluid to a Mott insulator *Phys. Rev. Lett.* **92** 130403
[112] Roy D, Singh R and Moessner R 2015 Probing many-body localization by spin noise spectroscopy *Phys. Rev.* B **92** 180205
[113] Roy D, Yang L, Crooker S A and Sinitsyn N A 2015 Cross-correlation spin noise spectroscopy of heterogeneous interacting spin systems *Sci. Rep.* **5** 9573
[114] Sinitsyn N A and Pershin Y V 2016 The theory of spin noise spectroscopy: a review *Rep. Prog. Phys.* **79** 106501
[115] Fröwis F, Fadel M, Treutlein P, Gisin N and Brunner N 2019 Does large quantum Fisher information imply Bell correlations? *Phys. Rev.* A **99** 040101
[116] Deffner S and Campbell S 2017 Quantum speed limits: from Heisenberg's uncertainty principle to optimal quantum control *J. Phys. A: Math. Theor.* **50** 453001
[117] Gessner M and Smerzi A 2018 Statistical speed of quantum states: generalized quantum Fisher information and Schatten speed *Phys. Rev.* A **97** 022109
[118] del Campo A, Egusquiza I L, Plenio M B and Huelga S F 2013 Quantum speed limits in open system dynamics *Phys. Rev. Lett.* **110** 050403
[119] Campaioli F, Pollock F A, Binder F C and Modi K 2018 Tightening quantum speed limits for almost all states *Phys. Rev. Lett.* **120** 060409
[120] Deffner S and Lutz E 2013 Quantum speed limit for non-Markovian dynamics *Phys. Rev. Lett.* **111** 010402
[121] Shanahan B, Chenu A, Margolus N and del Campo A 2018 Quantum speed limits across the quantum-to-classical transition *Phys. Rev. Lett.* **120** 070401
[122] Fröwis F 2012 Kind of entanglement that speeds up quantum evolution *Phys. Rev.* A **85** 052127
[123] Beau M and del Campo A 2017 Nonlinear quantum metrology of many-body open systems *Phys. Rev. Lett.* **119** 010403
[124] Breuer H-P, Laine E-M, Piilo J and Vacchini B 2016 Colloquium: non-Markovian dynamics in open quantum systems *Rev. Mod. Phys.* **88** 021002
[125] Rivas Á, Huelga S F and Plenio M B 2014 Quantum non-Markovianity: characterization, quantification and detection *Rep. Prog. Phys.* **77** 094001
[126] de Vega I and Alonso D 2017 Dynamics of non-Markovian open quantum systems *Rev. Mod. Phys.* **89** 015001
[127] Lu X-M, Wang X and Sun C P 2010 Quantum Fisher information flow and non-Markovian processes of open systems *Phys. Rev.* A **82** 042103
[128] Song H, Luo S and Hong Y 2015 Quantum non-Markovianity based on the Fisher-information matrix *Phys. Rev.* A **91** 042110
[129] Lu X-M, Ma Z and Zhang C 2004 Generalized-mean Cramér–Rao bound for multiparameter quantum metrology (arXiv:1010.06035)
[130] Wasserman L 2004 *All of Statistics: a Concise Course in Statistical Inference* (New York: Springer)
[131] Matsumoto K 2002 A new approach to the Cramér–Rao-type bound of the pure-state model *J. Phys. A: Math. Gen.* **35** 3111
[132] Vidrighin M D, Donati G, Genoni M G, Jin X-M, Kolthammer W S, Kim M S, Datta A, Barbieri M and Walmsley I A 2014 Joint estimation of phase and phase diffusion for quantum metrology *Nat. Commun.* **5** 3532

[133] Crowley P J D, Datta A, Barbieri M and Walmsley I A 2014 Tradeoff in simultaneous quantum-limited phase and loss estimation in interferometry *Phys. Rev.* A **89** 023845
[134] Vaneph C, Tufarelli T and Genoni M G 2013 Quantum estimation of a two-phase spin rotation *Quantum Meas. Quantum Metrol.* **1** 12
[135] Gill R D and Guţă M 2013 On asymptotic quantum statistical inference *IMS Collect. Probab. Stat. Back: High-Dimensional Models Process.* **9** 105–27
[136] Ragy S, Jarzyna M and Demkowicz-Dobrzański R 2016 Compatibility in multiparameter quantum metrology *Phys. Rev.* A **94** 052108
[137] Pezzè L, Ciampini M A, Spagnolo N, Humphreys P C, Datta A, Walmsley I A, Barbieri M, Sciarrino F and Smerzi A 2017 Optimal measurements for simultaneous quantum estimation of multiple phases *Phys. Rev. Lett.* **119** 130504
[138] Yang J, Pang S, Zhou Y and Jordan A N 2019 Optimal measurements for quantum multi-parameter estimation with general states *Phys. Rev.* A **100** 032104
[139] Yurke B, McCall S L and Klauder J R 1986 SU(2) and SU(1,1) interferometers *Phys. Rev.* A **33** 4033
[140] Demkowicz-Dobrzański R, Banaszek K and Schnabel R 2013 Fundamental quantum interferometry bound for the squeezed-light-enhanced gravitational wave detector GEO 600 *Phys. Rev.* A **88** 041802
[141] Branford D, Miao H and Datta A 2018 Fundamental quantum limits of multicarrier optomechanical sensors *Phys. Rev. Lett.* **121** 110505
[142] Caves C M 1981 Quantum-mechanical noise in an interferometer *Phys. Rev.* D **23** 1693
[143] Xiao M, Wu L-A and Kimble H J 1987 Precision measurement beyond the shot-noise limit *Phys. Rev. Lett.* **59** 278
[144] Grangier P, Slusher R E, Yurke B and LaPorta A 1987 Squeezed-light-enhanced polarization interferometer *Phys. Rev. Lett.* **59** 2153
[145] Lang M D and Caves C M 2013 Optimal quantum-enhanced interferometry using a laser power source *Phys. Rev. Lett.* **111** 173601
[146] Takeoka M, Seshadreesan K P, You C, Izumi S and Dowling J P 2017 Fundamental precision limit of a Mach–Zehnder interferometric sensor when one of the inputs is the vacuum *Phys. Rev.* A **96** 052118
[147] Polino E, Riva M, Valeri M, Silvestri R, Corrielli G, Crespi A, Spagnolo N, Osellame R and Sciarrino F 2019 Experimental multiphase estimation on a chip *Optica* **6** 288–95
[148] Altorio M, Genoni M G, Vidrighin M D, Somma F and Barbieri M 2015 Weak measurements and the joint estimation of phase and phase diffusion *Phys. Rev.* A **92** 032114
[149] Hu X-L, Li D, Chen L Q, Zhang K, Zhang W and Yuan C-H 2018 Phase estimation for an SU(1,1) interferometer in the presence of phase diffusion and photon losses *Phys. Rev.* A **98** 023803
[150] Roccia E, Gianani I, Mancino L, Sbroscia M, Somma F, Genoni M G and Barbieri M 2018 Entangling measurements for multiparameter estimation with two qubits *Quantum Sci. Technol.* **3** 01LT01
[151] Ciampini M A, Spagnolo N, Vitelli C, Pezze L, Smerzi A and Sciarrino F 2016 Quantum-enhanced multiparameter estimation in multiarm interferometers *Sci. Rep.* **6** 28881
[152] Humphreys P C, Barbieri M, Datta A and Walmsley I A 2013 Quantum enhanced multiple phase estimation *Phys. Rev. Lett.* **111** 070403
[153] Zhang L and Chan K W C 2018 Scalable generation of multi-mode noon states for quantum multiple-phase estimation *Sci. Rep.* **8** 11440
[154] Yao Y, Ge L, Xiao X, Wang X and Sun C P 2014 Multiple phase estimation for arbitrary pure states under white noise *Phys. Rev.* A **90** 062113
[155] Yao Y, Ge L, Xiao X, Wang X and Sun C P 2014 Multiple phase estimation in quantum cloning machines *Phys. Rev.* A **90** 022327
[156] Yue J-D, Zhang Y-R and Fan H 2014 Quantum-enhanced metrology for multiple phase estimation with noise *Sci. Rep.* **4** 5933
[157] Joo J, Munro W J and Spiller T P 2011 Quantum metrology with entangled coherent states *Phys. Rev. Lett.* **107** 083601
[158] Liu J, Lu X-M, Sun Z and Wang X 2016 Quantum multiparameter metrology with generalized entangled coherent state *J. Phys. A: Math. Theor.* **49** 115303
[159] Zhang L and Chan K W C 2017 Quantum multiparameter estimation with generalized balanced multimode noon-like states *Phys. Rev.* A **95** 032321

[160] Knott P A, Proctor T J, Hayes A J, Ralph J F, Kok P and Dunningham J A 2016 Local versus global strategies in multiparameter estimation *Phys. Rev.* A **94** 062312
[161] Ge W, Jacobs K, Eldredge Z, Gorshkov A V and Foss-Feig M 2018 *Phys. Rev. Lett.* **121** 043604
[162] Gessner M, Pezzé L and Smerzi A 2018 Sensitivity bounds for multiparameter quantum metrology *Phys. Rev. Lett.* **121** 130503
[163] Hyllus P, Pezzé L and Smerzi A 2010 Entanglement and sensitivity in precision measurements with states of a fluctuating number of particles *Phys. Rev. Lett.* **105** 120501
[164] De Pasquale A, Facchi P, Florio G, Giovannetti V, Matsuoka K and Yuasa K 2015 Two-mode bosonic quantum metrology with number fluctuations *Phys. Rev.* A **92** 042115
[165] Tsang M and Nair R 2012 Fundamental quantum limits to waveform detection *Phys. Rev.* A **86** 042115
[166] Tsang M, Wiseman H M and Caves C M 2011 Fundamental quantum limit to waveform estimation *Phys. Rev. Lett.* **106** 090401
[167] Berry D W, Tsang M, Hall M J W and Wiseman H M 2015 Quantum Bell–Ziv–Zakai bounds and Heisenberg limits for waveform estimation *Phys. Rev.* X **5** 031018
[168] Tsang M 2012 Ziv–Zakai error bounds for quantum parameter estimation *Phys. Rev. Lett.* **108** 230401
[169] Yuan H and Fung C-H F 2015 Optimal feedback scheme and universal time scaling for Hamiltonian parameter estimation *Phys. Rev. Lett.* **115** 110401
[170] Yang J, Pang S and Jordan A N 2017 Quantum parameter estimation with the Landau–Zener transition *Phys. Rev.* A **96** 020301
[171] Liu J and Yuan H 2017 Control-enhanced multiparameter quantum estimation *Phys. Rev.* A **96** 042114
[172] Liu J and Yuan H 2017 Quantum parameter estimation with optimal control *Phys. Rev.* A **96** 012117
[173] Khaneja N, Reiss T, Hehlet C, Schulte-Herbruggen T and Glaser S J 2005 Optimal control of coupled spin dynamics: design of NMR pulse sequences by gradient ascent algorithms *J. Magn. Reson.* **172** 296
[174] Reich D, Ndong M and Koch C P 2012 Monotonically convergent optimization in quantum control using Krotov's method *J. Chem. Phys.* **136** 104103
[175] Goerz M H, Whaley K B and Koch C P 2015 Hybrid optimization schemes for quantum control *EPJ Quantum Technol.* **2** 21
[176] Rondin L, Tetienne J-P, Hingant T, Roch J-F, Maletinsky P and Jacques V 2014 Magnetometry with nitrogen-vacancy defects in diamond *Rep. Prog. Phys.* **77** 056503
[177] Schloss J M, Barry J F, Turner M J and Walsworth R L 2018 Simultaneous broadband vector magnetometry using solid-state spins *Phys. Rev. Appl.* **10** 034044
[178] Li B-B, Bílek J, Hoff U B, Madsen L S, Forstner S, Prakash V, Schäfermeier C, Gehring T, Bowen W P and Andersen U L 2018 Quantum enhanced optomechanical magnetometry *Optica* **5** 850–6
[179] Sheng D, Li S, Dural N and Romalis M V 2013 Subfemtotesla scalar atomic magnetometry using multipass cells *Phys. Rev. Lett.* **110** 160802
[180] Jing X X, Liu J, Xiong H N and Wang X 2015 Maximal quantum Fisher information for general su(2) parametrization processes *Phys. Rev.* A **92** 012312
[181] Baumgratz T and Datta A 2016 Quantum enhanced estimation of a multidimensional field *Phys. Rev. Lett.* **116** 030801
[182] Hou Z, Wang R-J, Tang J-F, Yuan H, Xiang G-Y, Li C-F and Guo G-C 2019 Control-enhanced sequential scheme for general quantum parameter estimation at the Heisenberg limit *Phys. Rev. Lett.* **123** 040501
[183] Apellaniz I, Urizar-Lanz I, Zimborás Z, Hyllus P and Tóth G 2018 Precision bounds for gradient magnetometry with atomic ensembles *Phys. Rev.* A **97** 053603
[184] Altenburg S, Oszmaniec M, Wölk S and Gühne O 2017 Estimation of gradients in quantum metrology *Phys. Rev.* A **96** 042319
[185] Xu H, Li J, Liu L, Wang Y, Yuan H and Wang X 2019 Transferable control for quantum parameter estimation through reinforcement learning *npj Quantum Inf.* **5** 82
[186] Zhuang M, Huang J and Lee C 2018 Multiparameter estimation via an ensemble of spinor atoms *Phys. Rev.* A **98** 033603
[187] Liu N and Cable H 2017 Quantum-enhanced multi-parameter estimation for unitary photonic systems *Quantum Sci. Technol.* **2** 025008

[188] Proctor T J, Knott P A and Dunningham J A 2018 Multiparameter estimation in networked quantum sensors *Phys. Rev. Lett.* **120** 080501
[189] Correa L A, Mehboudi M, Adesso G and Sanpera A 2015 Individual quantum probes for optimal thermometry *Phys. Rev. Lett.* **114** 220405
[190] Nair R 2018 Quantum-limited loss sensing: multiparameter estimation and bures distance between loss channels *Phys. Rev. Lett.* **121** 230801
[191] Tsang M, Nair N and Lu X-M 2016 Quantum theory of superresolution for two incoherent optical point sources *Phys. Rev.* X **6** 031033
[192] Nair R and Tsang M 2016 Interferometric superlocalization of two incoherent optical point sources *Opt. Express* **24** 3684–701
[193] Wang L 2016 Discovering phase transitions with unsupervised learning *Phys. Rev.* B **94** 195105
[194] van Nieuwenburg E P L, Liu Y-H and Huber S D 2017 Learning phase transitions by confusion *Nat. Phys.* **13** 435–9
[195] Tranter A D, Slatyer H J, Hush M R, Leung A C, Everett J L, Paul K V, Vernaz-Gris P, Lam P K, Buchler B C and Campbell G T 2018 Multiparameter optimisation of a magneto-optical trap using deep learning *Nat. Commun.* **9** 360
[196] Dunjko V and Briegel H J 2018 Machine learning and artificial intelligence in the quantum domain: a review of recent progress *Rep. Prog. Phys.* **81** 074001
[197] Hentschel A and Sanders B C 2010 Machine learning for precise quantum measurement *Phys. Rev. Lett.* **104** 063603
[198] Eberhart R and Kennedy J 1995 *Proc. 6th Int. Symp. on Micro Machine and Human Science* (New York: IEEE)
[199] Lumino A, Polino E, Rab A S, Milani G, Spagnolo N, Wiebe N and Sciarrino F 2018 Experimental phase estimation enhanced by machine learning *Phys. Rev. Appl.* **10** 044033
[200] Greplova E, Andersen C K and Mølmer K 2017 Quantum parameter estimation with a neural network (arXiv:1711.05238)
[201] Zhang Y R and Fan H 2014 Quantum metrological bounds for vector parameters *Phys. Rev.* A **90** 043818
[202] Albarelli F, Friel J F and Datta A 2019 Evaluating the Holevo Cramér–Rao bound for multi-parameter quantum metrology *Phys. Rev. Lett.* **123** 200503
[203] Macieszczak K, Fraas M and Demkowicz-Dobrzański R 2014 Bayesian quantum frequency estimation in presence of collective dephasing *New J. Phys.* **16** 113002
[204] Rzadkowski W and Demkowicz-Dobrzański R 2017 Discrete-to-continuous transition in quantum phase estimation *Phys. Rev.* A **96** 032319
[205] Kiilerich A H and MØlmer K 2016 Bayesian parameter estimation by continuous homodyne detection *Phys. Rev.* A **94** 032103
[206] Rubio J and Dunningham J 2019 Quantum metrology in the presence of limited data *New J. Phys.* **21** 043037
[207] Rubio J and Dunningham J 2019 Bayesian multi-parameter quantum metrology with limited data (arXiv:1906.04123)
[208] Lu X-M and Tsang M 2016 Quantum Weiss–Weinstein bounds for quantum metrology *Quantum Sci. Technol.* **1** 015002
[209] Liu J and Yuan H 2016 Valid lower bound for all estimators in quantum parameter estimation *New J. Phys.* **18** 093009
[210] Yang Y, Chiribella G and Hayashi M 2019 Attaining the ultimate precision limit in quantum state estimation *Commun. Math. Phys.* **368** 223–93
[211] Guţă M *et al* 2019 Multiparameter estimation beyond quantum Fisher information *J. Phys. A: Math. Theor.* (submitted)
[212] Suzuki J, Yang Y and Hayashi M 2019 Quantum state estimation with nuisance parameters (arXiv:1911.02790)